Dissertation zur Erlangung des Doktorgrades

der Fakultät für Chemie und Pharmazie

der Ludwigs-Maximilians-Universität München

Filamin A interacts with the co-activator MKL1 to promote the activity of transcription factor SRF and cell migration

Philipp Oliver Kircher

aus

Weilheim i OB

2016

Erklärung:

Diese Dissertation wurde im Sinne von §7 der Promotionsordnung vom 28. November 2011 von Herrn Prof. Dr. Thomas Gudermann betreut und von Herrn Prof. Dr. Martin Biel von der Fakultät für Chemie und Pharmazie vertreten.

Eidesstattliche Versicherung:

Diese Dissertation wurde eigenständig und ohne unerlaubte Hilfe erarbeitet.

München, den 12.05.2016

_____

Philipp Kircher

Dissertation eingereicht am 02.06.2016

1. Gutachter: Herr Prof. Dr. Martin Biel

2. Gutachter: Herr Prof. Dr. Thomas Gudermann

Mündliche Prüfung am 18.07.2016

Table of content

1 Summary

Megakaryoblastic Leukemia 1 (MKL1, MRTF-A, MAL) is a transcriptional co-activator of Serum response factor (SRF) that promotes the expression of genes involved in cell proliferation, motility, adhesion and differentiation-processes. It thereby holds an essential part in controlling fundamental biological processes like heart, cardiovascular system or brain development. MKL1 is inactive when bound to monomeric actin (G-actin), thus nuclear access is denied. However, signals that activate the small GTPase RhoA cause actin polymerization (F-actin) and MKL1 dissociation from G-actin, this way allowing successful MKL1 shuttling into the nucleus and conveying signals from RhoA into SRF activity.

Filamin A (FLNA) belongs to the group of actin-binding proteins. It is indispensable for filamentous F-actin cross-linking, thus contributes to cytoskeletal dynamics, cell mobility and stability in a crucial way.

In this work, we found a new central mechanism of MKL1 activation that is mediated through its binding to FLNA as a novel interaction partner. We provide evidence that the interaction of MKL1 and FLNA is required for the expression of MKL1 target genes and MKL1-dependent cell motility. We map MKL1 and FLNA regions responsible for the interaction and demonstrate, that cells expressing a MKL1 mutant unable to bind FLNA showed reduced expression of MKL1 target genes and impaired cell motility. Furthermore we indicate that induction and repression of MKL1 target genes correlate with increased or decreased quantity of the MKL1-FLNA interaction. A dynamic flow was revealed, as lysophosphatidic acid-induced RhoA activity in primary human fibroblasts promoted the association of endogenous MKL1 with FLNA, whereas exposure to an actin polymerization inhibitor dissociated MKL1 from FLNA and decreased MKL1 target gene expression in melanoma cells.

Thus FLNA binding to MKL1 functions as a novel cellular transducer linking actin polymerization to SRF activity, counteracting the known repressive complex of MKL1 and monomeric G-actin, which advances to our mechanistic understanding of MKL1 regulation.

2 Introduction

2.1 Megakaryoblastic Leukemia 1: A first look and brief history

Versatility and specificity in gene regulation is achieved with the association of transcriptional co-activators with specific DNA-binding proteins. Megakaryoblastic Leukemia 1 (MKL1, MRTF-A, MAL) is a strong transcriptional co-activator, which has been introduced for the first time as a trigger for acute megakaryoblastic leukemia (AMKL), a rare and aggressive form of childhood leukemia (Mercher T., Coniat MB. et al, 2001). AMKL's signature trademark is the stoppage of thrombocytes development during the stage of immature megakaryoblasts. Formation of a MKL1 fusion protein (RBM15-MKL1/ RNA-binding motif protein 15 or OTT-MAL/ one-twenty-two-myeloid acute leukemia) is expected to be the cause. In contrast to regular MKL1, RBM15-MKL1 acts independently of G-actin, which naturally controls MKL1 shuttling mechanism in and out of the nucleus. Therefore, RBM15-MKL1 remains in the nucleus, resulting in a non-stop stimulation of MKL1 target genes, thus promoting tumor progression (Descot A., Rex-Haffner M. et al, 2008). Besides the involvement of MKL1 in acute megakaryoblastic leukemia, MKL1 is also required for tumor cell invasion and metastasis since knockdown of MKL1 revoked cell invasion and motility of human breast carcinoma and mouse melanoma cells (Medjkane S., Perez-Sanchez C. et al, 2009).

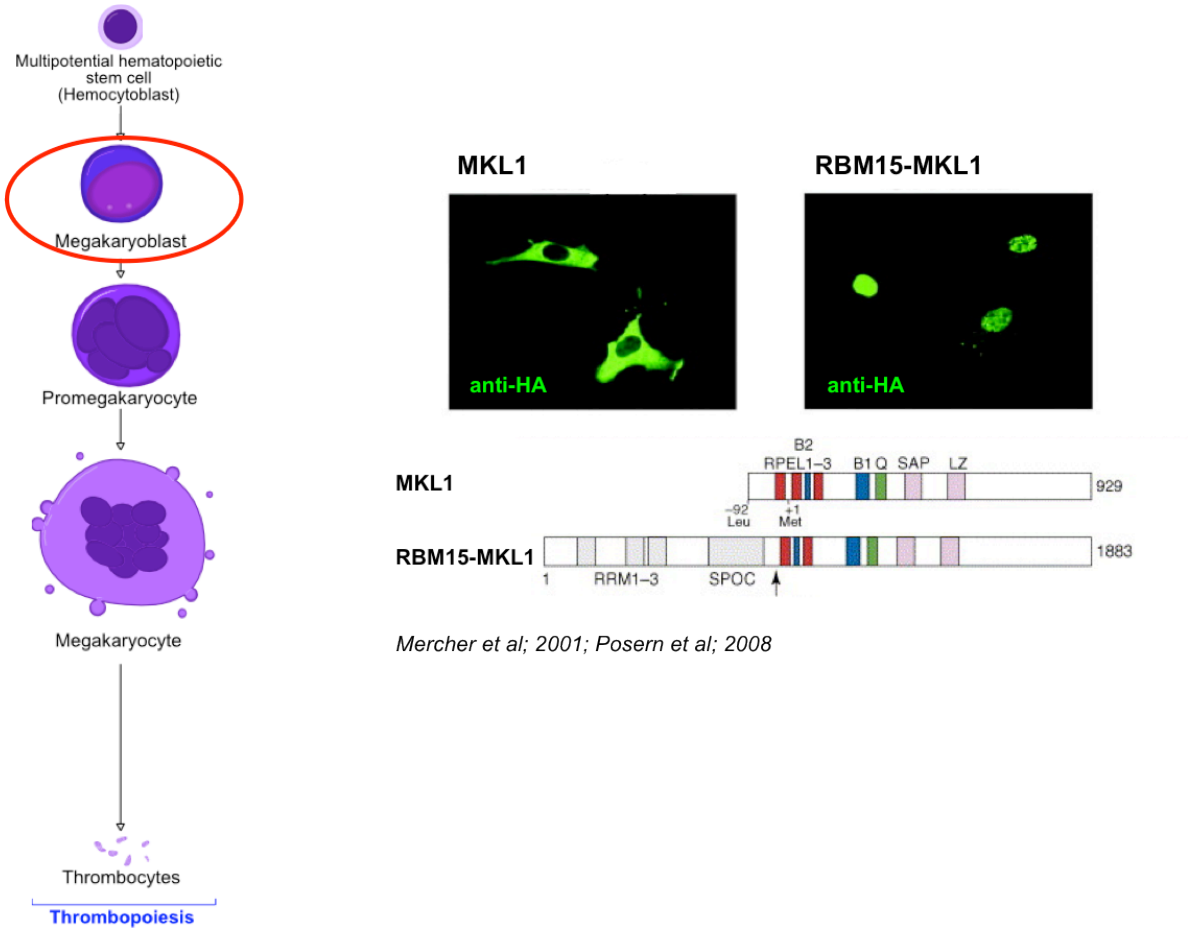

Figure 1: (Left) Thrombocytes development/stoppage at stage of immature megakaryoblastics (red circle) in acute megakaryoblastic leukemia (AMKL). (Right) Formation of the RBM15-MKL1-fusion protein, which remains in the nucleus. Taken from Mercher et al, 2001; Posern et al, 2008.

2.2 Serum Response factor (SRF): Engine of transcriptional activity and director of elementary biological functions

Transcription factors mediate genetic execution in response to cellular signals, this way playing major roles helping the cell adapting to changed demands. Serum response transcriptional factor (SRF) which is activated by MKL1, directly regulates the transcription of a large variety of genes involved in cell proliferation, cell motility, cell adhesion, cell differentiation and organization of the cytoskeleton (Johansen FE., Prywes R., 1995; Treisman R., 1986). This way the MKL1/SRF complex obtains an essential part in controlling fundamental biological processes like heart, muscle, cardiovascular system or brain

development and its crucial necessity is strengthened by the early embryonic death of SRF knockout mice (Arsenian S., Weinhold B. et al, 1998), malfunction in cardiac muscle differentiation in transgenic mice containing dominant-negative SRF mutants (Zhang X., Chai J. et al, 2001; Zhang X., Azhar G. et al, 2001) and thin muscle fiber development in dominant negative mutants of MKL1 (Salvaraj A., Prywes R., 2003). Furthermore, knockout of MKL1 in the brain caused morphological abnormalities and defects due to a failure of actin polymerization and dysfunctional cytoskeletal organization resulting in impaired neuronal migration (Mokalled MH., Johnson A. et al, 2010). The importance of the partnership between MKL1 and SRF is illustrated by the fact that SRF by itself is considered a rather weak transcriptional factor not unfolding its full transcriptional diversity in before MKL1 binding (Spiegelman BM., Heinrich R., 2004).

SRF belongs to the MADS-box family of transcription factors, named after the founding members MCM1, Agamous, Deficiens and SRF. As a unique characteristic, all members of the MADS-box family share the presence of a DNA binding domain (Pellegrini L., Tan S. et al, 1995), mediating SRFs large variety of biological effects. Examining its evolution, the importance of this sequence for SRF clarifies, reflected in a high degree of conservation in all eukaryotic kingdoms. SRF conveys gene expression via binding to this highly conserved sequence of nucleotides named serum response element (SRE) or CArG box (CC AT-rich GG) due to the conservation of the central A/T rich region and the flanking C-G base pairs (Pellegrini L., Tan S. et al, 1995). The CArG box is found within the promoters of known SRF target genes. SRF target genes involved in cell growth can often be distinguished from those involved in myogenesis by the degree of their CArG box binding. For example CArG-boxes in the promoters of several muscle genes differ more from the consensus sequence then those which are involved in cell growth, resulting in a reduction in SRF-binding affinity (Chang PS., Li L. et al, 2001).

Representable and fine described SRF targets are the connective tissue growth factor (*CTGF*) (Muehlich S., Cicha I. et al, 2007; Hinkel R., Trenkwalder T. et al., 2014), Integrin alpha-5 (*ITGA5*) (Muehlich S., Hampl V. et al, 2012) and Transgelin *(SM22)* (Olson E., Nordheim A., 2010). All three of them were frequently used in this work, showing prime examples for MKL1 activity.

CTGF belongs to the family of subset ECM proteins, known as matricellular proteins. Besides serving as a scaffold for arranging cells in tissue, the extracellular matrix (ECM) behaves as a multifunctional cellular regulator. ECM proteins are able to modulate the activity of extracellular signaling molecules such as growth factors or inflammatory cytokines. Matricellular proteins in particular serve primarily regulatory rather than structural roles. *CTGF* itself exercises important roles in lots of biological processes, for example cell adhesion, migration or proliferation but also tissue wound healing and injury repair, where its expression is highly increased (Chen C-C., Lau LF., et al, 2009). Deregulation of its expression or activity contributes to inflammation and mediation of metastasis to the bone in breast cancer, which makes it an interesting target for future therapeutic drug administration (Muehlich S., Cicha I. et al, 2007), while expression levels are low under physiological conditions. It also may enhance tumor growth through their potent angiogenic activity (Shimo T., Nakanishi T., et al, 2001). Accordingly, expression of *CTGF* in breast cancer cells enhances microvessel density of xenograft tumor in mice (Yin D., Chen W. et al, 2010). Consistently, xenograft tumor growth is inhibited by silencing CTGF expression in cancer cells of prostate and pancreas (Bennewith KL., Huang X., et al, 2009).

Integrins are transmembrane receptors that are bridges for cell-cell and cell-extracellular matrix (ECM) attachment. They are found in multiple tissues and cells and when triggered activate chemical pathways to the interior. This allows rapid and flexible response to events at the cell surface. Similar to *CTGF*, raised *ITGA5* levels take place in a multitude of disease patterns (Arosio D., Casagrande C. et al, 2012).

Transgelin *(SM22)* is an actin binding protein, which is plentifully expressed in smooth muscle cells (SMC) (Sayar N., Karahan G. et al, 2015). Smooth muscle can be found within the walls of blood vessels such as arteries and veins but also in the urinary bladder, uterus, gastrointestinal tract and in the iris of the eye. In contrast to skeletal and cardiac muscle, smooth muscle tissue tends to demonstrate higher elasticity. This ability to stretch and still maintain contractility is important to organs like the urinary bladder. It has been shown, that *SM22* is increased in gastric and colon cancer (Li N., Zhang J. et al, 2007; Lin Y., Buckhaults PJ. et al, 2009).

In summary SRF acts as a docking platform for diverse signal regulated and cell type specific cofactors triggering their distinct responses.

2.2.1 Serum Response factor (SRF): Two different pathways of activation

SRF stimulation is achieved via two parallel but independent signaling pathways that involve mitogen-activated protein (MAP) kinase/TCF on the one hand and Rho/actin dynamics on the other.

2.2.1.1 The ternary complex factor (TCF) dependent signaling pathway

First, stimulation with extracellular stimuli (serum, LPA, growth factors) leads to direct phosphorylation of the ternary complex factors (TCFs) by the three major groups of MAP kinase (Extracellular signal Regulated Kinase (ERK), c-Jun N-terminal Kinase (JNK) and p38) (Sotiropoulos A., Gineitis A. et al, 1999). Next, phosphorylated TCFs bind SRF to trigger the expression of target genes. The TCFs act as transcriptional co-activators and are composed of Elk-1, SAP-1 and Net which belong to the Ets group of transcription factors, one of the largest family of transcription factors (Sharrocks AD., 2001). Ets domain transcription factors recognize an Ets Binding Site (EBS) which flanks the CArG boxes and which is required for the ternary complex formation between TCFs and SRF (Treisman R., 1995).

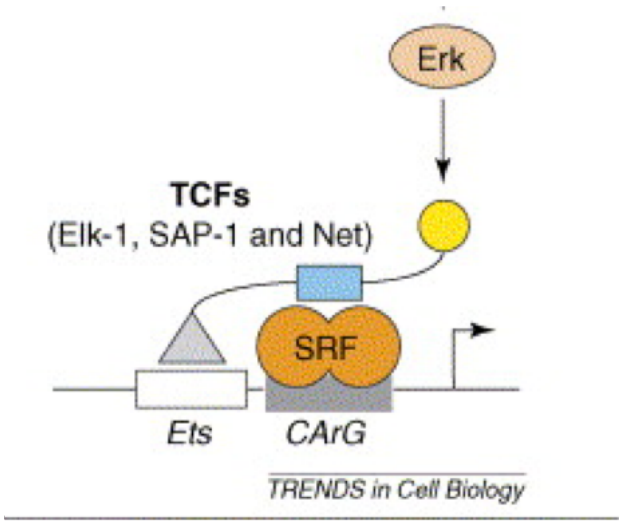

Figure 2: Model of SRF activity through TCF phosphorylation. Taken from Posern G., Treisman R., 2006

2.2.1.2 The Rho-actin signaling pathway and cytoskeleton actin dynamics

The second SRF activating pathway involves the small GTPase RhoA of the Rho family, which belongs to the Ras superfamily of GTP-binding proteins. Activation of growth factors as well as G-protein coupled receptors and integrins result in the activation of RhoA GTPase (Olson EN., Nordheim A. et al, 2010). A fundamental characteristic of RhoA is the capability of controlling actin assembly in response to extracellular signals (Vartiainen MK., Guettler S. et al, 2007). RhoA has been described to be involved in plenty of cellular processes such as cytoskeleton organization, gene transcription, cell migration and cell growth (Jaffe AB., Hall A., 2005). Rho/RhoA are able to act as a molecular switch by converting external indications to intracellular signaling pathways. This happens due to shuttling between an active, GTP-bound and an inactive, GDP-bound state. Rho/RhoA activation is promoted by GEF (guanine nucleotide exchange factor), which catalyzes the exchange of GDP to GTP (Jaffe AB., Hall A., 2005). On the other hand, GAP (GTPase activating protein) stimulates Rho GTPase activity to hydrolyze bound GTP. Thus, the activity of Rho GAP promotes the return of Rho GTPases in their inactive GDP bound state (Jaffe AB., Hall A., 2005).

First proof of a secondary, TCF-independent activation of SRF was recorded by the findings that mutation of the TCF-binding site within target gene promoters did not completely abolish the serum-induced activation of the promoter (Hill C., Wynne J. et al, 1994). Furthermore, SRF activation was blocked by Rho inhibition and activated upon microinjection of active RhoA (Hill C., Wynne J. et al, 1995). In 1999, Sotiropoulos A. et al. brought up cytoskeleton actin dynamics and linked it successfully to Rho/RhoA signaling. Actin is a highly conserved, 42kDa large structure protein, which is ubiquitary expressed in eukaryotic cells (Olson EN., Nordheim A. et al, 2010). Sotiropoulos et al showed that Rho/RhoA signaling leads to the accumulation of filamentous actin (F-actin) through both filament stabilization and de novo polymerization. This led to stimulation of the SRF signaling process. Combined with depletion of cellular monomeric G-actin levels, first evidence of direct influence of actin treadmilling to SRF activity was given, which was highlighted by Posern G. et al (2002), who indicated that overexpression of non-polymerizable actin mutants showed no success in activating SRF. In general, the actin circuit is subject to an ongoing process of polymerization and decay (Holmes KC., Popp D. et al, 1990). This sensitive cycle is controlled by the ATPase activity of actin in a crucial manner. ATP-bound

monomeric actins are getting linked to actin filaments, followed by ATP hydrolysis, while in contrast ADP-bound actins remain in their monomeric state.

In variation to cytoplasmic actin, which is investigated in great detail, mystery still remains about functions of nuclear actin. Recently it has been shown that nuclear and cytoplasmic actin pools are in dynamic communication (Dopie J., Skarp KP. et al, 2012). On the one hand Dopie J. et al used fluorescence loss in photobleaching (FLIP) to address nuclear actin export and showed that most GFP-actin is subject to rapid nuclear export, setting nuclear G-actin availability as a standard for export rate. On the other hand fluorescence recovery after photobleaching (FRAP) indicated a rapid G-actin import recovery phase followed by a slower phase corresponding to reincorporation of actin into stable nuclear complexes. In 2013, Baarlink C. et al expanded the current actin paradigm by presenting an new model in which the formin mDia, an effector of Rho GTPase does not only force cytoplasmic, but also nuclear actin polymerization in fibroblasts after serum stimulation (Baarlink C., Wang H., Grosse R., 2013). They further advanced to our knowledge by pointing out that nuclear-targeted mutants of mDia proteins inhibit MKL1 activation without affecting cytoplasmic F-actin. This way they suggested that MKL1 activation requires active nuclear actin polymerization rather then simple equilibration of cytoplasmic and nuclear actin pools. Taken together, recent findings support actin dynamics regulating SRF gene activity with comparable results regardless of whether positioned to the cytoplasm or nucleus.

Previously it has been shown that nuclear actin is also connected to virus infection, e.g. herpes simplex virus (HSV) (Roberts KL., Baines JD., 2011). Kokai E. et al (2013) further demonstrated that overexpression of nuclear wild-type actin reduced the percentage of HSV-infected cells. Under physiological conditions instead, actin levels are kept low in most cell types, thereby preventing nuclear F-actin generation. Cell stimulation with various stress factors including ATP depletion and neurodegenerative stimuli (Domazetovska A., Ilkovski B. et al, 2007) lead to F-actin polymerization favoring conditions and nuclear resident actin networks comparable to the ones in the cytoplasm.

2.2.1.3 SRF activating pathways in comparison: A competition for cell development

As it has been described in *2.2.1.1* and *2.2.1.2*, both the Rho-actin-MKL1 pathway and the TCF cascade lead to SRF activation and contact the same surface on SRF in an exclusive manner (Wang Z., Wang DZ. et al, 2004).

Growth promoting factors induce TCFs, which are able to dislocate MKL1 from SRF suggesting that TCF binding might block activation by these co-activators in a competitive manner (Wang Z., Wang DZ. et al, 2004). Consistent with that, mutation of the TCF site results in an increased activation rate by MKL1 (Wang Y., Falasca M. et al, 1998). Since TCF is activated by MAP kinase, this would allow growth signals to prefer TCF while differentiation signals could favor MKL1. Interestingly, in case of smooth muscle cells, the replacement of Myocardin (founding member of the MRTF/MKL1 family, also see *2.3*) with the TCF Elk1 results in an overall repression of transcription, since Myocardin is a much more potent transcription factor than Elk1 (Wang Z., Wang DZ. et al, 2004). Further investigations have shown that competition between Elk1 and Myocardin in smooth muscle cells can be characterized as switch among proliferation and differentiation upon extra cellular signals (Wang Z., Wang DZ. et al, 2004). In case of muscle cell proliferation the TCF cascade is active while the differentiation program controlled by Myocardin is off.

2.2.1.4 Rho in cancer development and the tumor suppressor DLC1

There is a rising evidence that deregulated Rho GTPase signaling contributes to cancer initiation, tumor progression and survival (Ahronian LG., Zhu LJ. et al, 2016; Kümper S., Mardakheh FK. et al, 2016). This can often be determined in overexpressed Rho protein levels (Sahai E., Marshall CJ., 2002). Besides pro migratory properties, increased Rho GTPase expression promoted the expression of pro-angiogenetic factors facilitating tumor vascularization (Turcotte S., Desrosiers RR. et al, 2003). This is key since tumor cells are not able to grow without the appropriate blood vessel support. In addition to constitutive activation of GEF, deletion of GAP is another mechanistic way to achieve Rho GTPase overexpression. One important group of Rho GAP proteins in tumorigenesis is the tumorsuppressor deleted in liver cancer (DLC1) protein family. Similar to other classical tumorsuppressors like p53, which prevent tumor progression, downregulation or deletion of DLC1 has been discovered in many human cancers including breast, lung and colon (Guan M., Zhou X. et al, 2006; Kim TY., Jong HS. et al, 2003; Seng TJ., Low JS. et al, 2007). Previously

to this thesis our group provided evidence that loss of DLC1 in hepatocellular carcinoma (HCC) leads to activation of RhoA combined with an increased amount of actin polymerization and MKL1 activation (Muehlich S., Hampl V. et al, 2011).

2.3 Myocardin-related transcription factors: A closer insight

Before identifying MKL1 (*2.1*), Wang et al marked a novel group of transcriptional co-activators called the family of myocardin-related transcription factors (MRTFs). The fact that the ubiquitously expressed SRF is required for the expression of muscle genes suggests that muscle-specific SRF cofactors contribute to the muscle specificity of SRF target genes. Myocardin, the founding member of this family was discovered in a bioinformatics screen for murine cardiac specific genes and is particularly expressed in cardiac and smooth muscle cells (Wang D., Chang PS. et al, 2001). In contrast, MKL1 and the third member of the family, MKL2 (MAL16, MRTF-B; Selvaraj A., Prywes R., 2003) are spread out more widely in the organism (Wang DZ., Li S. et al, 2002).

2.3.1 Myocardin-related transcription factors: Structure

The myocardin family proteins share a high degree of similarity in multiple regions. The conserved N-terminus contains three RPEL motifs (Arg-Pro-X-X-X-Glu-Leu), which represent a novel binding structure for monomeric G-actin thus maintaining MKL1 in the cytoplasm in un-stimulated cells (Miralles F., Posern G. et al, 2003; Posern G., Miralles F., et al, 2004). It has been predicted that binding of the RPEL motif to G-actin occurs competitively with binding to the major G-actin-binding-proteins profilin and thymosin ß4, as well as with assembly of F-actin (Dominguez R., 2004; Posern G., Miralles F., et al, 2004). Profilin-G-actin complexes are introduced into growing actin polymers by formins, this way profilin performs a role of monomeric actin recruiting in the act of polymerization (Carlsson L., Nyström LE. et al, 1977). Binding of G-actin to thymosin ß4 opposes this procedure by sequestering G-actin.

Mouilleron S. et al. unveiled two crystal forms of the RPEL-actin domain complex (2011). In a pentavalent actin-RPEL domain assembly, each of the three RPEL motif engages an actin (RPEL-actins, R1, R2, R3) and additionally two more actins are bound via RPEL2 and RPEL3 at their N-terminal extensions (spacer-actins, S1, S2) while the trivalent complex in contrast

only contains two RPEL- and one spacer-actin (R1-S1-R2). Moreover it has been shown that RPEL3 (R3) has the lowest actin-binding affinity of the three RPEL motifs, which leads to the conclusion of a more stable trimeric complex compared with the pentavalent one (Mouilleron S., Langer C. et al, 2011). To highlight the important role of spacer-actins for MKL1 localization, disruptions of both actin S1 and S2 contacts by introducing mutations in spacer1 and spacer2, resulted in effectively complete nuclear accumulation of MKL1 in un-stimulated cells (Mouilleron S., Langer C. et al, 2011). In contrast, myocardin is exclusively localized to the nucleus, which is likely due to sequence divergence of its RPEL domains and consequent inability to bind monomeric actin (Miralles F., Posern G. et al, 2003).

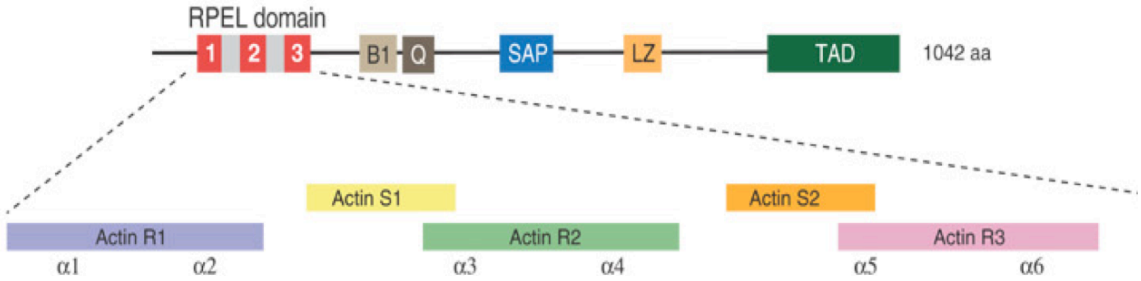

Figure 3: Model of the RPEL domain and binding to actin as a tri- or pentavalent complex (Actin R1,R2,R3 = RPEL-actins, Actin S1,S2 = Spacer-actins). Taken from Mouilleron S., Langer C. et al, 2011

Association of MKL1 and its family members with SRF takes place through a basic region and a glutamin-rich domain (Wang D., Chang PS. et al, 2001; Cen B., Selvaraj A. et al, 2003). Another important domain of the myocardin family is illustrated by a 35-amioacid long SAP domain, named after SAF-A, Acinus and Pias. Its main functions lies in DNA-binding and apoptosis (Aravind L., Koonin EV. et al, 2000). SAP deletion mutants showed to be defective in simulating SRF activity on some promoters, which suggests a certain role of the SAP domain regarding promoter specificity (Wang D., Chang PS. et al, 2001). Homo- and heterodimerization of MKL1 is mediated by a leucine zipper (Wang D., Chang PS. et al, 2001) and the C-terminal TAD domain is responsable for activiation of transcriptional activity (Cen B., Selvaraj A. et al, 2003).

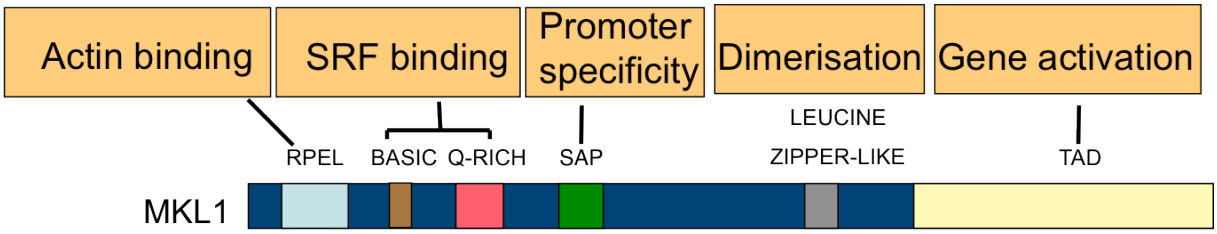

Figure 4: Model of MKL1 and its consisting domains

2.3.2 Myocardin-related transcription factors: Subcellular localization

Following the findings of Sotiropoulos A. et al. that cytoskeleton actin dynamics are linked to Rho signaling (1999), Miralles F. et al indicated a complex of MKL1 and actin (2003). Simultaneously, serum has been assigned to be the cause for translocation of MKL1 from the cytoplasm to the nucleus in NIH3T3 fibroblasts (Miralles F., Posern G. et al, 2003). As already mentioned in *2.2.1.2,* these results are further supporting thoughts that G-actin binding maintains MKL1 in the cytoplasm. Consistent with that, depletion of G-actin and polymerization into F-actin leads to a release of MKL1 from the inhibitory complex and translocation in the nucleus followed by SRF activation.

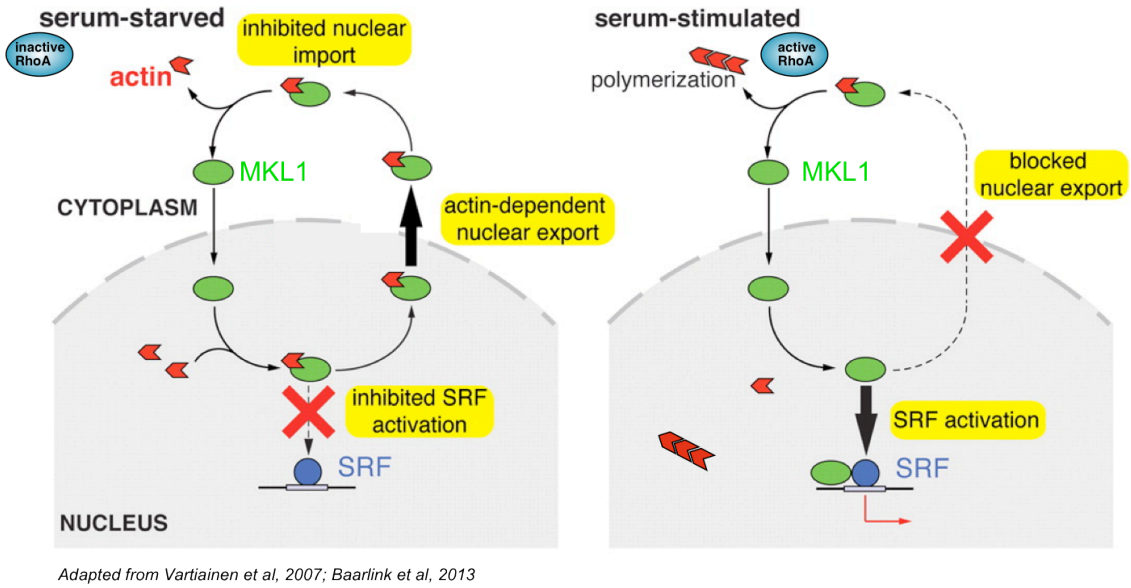

Adapted from Vartiainen et al, 2007; Baarlink et al, 2013

Figure 5: Model of the multiple roles for actin in MKL1 regulation. (Right) Upon stimulation through RhoA and serum, decreased export includes nuclear MKL1 accumulation and abolished interaction with monomeric G-actin, which allows SRF activation. (Left) Serum starved conditions lead to increased nuclear MKL1 export and elevated levels of MKL1-G-actin association. Taken from Vartiainen M., Guettler S. et al, 2007.

In biochemistry the reversible process of phosphorylation, governed by kinases, and the resulting phospho-proteins are one of cells most important regulatory actions. Due to its charge and polarity, phosphorylation leads to a change in protein conformation, resulting in two different possible catalytic-reactive protein forms. Thus, a protein can be either activated or inactivated by phosphorylation. Phosphorylation only occurs at the side chains of three amino acids, named serine, threonine and tyrosine. In a mechanistic way the amino acids nucleophilic –OH group attacks the terminal phosphate group of the universal donor ATP, resulting in a transfer of the phosphate group to the amino acid side chain. Many transcription factors like SRF or G-protein coupled receptors are activated this way *(2.2.1.1)*. Today, it is estimated that 1/10 to ½ of all available proteins are phosphorylated in some cellular state (Cohen AW., Park DS. et al, 2002). Therefore, understanding the state of phosphorylation is essential for judging on cell status, especially regarding abnormal phosphorylation and connected diseases.

Besides nuclear MKL1 translocation, serum stimulation also leads to extracellular signal-regulated kinase 1/2 (ERK1/2) dependent phosphorylation of MKL1 at serine 454 (Muehlich S., Wang R. et al, 2008), also visible in a MKL1 mobility shift in SDS-Page. Nuclear MKL1 export is facilitated by MKL1 phosphorylation through provoking MKL1-G-actin binding, thereby working as a switch-off for MKL1/SRF signaling, correlating well with target gene repression. Furthermore a non-phosphoryable MKL1 mutant showed a constant nuclear localization (Muehlich S., Wang R. et al, 2008). One expects that the nuclear export rate is the determining factor for the subcellular localization of MKL1 (Vartiainen MK., Guettler S. et al, 2007) and that the phosphorylation this way is likely terminating induction of MKL1 target genes. This portrayed mechanism of nuclear-cytoplasmic shuttling of MKL1 is well established for fibroblasts and muscle cells.

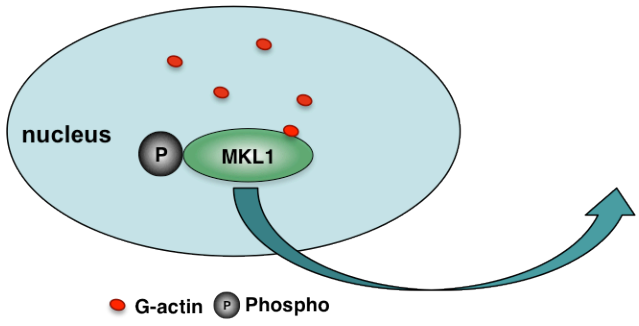

Figure 6: Model of nuclear MKL1 export, initiated by a combination of MKL1 phosphorylation and G-actin binding.

2.4 Filamin A: Rising of a new MKL1 interaction partner

2.4.1 The cytoskeleton: A cell stabilizer and more

A complex network of protein fibers in eukaryotic cells, the cytoskeleton provides rigid structural support that is responsible for maintaining cell shape and stability. Paradoxically, this rigid network is also highly active and dynamic, providing cells with plasticity and the ability to respond to stimuli from the surrounding environment. Besides its effects on cell firmness the cytoskeleton is crucial for maintaining regular cell activity, including cellular motion and intracellular transport (Yue J., Huhn S. et al, 2013). Eukaryotic cells contain three major components: microfilaments, intermediate filaments and microtubules. Microfilaments (actin filaments or F-actin) are composed of linear polymers of actin that form the thinnest filaments of the cytoskeleton. A unique feature of microfilaments is the dynamic interaction with each other (elongation and shrinkage), which generates force and causes movement (Galkin VE., Orlova A. et al, 2012). They also act as tracks for the motion of myosin molecules that attach to the microfilaments and head along, thereby once more generating force and contributing to cell locomotion via forming of actin rich focal cell adhesions (Dominguez R., Holmes KC, 2011). In addition to linear formation, microfilaments are also able to cross-link into 3D bundles (Cunningham CC., Vegners R. et al, 2001), which is essential for dynamic remodeling of the cytoskeleton. This cross-linking process is orchestrated by actin-binding-proteins (ABP) which typically share a conserved F-actin binding domain (ABD) (Van Troys M., Vandekerckhove J., 1999). In summary mechanical properties of cells are generated by the combined interactions of the cytoskeletal elements.

2.4.2 The family of the filamins: Structure

One important group of the actin binding proteins is the filamin family, which has been discovered in 1975 as the first non-muscle actin filament crosslinking protein. The family consists of three homologous proteins (FLNA, FLNB, FLNC) of which Filamin A (FLNA, human actin-binding protein 280, filamin 1) is the most abundant one and its structure today is discovered in great detail. The protein is a homodimer with two large subunits of high molecular weight (280 kDa), which form a V-shaped structure (van der Flier A., Sonnenberg A., 2001). It consists of 2467 amino acids, including an actin binding domain located at the amino terminus of each monomer, followed by 24 tandem repeats of 96 amino acids. A first hinge region (H1) is located between repeat 15 and 16 and a second one (H2) is situated between repeat 23 and 24. Both add much needed flexibility to the framework. Repeats 1 to 15 are named Rod1, while repeats 16 to 23 are called Rod2. Dimerization and V-shape structure is mediated by the C terminus of repeat 24 (Gorlin JB., Yamin R. et al, 1990). Interestingly besides the 280 kDa full-length Filamin A, the relative hinge regions represent cleavage sites for the calcium dependent protease calpain that leads to two shortened variations: A 170 kDa fragment composed of the actin binding domain plus the first 15 repeats and a second 110 kDa fragment consistent of the repeats 16 to 24 (O'Connell MP., Fiori JL. et al, 2009).

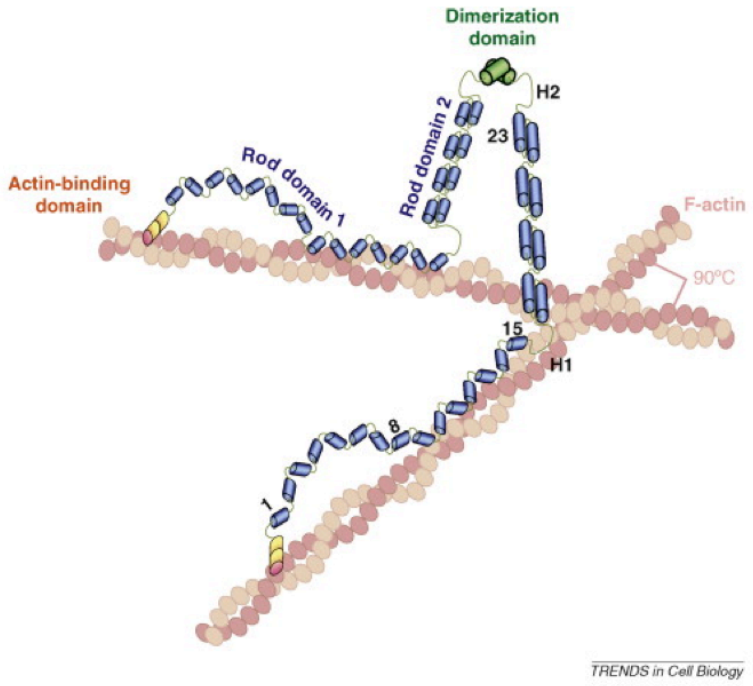

Figure 7: Model of FLNA (blue) association with F-actin (red). Taken from Zhou A., Hartwig J. et al, 2010.

2.4.3 The family of the filamins: Broad variety of functions

One look at bushes and trees is enough to state how branched scaffoldings can produce a tremendous variety of shapes. A fundamental role of FLNA, attributed to its unique structure, is binding and cross-linking actin filaments into a dynamic three-dimensional structure through its actin-binding domain, adding flexibility or stiffness if needed, for example in case of shear stress or hydrostatic pressure (Gardel MK., Nakamura F. et al, 2006). Zhou A. et al (2010) indicated that actin stabilization takes place in an orthogonal structure (Fig. 7), which makes it possible to combine a maximum number of actin filaments with a modest investment of energy.

Cell adhesion and migration heavily rely on active and even more important reversible changes in the mechanical properties of the cell. Besides providing cell stability, FLNA adds to the ability of the cell to become mobile, which features formation of filopodia and lamellipodia. These slender cytoplasmic projections, composed of cross-linked actin bundles by FLNA, extend beyond the leading edge in migrating cells. Elements which spread beyond the lamellipodium frontier are called filopodia (Small JV., Stradal T. et al, 2002). Many types of migrating cells display filopodia, which are thought to be involved in sensing, conveying changes in direct locomotion and cell-cell interaction (Nakamura F., Stossel T. et al, 2011). FLNA knockdown results in inhibition of these formations and depletes cell migration in a drastic manner (Kim H., Nakamura F. et al, 2010). Furthermore for wound closure, growth factors stimulate the formation of filopodia in fibroblasts and they also have been linked to dendrite creation when new synapses are formed in the brain and phagocytosis where filopodia act as phagocytic tentacles, pulling bound objects towards the cell for phagocytosis (Kress H., Stelzer EH. et al, 2007). On the other hand, filopodia are also used for movement of bacteria and viruses between cells to evade the host immune system (Lehmann MJ., Sherer NM. et al, 2005).

The human interactome embraces a network of an estimated number of 650000 molecular interactions of which just about 0.3% are yet discovered (Stumpf MP., Kelly WP. et al, 2007, Amaral LA, 2008) and what today stands more and more as a benchmark for complexity of the human organism. FLNA interacts and serves as a scaffold for a large variety of more than 90 functionally diverse cellular proteins like ion channels, receptors and signaling molecules which implies that FLNA is a key component of a versatile signaling complex (Stossel T.,

Condeelis J. et al, 2001; Feng Y., Walsh C., 2004). FLNA also has a direct influence on transfection via interaction with an androgen receptor (Loy CJ., Sim K. et al, 2003; Ozanne D., Brady M. et al, 2000), the tumor suppressor BRCA1/2 (Yuan Y., Shen Z., 2001), the transcription factor FOXC1 (Berry F., O'Neill M. et al, 2005) and SMAD-protein (Sasaki A., Masuda Y. et al, 2001). This way, gene expression is not only regulated by keeping transcription factors in a certain area, but also via direct interaction with FLNA. This is highly important regarding the background of this thesis and the examined MKL1-FLNA interaction. In contrast to FLNB and FLNC, Filamin A is widely expressed and its drastic importance for cell function can easily be seen in a loss of cell locomotion and the occurrence of blebbing (loss of mechanic cell stabilization due to the absence of FLNA and cell damage caused by hydrostatic cell pressure) in FLNA deficient M2 melanoma cells (Cunningham CC., Gorlin JB. et al, 1992; Nakamura F., Stossel T. et al, 2001). In summary, FLNA is positioned at both the leading edge and the rear part of the cell, orchestrating the engineering of the cytoskeleton, migration and interacting with partner proteins, thus representing an extraordinary example of multi-functionality in cell biology.

2.4.4 The family of the filamins: Pathogenesis and tumorigenesis

Genetic evidence links FLNA as an essential protein for human development. According to its versatile functions, mutations and deletions in the human FLNA genes result in a wide spectrum of cell anomalies and development malformations with often lethal consequences. Most of FLNA deficient, genetic diseases are based on disruption of cell motility and signaling, this way affecting organogenesis. Since directed cell movement is essential for embryonic development, aberrant unregulated migration leads to pathological processes (Feng Y., Chen MH. et al, 2006).

The first disease linked to FLNA mutations is the brain malformation known as periventricular heterotopia. A typical periventricular heterotopia brain is characterized by an abnormal appearance of collections of neurons along walls of the lateral ventricle, where neurons are originally generated during corticogenesis, instead of migrating to the correct cortical site (Fox JW., Lamperti ED. et al, 1998). The major clinical syndrome of periventricular heterotopia is late-onset epilepsy that often starts in the second decade of life.

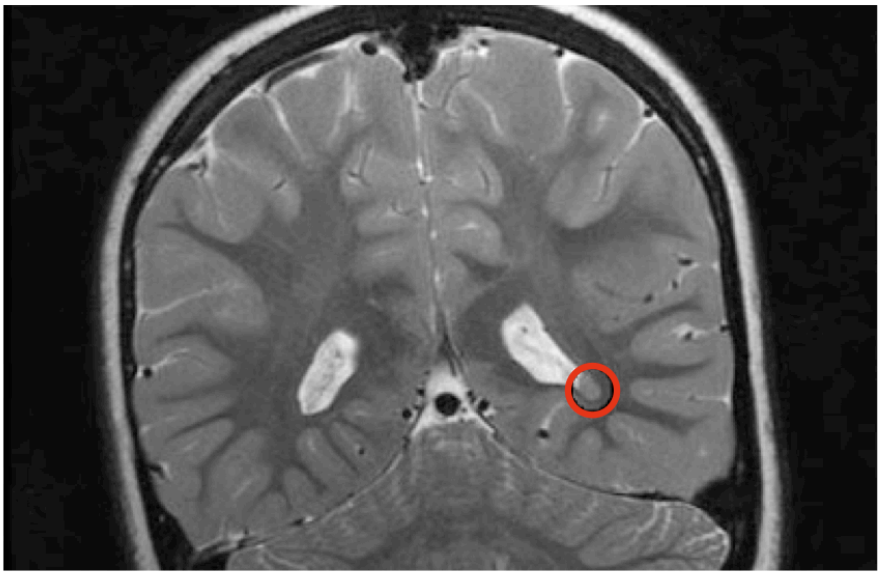

Figure 8: Periventicular heterotopia. Deregulated neuron migration leads to mal-localization as seen in red circle. Taken from Gonzalez G., Vedolin L. et al, 2012

Loss of FLNA expression in mice causes embryonic lethality with severe defects in cardiovascular formation and bone development. FLNA deficient M2 melanoma cells fail to move because they have highly unstable surfaces, while restoring regular levels of FLNA rescues motility. Furthermore, FLNA restored A7 melanoma cells showcased a need of more than twice the amount of shear stress to achieve a given deformation then the FLNA depleted M2 cells (Cunningham CC., Gorlin JB. et al, 1992).

Cancer has been described as the product of development error leading to the acquisition of a unique cell character (da Costa LF., 2001). It is a multistep process that transforms a normal cell into one that evades apoptosis, grows irrepressibly, promotes angiogenesis to support the tumor and finally invades surrounding tissue and metastasizes (Hanahan D., Weinberg RA., 2000). Tracing has shown that stem cells are mobilized to repair skin wounds and that this process may contribute to skin tumor development (Arwert EN., Hoste E. et al, 2012). In many cases cancer can be thought of as continued and unwanted regeneration that does not know how to stop resulting in overexpression of certain key proteins. FLNA's function as a scaffolding protein and its vital importance in cell migration can transform it into an extremely potent cancer promoting protein. FLNA has been observed being overexpressed in multiple types of cancer, including prostate (Bedolla RG., Wang Y. et al, 2009), breast (Tian HM., Liu XH. et al, 2013), lung cancer (Uramoto H., Akyürek LM. et al, 2010), colon cancer (Larriba MJ., Martin-Villar E. et al, 2009), melanoma (Flanagan LA., Chou J. et al, 2001) and neuroblastoma (Bachmann AS., Howard JP. et al, 2006). Although this large volume of studies linking FLNA with cancer metastasis, the specific roles of FLNA during metastatic invasion remains elusive. This enigma is a reflection of metastasis complex nature. Metastasis, or leaving the primary tumor for invasion into other tissue parts, requires a strict cascade of locomotion events, including tumor cell detachment from the primary site, followed by tumor cell invasion, migration and colonization at the secondary sites (Arwert EN., Hoste E. et al, 2012). Metastasis requires the cancer cells to be able to adept to different cell shapes, resist to mechanical stress and to be highly motile (Yue J., Huhn S. et al, 2013). A great amount of these key processes are driven by FLNA as described in *2.4.3*. Thus, it is conceivable that lack of FLNA would decrease the tumor cells ability regarding mobility and invasiveness and furthermore cause them to be more sensitive to mechanical stress (Yue J., Huhn S. et al, 2013). This demonstrates the irreparable role of

FLNA in tumorigenesis and its medical relevance during the process of developing malfunctions.

3 Aim of thesis

Previously to this thesis, Filamin A has been identified as a novel interaction partner of MKL1 via yeast two-hybrid assay by Dr. S. Muehlich (Kircher P., Hermanns C. et al, 2015).

This thesis covers the interaction of MKL1 and FLNA and takes a detailed look at functionality behind the complex formation.

In particular the thesis addresses the following issues:

1. Confirming the interaction between MKL1 and FLNA in physiological and pathophysiological cell systems and furthermore map the necessary interacting domains on the respective protein.
2. Stating the cell compartment in which the MKL1-FLNA interaction takes place.
3. Correlating the MKL1-FLNA interaction with induction and repression of MKL1-SRF target genes.
4. Introducing FLNA as a transducer of actin polymerization into SRF activity.
5. Presenting the MKL1-FLNA interaction as a requirement for MKL1-dependant cell migration, invasion and expression of MKL1 target genes.

Since MKL1 and FLNA are both involved in diseases and cancer development, mainly regarding migratory processes like tumor motility, proliferation and metastasis, gaining new insights into functional effects of the interaction are of great value for future drug development including MKL1 and FLNA as possible pharmacological targets.

4 Materials

4.1 Cell culture

4.1.1 Cell lines

Cell line	Organism/ Cell Type	Culture conditions	Provider/ Origin
A7	Human melanoma	MEM	Stossel TP., ATCC #CRL-2500, Boston
M2	Human FLNA-deficient melanoma	MEM	Stossel TP., Ohta Y., Boston
HuH7	Human hepatocellular carcinoma	DMEM	Singer S., Heidelberg
MDA-MB-468	Human breast carcinoma	DMEM	Parsons R., New York
NIH-3T3	Mouse embryonic fibroblasts	DMEM	Muehlich S., München
MEF	Mouse primary embryoic fibroblasts	DMEM	Sarikas A., München
HDFA	Human primary fibroblasts	Medium 106	Life Technologies, Darmstadt
MACS	Mouse neuronal cells	DMEM	Breit A., München
HEK-293	Human embryonic kidney cells	DMEM	Muehlich S., München

HLF	Human lung fibroblasts	DMEM	Muehlich S., München
HepG2	Human hepatoma	RPMI	Singer S., Heidelberg

4.1.2 Cell culture media and solutions

Reagent	Provider
Modified Eagle Medium (MEM)	Sigma-Aldrich, Taufkirchen, Germany
Dulbecco`s Modified Eagle Medium (DMEM)	Sigma-Aldrich, Taufkirchen, Germany
RPMI 1640 Medium	Sigma-Aldrich, Taufkirchen, Germany
Medium 106	Life Technologies, Darmstadt, Germany
Opi-MEM®	Gibco® Invitrogen, Karlsruhe, Germany
Fetal Bovine Serum (FBS)	Gibco® Invitrogen, Karlsruhe, Germany
Penicillin-Streptomycin (5000 U/mL)	Gibco® Invitrogen, Karlsruhe, Germany

4.1.3 Transfection reagents

Reagent	Provider
Lipofectamine® 2000	Invitrogen, Karlsruhe
Lipofectamine® RNAiMAX	Invitrogen, Karlsruhe
2 M Calcium-Phosphat	selfmade
GenJet™DNA In Vitro Transfection Reagent	SignaGen Laboratories, Rochville, USA

4.1.4 Plasmid constructs

Plasmid construct	Vector	Provider
Wildtype FLAG-MKL1	pCMV	Prywes R., Columbia University, NY, USA
Wildtype MYC-FLNA	pCDNA3	Blenis J., Harvard Medical School, MA, USA
Wildtype FLAG-MKL2	pCMV	Prywes R., Columbia University, NY, USA
Wildtype MYC-Myocardin	pCDNA3	Prywes R., Columbia University, NY, USA
GFP-Actin	peGFP	Sheetz M., Columbia University, NY, USA
FLAG-MKL1 mutant N100	pCMV	Prywes R., Columbia University, NY, USA
FLAG-MKL1 mutant N300	pCMV	Prywes R., Columbia University, NY, USA
FLAG-MKL1 mutant C500	pCMV	Prywes R., Columbia University, NY, USA
FLAG-MKL1 mutant C630	pCMV	Prywes R., Columbia University, NY, USA
FLAG-MKL1 mutant C830	pCMV	Prywes R., Columbia University, NY, USA
FLAG-MKL1 mutant Δ301-380	pCMV	Prywes R., Columbia University, NY, USA

FLAG-MKL1 mutant Δ381-506	pCMV	Prywes R., Columbia University, NY, USA
FLAG-MKL1 mutant Δ301-342	pCMV	Kircher P., LMU, München
FLAG-MKL1 mutant Δ321-342	pCMV	Kircher P., LMU, München
FLAG-MKL1 mutant Δ301-310	pCMV	Kircher P., LMU, München
FLAG-MKL1 mutant Δ305	pCMV	Kircher P., LMU, München
FLAG-MKL1 mutant Δ312	pCMV	Kircher P., LMU, München
FLAG-MKL1 mutant ΔSAP	pCMV	Prywes R., Columbia University, NY, USA
FLAG-STS/A mutant MKL1	pCMV	Prywes R., Columbia University, NY, USA
MYC-FLNA mutant 1-275	pCI-HA	Berry F., University of Alberta, Edmonton, CA
MYC-FLNA mutant 276-570	pCI-HA	Berry F., University of Alberta, Edmonton, CA
MYC-FLNA mutant 571-866	pCI-HA	Berry F., University of Alberta, Edmonton, CA
MYC-FLNA mutant 1155-1442	pCI-HA	Berry F. , University of Alberta, Edmonton, CA
MYC-FLNA mutant 1779-2284	pCI-HA	Berry F., University of Alberta, Edmonton, CA
MYC-FLNA mutant 2285-2729	pCI-HA	Berry F., University of Alberta, Edmonton, CA
R62D-FLAG-Actin	pEF	Posern G., Martin Luther University, Halle, Germany
NLS-R62D-FLAG-Actin	pEF	Posern G., Martin Luther

		University, Halle, Germany
S14C-FLAG-Actin	pEF	Posern G., Martin Luther University, Halle, Germany
GFP-MKL1	peGFP	Prywes R., Columbia University, NY, USA
mDiaNES	pEF	Posern G., Martin Luther University, Halle, Germany
mDiact	pEF	Posern G., Martin Luther University, Halle, Germany
Empty Vector	peGFP	Prywes R., Columbia University, NY, USA
5 x SRE	pCMV	Prywes R., Columbia University, NY, USA
Renilla Luciferase SV40	pSV	Prywes R., Columbia University, NY, USA

4.1.5 siRNA sequences

All siRNA oligonucleotides were custom synthesized by Sigma-Aldrich, Taufkirchen, Germany.

Lyophilized siRNA oligonucletodides were dissolved in water to a concentration of 50 µM and stored in aliquotes at -20˚C.

Target	**Sequence [5`-3`]**
siRNA Neg. ctrl	CGU ACG CGG AAU ACU UCG A [dT] [dT]

siFLNA	AAA AUG CAC CGC AAG CAC AAC [dT] [dT]
siMKL1	GAA UGU GCU ACA GUU GAAA [dT] [dT]
siSRF	GAU GGA GUU CAU CGA CAA CAA [dT] [dT]

4.1.6 Selection antibiotic for cell culture

Antibiotic	Stock solution	Final concentration	Provider
Geneticin (G418 Sulfate)	50 mg/mL	200 µg/mL	Carl Roth, Karlsruhe, Germany

4.1.7 Inhibitors and stimulants

Inhibitor/Stimulant	Final concentration	Provider
Lysophosphatidic acid(LPA)	10 µM	Sigma-Aldrich, Taufkirchen, Germany
Latrunculin B (LatB)	0.3 µM	Merck, Darmstadt, Germany
Jasplakinolide	0.5 µM	CalBiochem, Darmstadt, Germany
Calpain Inhibitor III	1 µM, 10 µM	AppliChem, Darmstadt, Germany

4.2 Antibodies

4.2.1 Primary antibodies

All antibodies were diluted in TBS-T and conserved with BSA and 10 % NaN_3

Primary antibody	Dilution	Provider
Alexa Fluor® Phalloidin	1:500	Invitrogen, Karlsruhe, Germany
FLAG M2 (mouse monoclonal)	1:500	Sigma-Aldrich, Taufkirchen, Germany
FLNA (human)	1:1000	Abcam, Cambridge, UK
FLNA MAB 1678 (human)	1:1000 1:100 in PBS (IF)	Chemicon Millipore, Schwalbach, Germany
FLNA (rabbit)	1:1000	Cell Signaling Technology, USA
GFP (FL) (human)	1:200	Santa Cruz Biotechnology, CA, USA
HA (3F10) (goat monoclonal)	1:500	Roche Applied Science, Germany
HSP90 (mouse monoclonal)	1:500	Santa Cruz Biotechnology, CA, USA
MKL1 (rabbit)	1:500	Muehlich S., Munich, Germany
MRTF-A (C19) (goat polyclonal)	1:100 in PBS (IF)	Santa Cruz Biotechnology, CA, USA
P-MKL1	1:250	Muehlich S., Munich, Germany

4.2.2 Secondary antibodies

Secondary antibody	Target	Dilution	Provider
Alexa Fluor®488	Mouse	1:1000	Invitrogen, Karlsruhe
Alexa Fluor®488	Rabbit	1:1000	Invitrogen, Karlsruhe
Alexa Fluor®555	Goat	1:1000	Invitrogen, Karlsruhe
Anti-rabbit IgG HRP-conj	Rabbit	1:10000	Cell Signaling Technology, USA
Anti-mouse IgG HRP-conj	Mouse	1:10000	Cell Signaling Technology, USA
Anti-goat IgG HRP-conj	Goat	1:50000	Santa Cruz Biotechnology, CA, USA

4.3 Nucleotides

4.3.1 Random Hexamers

Nucleotide	Sequence [5`-3`]	Provider
Random Hexamers (0.02 µM)	NNN NNN	Metabion International AG, Martinsried, Germany

4.3.2 Real-time PCR primers

Target gene specific primers were designed with the software Universal Probe Library from Roche. Custom-synthesized primers were purchased by Metabion International AG, Martinsried, Germany. The real-time PCR primers were diluted to a concentration of 100 µM and stored at -20˚C.

h=human; F=forward; R=reverse

Name	**Sequence [5`-3`]**
h18s rRNA F	TCG AGG CCC TGT AAT TGG AAT
h18s rRNA R	CCC TCC AAT GGA TCC TCG TTA
hCNN1 F	GCT GTC AGC CGA GGT TAA GA
hCNN1 R	CCC TCG ATC CAC TCT CTC AG
hCTGF F	TTG GCA GGC TGA TTT CTA GG
hCTGF R	GGT GCA AAC ATG TAA CTT TTG G
hFLNA F	TCG CTC TCA GGA ACA GCA
hFLNA R	TTA ATT AAA GTC GCA GGC ACC TA
hGLIPR1 F	TCT TTC CAA TGG AGC ACA TTT
hGLIPR1 R	TCT TAT ATG GCC AAG TTG GGT AA
hITGA5 F	TGC AGT GTG AGG CTG TGT ACA
hITGA5 R	GTG GCC ACC TGA CGC TCT
hMKL1 F	CCC AAT TTG CCT CCA CTT AG
hMKL1 R	CCT TGG CTC ACC AGT TCT TC
hSM22 F	GGC CAA GGC TCT ACT GTC TG

hSM22 R	CCC TTG TTG GCC ATG TCT
hTGF-beta F	TCT TTC CAA TGG AGC ACA TTT
hTGF-beta R	TCT TAT ATG GCC AAG TTG GGT AA
hFHL2 F	GCT GTC AGC CGA GGT TAA GA
hFHL2 R	CCC TCG ATC CAC TCT CTC AG
hSRF F	AGC ACA GAC CTC ACG CAG A
hSRF R	GTT GTG GGC ACG GAT GAC

4.4 Bacterial strains and media

Bacterial strain	**Provider**
E.coli DH5α	Takara BIO

LB agar
1% sodium chloride
1% bacto tryptone
0.5% yeast extract
1.5% bacto agar

LB liquid medium
1% sodium chloride
0.5% yeast extract
1% bacto tryptone
Adjustment to pH 7.5 with 10 N NaOH

4.5 Kits

Reagent	**Provider**
Q5® Site-Directed Mutagenesis Kit	New England Biolabs, MA, USA
GenElute™ HP Plasmid Midiprep Kit	Sigma-Aldrich, Taufkirchen, Germany
Dual Luciferase® Reporter Assay System	Promega, Mannheim, Germany

4.6 Reagents

Reagent	Provider
Protease Inhibitor, Cocktail Set III, Animal Free	Calbiochem, Darmstadt, Germany

Spectra™ Multicolor Broad Range Protein Ladder	Fermentas, St. Leon-Rot, Germany
Rec-Protein G-Sepharose® 4B conjugate	Invitrogen, Karlsruhe, Germany
Roti ®-Quant	Carl Roth, Karlsruhe, Germany
Roti ®-Lumin 1; Roti ®-Lumin2	Carl Roth, Karlsruhe, Germany
Super Signal West Femto Trialkit (Enhancer peroxide solution)	Thermo Scientific, Schwerte, Germany
Trizol® LS Reagent	Invitrogen, Karlsruhe, Germany

4.7 Enzymes

Reagent	**Provider**
SuperScript II Reverse Transcriptase	Invitrogen, Karlsruhe, Germany
RNaseA	Fermentas, St. Leon-Rot, Germany
Trypsin-EDTA 0.05 %	Sigma-Aldrich, Taufkirchen, Germany

4.8 Buffers and solutions

4.8.1 cDNA synthesis/ RT-PCR

Reagent	Provider
5 x First-Strand Buffer	Invitrogen, Karlsruhe, Germany
dNTPs (10 mM)	Invitrogen, Karlsruhe, Germany
LightCycler® 480 SYBR Green I Master	Roche, Penzberg, Germany

4.8.2 Protein analysis

2.5 M $CaCl_2$ solution

87.6 g $CaCl_2$*$6H_2O$ ad 200 mL destilled water, sterilfiltration

2xHBS

8.0 g NaCl

0.2 g Na_2HPO_4*7 H_2O

6.5 g HEPES

Adjustment of pH to 7.0

Ad 500 mL destilled water

Kralewski cell lysis buffer

50 mM HEPES (pH 7.4)

150 mM NaCl

1 % Triton X-100

1 mM EDTA

10 % Glycerol

4x SDS loading/Laemmli Sample Buffer (4xLSB)

1 M TRIS/HCL (pH 8.8)

0.01 % (w/v) Bromphenolblau

20 % (w/v) SDS

2 % (v/v) Glycerol

0.5 M EDTA

5 % (v/v) ß-Mercaptoethanol

10 x PBS pH 7.4

140 mM NaCl

2.7 mM KCl

10 mM Na_2HPO_4

1.8 mM KH_2PO_4

10 x Gel running buffer (pH 8.3)

0.25 M TRIS

2 M Glycin

1 % (w/v) SDS

H_2O ad 1000 mL

10 x TBS

0.2 M TRIS

1.4 M NaCl

H_2O ad 5000 mL

10 x TBST

0.2 M TRIS

1.4 M NaCl

1 % Tween 20

H_2O ad 5000 mL

10 x Blotting buffer

7.25 g TRIS

3.65 g Glycine

0.47 g SDS

200 mL Methanol

H_2O ad 1000 mL

1.5 M TRIS (pH 6.8)

121.1 g TRIS

Adjustment of pH with 1 N HCL to 6.8

H_2O ad 1000 mL

1.5 M TRIS (pH 8.8)

121.1 g TRIS

Adjustment of pH with 1 N HCL to 8.8

H_2O ad 1000 mL

1 % Triton IP Lysisbuffer

50 mM Tris

150 mM NaCl

1 % Triton X-100

10 % Glycerol

Add before usage: 0.2 % PMSF, protease inhibitor cocktail

Enhanced Chemiluminescence solution (ECL) S1 and S2

S1 solution

80 mL H_2O

10 mL 1 M TRIS/HCL pH 8.5

1 mL 250 mM 3-Aminophtalhydrazide

0.44 mL 90 mM p-Coumaric acid

H_2O ad 100 mL

S2 solution

80 mL H_2O

10 mL 1 M TRIS/ HCl pH 8.5

60 µL 30% H_2O_2

H_2O ad 100 mL

Both solutions were stored at -20˚C an thawed prior to use. Both solutions were mixed at a ratio of 1:1 to yield the ready-to-use assay solution.

1 % Toluidine staining solution
0.1 g toluidine blue dye
0.1 g Sodium tetraborate decahydrate
Dissolved in 100 mL destilled water

4.9 Chemicals

Chemicals	**Provider**
2-Propanol	Carl Roth, Karlsruhe, Germany
4,6 Diamidin-2-phenylindol (DAPI)	Sigma Aldrich, Taufkirchen, Germany
30 % Acrylamid, Rotiphorese ® Gel 30	Carl Roth, Karlsruhe, Germany
Agarose	PEQLAB, Erlangen, Germany
Ammonium peroxodisulfat (APS)	Carl Roth, Karlsruhe, Germany
Ampicillin	Gibco® Invitrogen, Karlsruhe, Germany
ß- Mercaptoethanol	Serva, Heidelberg, Germany

Bovine serum albumin	Carl Roth, Karlsruhe, Germany
Bromphenol blue	Carl Roth, Karlsruhe, Germany
Calcium chloride ($CaCl_2$)	Carl Roth, Karlsruhe, Germany
Chloroform	VWR, Ismaning, Germany
Citric acid	Carl Roth, Karlsruhe, Germany
Desoxynucleosid triphosphates (dATP, dCTP, dGTP, dTTP)	Invitrogen, Karlsruhe, Germany
Dimethyl sulfoxide (DMSO)	Carl Roth, Karlsruhe, Germany
Dithiothreitol (DTT)	Carl Roth, Karlstuhe, Germany
DMF (N,N-Dimethylformamide)	Sigma Aldrich, Taufkirchen, Germany
ECM gel from Engelbert-Holm-Swarm mouse sarcoma	Sigma Aldrich, Taufkirchen, Germany
Ethylenediaminetetraacetic acid	Carl Roth, Karlsruhe, Germany
Ethanol	Carl Roth, Karlsruhe, Germany
Fetal bovine serum FBS	Sigma Aldrich, Taufkirchen, Germany
FBS "South American"	Life Technologies, Darmstadt, Germany
Fluoromount	Sigma Aldrich, Taufkirchen, Germany
Glycine	Carl Roth, Karlsruhe, Germany
Glycerol	Carl Roth, Karlsruhe, Germany
HEPES	Carl Roth, Karlsruhe, Germany
Immersion Oil 518F	Zeiss, Oberkochen, Germany
Low fat milk powder	Vitalia, Bruckmühl, Germany
Methanol	Carl Roth, Karlsruhe, Germany
Mounting Fluoromount	Sigma Aldrich, Taufkirchen, Germany

Paraformaldehyd (PFA)	Carl Roth, Karlsruhe, Germany
Penicillin	Gibco® Invitrogen, Karlsruhe, Germany
Phenylmethylsulfonylfluorid (PMSF)	Callbiochem, Darmstadt, Germany
Protease Inhibitor, Cocktail Set III Animal Free	Callbiochem, Darmstadt, Germany
Roti-Lumin, 1+2	Carl Roth, Karlsruhe, Germany
Roti-Quant®	Carl Roth, Karlsruhe, Germany
Saccharose	Carl Roth, Karlsruhe, Germany
Sodium chloride	Carl Roth, Karlsruhe, Germany
Sodium dodecyl sulfate (SDS)	Carl Roth, Karlsruhe, Germany
Sodium hydrogen phosphate	Carl Roth, Karlsruhe, Germany
Sodium tetraborate decahydrate	Carl Roth, Karlsruhe, Germany
Streptomycin	Gibco® Invitrogen, Karlsruhe, Germany
TEMED	Carl Roth, Karlsruhe, Germany
TRIS tris(hydroxymethyl)aminomethane	Carl Roth, Karlsruhe, Germany
Trisoidum citrate	Carl Roth, Karlsruhe, Germany
Triton X-100	Carl Roth, Karlsruhe, Germany
Toluidine blue dye	Carl Roth, Karlsruhe, Germany
Tween®20	Carl Roth, Karlsruhe, Germany

4.10 Technical devices and other equipment

Device	Provider
24-well Transwell® inserts 8 µM	Millipore, Germany
BD BioCoat Matrigel Invasion Chamber	Thermo Scientific, Germany
BioPhotometer plus	Eppendorf, Hamburg, Germany
Blotting equipment Mini PROTEAN® TetraCell	Bio-Rad, Munich, Germany
Cell culture dishes	Sarstedt, Nümbrecht, Germany
Centrifuge 5424R	Eppendorf, Hamburg
Centrifuge 5804R	Eppendorf, Hamburg
Centrifuge Heraeus Biofuge Stratos	Thermo Scientific, Freiburg, Germany
Centrifuge Vials 15 mL, 50 mL	Sarstedt, Nürmbrecht, Germany
Chemiluminescent imager Chemismart 5100	PEQLAB, Erlangen, Germany
Confocal microscope LSM 510	Zeiss, Jena, Germany
Cryo vials CryoPure 1.6 mL	Sarstedt, Nümbrecht, Germany
Eppendorf tubes	Eppendorf, Hamburg
Falcon tubes	Sarstedt, Nümbrecht, Germany
Freezer	Liebherr, Biberach an der Riss, Germany
Fridge	Liebherr, Biberach an der Riss, Germany
Gelelectrophorese Device	Bio-Rad, Munich, Germany
Glas pearls	Carl Roth, Karlsruhe, Germany
Incubator for Bacteria MaxQ 6000	Thermo Scientific, Germany
Laminar Flow HERACell 150i	Thermo Scientific, Germany

Light Cycler®480	Roche, Penzberg, Germany
Light Cycler®480 Multiwell Plate 96	Roche, Penzberg, Germany
Light Cycler®480 Sealing Foil	Roche, Penzberg, Germany
Microscope Axiovert 135M	Zeiss, Göttingen
Neubauer cell counting chamber	Marienfeld, Lauda-Königshofen, Germany
PCR machine	Biometra GmbH, Göttingen
pH meter Lab850	Schott Instruments, SI Analytics, Mainz, Germany
Pipetus	Hirschmann, Eberstadt, Germany
Power supply PeqPower 300	PEQLAB, Erlangen, Germany
PVDF-membrane	Millipore, Billerica, MA
Rotation Incubator	Heidolph, Schwabach, Germany
SDS-PAGE equipment	BIORAD, München
Shaker Polymax 1040	Heidolph, Schwabach, Germany
Sterile cotton swabs	Carl Roth, Karlsruhe, Germany
Thermoblock	Eppendorf, Hamburg, Germany
UV-transparent cuvettes	Sarstedt, Nümbrecht, Germany
Vortex device	IKA, Staufen, Germany
Water bath	Memmert, Schwabach, Germany
Whatman Paper 0.8 mm	Optilab, München, Germany

5 Methods

5.1 Cell culture methods

5.1.1 Culturing and maintenance of eukaryotic cell lines

All cell work was carried out in a biosafety level S1 laboratory using sterile laminar flow cabinets.

Thawing was achieved by centrifugation of 5 mL appropriate cell medium including the pre-heated cell suspension taken out of the cyro vial. Next, peletted cells were re-suspended in fresh medium and cultured in cell culture dishes.

For freezing, centrifuged cells were re-suspended in FBS supplemented with Dimethyl-sulfoxide (DMSO), aliquoted into cryo vials and deposited at -80°C in 2-propanol chambers. 48 hours later, vials were transferred to liquid nitrogen for long-term storage.

All mammalian cells were maintained as monolayers at 37˚C in a humidified atmosphere containing 5 % CO_2 and cultured in the stated media, containing 10 % (v/v) heat inactivated fetal bovine serum and 5 % (v/v) penicillin/streptomycin. Passaging of cells was performed twice per week, using sterile buffered saline (PBS) for washing and trypsin to detach cells of cell culture dishes. Cell dilution was typically 1:10. Geneticin was added the following day to sustain FLNA expression in A7 cells.

5.1.2 Liposomal transient transfection

A Neubauer chamber was used for cell counting. 24 h after plating, cells at 60 % confluency were transfected with the DNA plasmid constructs using Lipofectamine 2000 reagent according to the manufacturer's instructions (Table 1). After 6 h of incubation in OptiMEM, medium was replaced with fresh medium. RNA and protein were harvested 24 to 48 h post-transfection for further analysis. Control cells were transfected in parallel. All transfections were performed in triplicate.

	DNA plasmid [µg]	Lipofectamine® 2000 [µL]	OptiMEM [µL]	Total medium volume post transfection [mL]
6-well dish	4	5	250	2
6 cm dish	8	10	500	4

Table 1: Required volumes for liposomal transfection

5.1.3 Calcium-phosphate transient transfection

Second to the liposomal transfection method, transient transfection was accomplished by calcium DNA-precipitation. Shortly prior to transfection, medium was replaced by fresh medium without antibiotics. For the actual transfection two solutions were prepared (Table 2) and Solution 1 was added drop by drop to Solution 2 while vortexing. Subsequently the mix was incubated for 5 minutes at room temperature and added to the cells. 24 h after transfection, cells were washed twice with PBS and medium was replaced with fresh medium including antibiotics.

	DNA plasmid [µg] (Solution 1)	2 M $CaCl_2$ [µL] (Solution 1)	2x HBS Buffer [µL] (Solution 2)	Total volume DNA cocktail ad H_2O [µL] (Solution 1)	Total medium volume post transfection [mL]
6-well dish	4	3.5	62.5	62.5	2
6 cm dish	8	7	125	125	4

Table 2: Required volumes for calcium-phosphate transfection

5.1.4 siRNA transient transfection

Knockdown of target genes by RNA interference (RNAi) results in a transient gene-specific reduction in gene expression. For RNA interference, cells were transfected with either 50 nM gene-specific small interfering RNA (siRNA) or 50 nM of negative control siRNA using Lipofectamine RNAiMAX according to the manufacturer's instructions.

All knockdown experiments were carried out in 6-well dishes and a reverse transfection method was used. 2 µl FLNA, MKL1 or negative control siRNA, 500 µL OptiMEM and 5 µL Lipofectamine RNAiMAX were furnished per dish and incubated for 20 minutes at room temperature. In the meantime 2 x 10^5 A7 or HuH7 were re-suspended in 1.5 mL OptiMEM and added to the prepared dishes. The next day, Medium was replaced by 2 mL fresh medium containing serum and antibiotics. Depending on type of analysis either 24, 48 or 72 h post transfection, knockdown efficiencies were assessed.

5.1.5 Serum starvation

Serum starvation was achieved by two time PBS washing, followed by incubation in culture medium supplemented wit 0.2 % fetal bovine serum without antibiotics for 16 h overnight.

5.1.6 Serum stimulation

After serum starvation, cells were stimulated with 20 % fetal bovine serum USA for 2 h or the indicated time intervals. The serum was directly added to the growth medium used for starvation.

5.1.7 Drug treatment

Lysophosphatidic acid (LPA), Latrunculin B (LatB), Jasplakinolide and Calpain Inhibitor III were diluted to the required working concentration with medium and exposed to the seeded cells for the precise amount of time.

5.1.8 Cell harvest and lysis

For harvesting, cells were washed twice with ice cold PBS to avoid degradation of proteins and lysed with 200 µL Kralewski buffer containing protease inhibitor cocktail 1:100, phenylmethanesulfonylfluoride (PMSF) 1:500 and dithiothreitol (DTT) 1:250 or in case of immunoprecipitation with 500 µL 1% Triton IP lysis buffer. Samples were incubated for 15 minutes (45 minutes for immunoprecipitation) on ice and pelleted by centrifugation at 13000 rpm for 15 minutes at 4˚C. The supernatant containing the extracted proteins was transferred into a new Eppendorf tube, supplemented with 4x SDS loading/Laemmli buffer and boiled at 95˚C for 10 minutes. The protein lysates were stored at -20˚C or directly used

for immunoblot analysis. If applicable, total protein concentration was measured prior to addition of Laemmli buffer using the Bradford method.

5.2 Protein biochemistry

5.2.1 Determination of total protein concentration

For measuring total protein concentration in cell lysates prior to immunoblot analysis, Roti-Quant® Bradford reagent was used according to the manufacturer's instructions. 2 µL lysis buffer served as blank and 2 µL of each sample were diluted with 1000 µL Roti-Quant® Bradford Reagent (Coomassie Brilliant Blue G-250 was diluted 1:5 with H_2O and filtrated) and incubated at room temperature for 5 minutes. The protein concentration was analyzed by measuring the absorbance at 595 nm with the BioPhotometer. Typically, 10 to 50 µg of total protein were subjected to immunoblot analysis.

5.2.2 Sodium dodecyl sulfate polyacrylamide gel electrophoresis (SDS-PAGE)

The SDS-PAGE method was used to separate proteins according to their molecular weight (Laemmli, 1970). Table 3 below illustrates the required volumes for a single 1.5 mm polyacrylamide gel.

Separating gel	5 %	10 %	12 %
H_2O [mL]	4.25	1.99	2.4
30 % polyacrylamide [mL]	1.25	1.67	3
1.5 M TRIS (pH 8.8) [mL]	1.875	1.25	1.95
10 % SDS [µL]	75	50	75

10 % APS [µL]	100	50	75
TEMED [µL]	6	2	3

Stacking gel	
H_2O [mL]	2.7
30 % polyacrylamide [mL]	0.67
1.5 M TRIS (pH 6.8) [mL]	1
10 % SDS [µL]	40
10 % APS [µL]	40
TEMED [µL]	4

Table 3: Composition of a 1.5 mm polyacrylamide gel.

Water, acrylamide and the corresponding TRIS buffer were pre-mixed. Polymerization reaction was started by adding APS and TEMED. The polymerized gel was clamped in the gel electrophoresis device (BioRad) and then filled with gel running buffer. The gel was loaded with the protein lysate probes denatured and heated in 95˚C in 4 x Laemmli buffer for 5 minutes. Spectra Multicolor Brad Range protein standard was used as a molecular weight marker in parallel. The gel electrophoresis ran at a constant current of 80 V.

5.2.3 Immunoblotting

After gel electrophoresis, proteins separated according to their mass were transferred from the SDS-gel onto a pre-activated polyvinylidene fluoride (PVDF) membrane using the minigel system (BIORAD) (Towbin et al, 1979). Using the wet blotting method and a transfer buffer, the proteins were blotted at a constant current of 350 mA for 105 minutes. Membranes were blocked directly in 5 % nonfat dry milk in TBS-T for 1 h at room temperature to prevent unspecific bindings and probed with the primary antibody overnight at 4 ˚C with gentle agitation. Next day, membrane was washed three times with TBS-T for 15 minutes and

thereafter probed with the horseradish peroxidase-conjugated secondary antibody in TBS-T for 1 h at room temperature. Final washing was done three times for 5 minutes with TBS-T. Protein bands were visualized via the enhanced chemiluminescence detection method at a luminescent imager by probing the membrane with enhanced chemiluminescece solution S1 and S2 for 1 minute. Detection with HSP90 antibody was used as a loading control.

5.2.4 Immunoprecipitation

For immunoprecipitation assays, cells were harvested 24 h after transfection or 24 h after seeding if endogenous interactions were determined. Lysis was accomplished by adding 500 µL 1% Triton IP lysisbuffer and by incubation on ice for 45 minutes followed by centrifugation (10 minutes, 13000 rpm, 4 ˚C). 20 µL lysate was taken and frozen for later examinations. The remaining 480 µL were immunoprecipitated with the help of the fitting antibody according to the plasmids tag. This pull-down was accomplished with 3 µL of a specific antibody against HA-FLNA, FLAG-MKL1 or endogenous MKL1, FLNA and overnight rotation at 4 ˚C. Next day, 100 µL of four times 1% Triton IP lysisbuffer washed, recombinant protein G-Sepharose beads in a 50 % slurry in immunoprecipitation buffer was added, and the lysates were rotated for 3 h at 4 ˚C. Next, beads-antibody immunoprecipitates were collected by centrifugation at 13000, washed four times with immunoprecipitation buffer, and then resolved with SDS-polyacrylamide gel electrophoresis. The proteins were then transferred to PVDF membranes and immunoblotted with the respective antibody.

5.2.5 Indirect Immunofluorescence

Cells grown on coverslips were washed with 1 mL PBS, fixed in 4 % paraformaldehyde for 10 minutes at room temperature and extracted with 0.2 % Triton X-100 in PBS for 7 minutes. Blocking of unspecific binding sites was performed by incubation in 1 % bovine serum albumin in PBS for 60 minutes at room temperature. Afterwards cells were incubated with the primary antibody (1:1000 dilution), phalloidin for F-actin staining or 4’6-diamidion-2-phenylindole (DAPI) for nuclei staining at room temperature for 1 h. Thereafter cells were washed three times each with PBS and incubated with fluorescently labeled secondary antibodies for 30 minutes at room temperature in the dark. In the concluding washing step, cells were washed two times with PBS. Finally, cells were embedded in the mounting medium (Fluoromount®). Depending of the nature of the experiment a snapshot

fluorescence microscope, or a confocal microscope was used. For normal fluorescence microscopy, images were obtained on a Zeiss LSM 510 microscope.

5.3 Scratch-wound assay

Cells were transfected and allowed to grow to a confluent monolayer. After a wound was scratched with the tip of a pipette, the mobilization of cells behind the wound edge was determined via cell counting, measuring the remaining wound gap in comparison to a control sample and immunoblotting. Images were acquired on a Zeiss microscope.

5.4 Invasion assay

The invasive capacity of tumor cells was tested using a BD BioCoat Matrigel Invasion Chamber. 5 x 10^4 cells in 200 µL medium supplemented with 1 % serum were placed in the upper chamber of the Transwell® insert whereas the lower chamber was filled with 600 µL medium containing 10 % serum as a chemoattractant. The cells were allowed to invade for 24 h at 37˚C. Invaded cells were visualized by toluidine staining. Non-invading cells were removed from the top of the gel with a sterile cotton swap. For fixation of invaded cells, inserts were incubated in 100 % methanol for 2 minutes and subsequently stained in 1 % toluidine blue solution for 2 minutes. Excess dye was removed by washing the inserts in distilled water. The inserts were allowed to air dry. Cells were quantified by counting the cell number of invaded, purple-colored cells using a Zeiss microscope.

5.5 Nucleic acid biochemistry

5.5.1 RNA isolation

For RNA preparation, cells were washed twice with PBS and 0.5 mL TRIzol® reagent per 6-well dish was added for harvesting. Cells were scrapped off, transferred into a tube and incubated for 5 minutes at room temperature. Next, 0.2 mL chloroform was added and the

tube was shaken for 15 seconds, followed by incubation for 3 minutes at room temperature. For phase separation the sample was centrifuged at 12700 rpm for 15 minutes at 4˚C. The aqueous phase, containing the RNA was removed and placed in a new tube. For precipitation of the RNA, 0.25 mL 2-propanol was added, followed by incubation at room temperature for 10 minutes. Collection of the RNA precipitate was achieved by centrifugation at 12000 rpm for 10 minutes at 4˚C followed by a careful removal of the supernatant. The RNA pellet was washed with 1 mL 75 % ethanol and then centrifuged again at 12000 rpm for 10 minutes at 4˚C. The supernatant was discarded and the RNA was allowed to air dry. The remaining RNA was re-suspended in nuclease-free water and dissolved by incubation at 55˚C for 10 minutes. RNA concentration and purity were determined by photometric measurement of the absorbance.

5.5.2 cDNA synthesis

cDNA synthesis was accomplished with help of reverse transcriptase. Therefore two cocktails were prepared (Table 4). For cocktail A, 1 µg of total RNA was primed with 1 µL of Random Hexamers (50 µM) and nuclease free water was added to reach a total volume of 5 µL. Denaturation was obtained by heating at 70˚C for 5 minutes, followed by incubation at 4˚C for 5 minutes. Meanwhile cocktail B (cDNA mix) mixed.

cDNA mix/cocktail B	
5x First Strand Buffer [µL]	4
0.1m DTT [µL]	2
10 µM dNTPs [µL]	1
Superscript Reverse Transcriptase II [µL]	1
Nuclease free water [µL]	7

Table 4: cDNA mix for RT-PCR

Following the preparation of cocktail A and B both mixtures were put together and heated at 25˚C for 5 minutes and then at 42˚C for 60 minutes. Next, reverse transcriptase was inactivated by heating to 70˚C for 15 minutes. The prepared cDNA was stored at -20˚C.

5.5.3 Real-time PCR

Quantification of gen expression was done with the SYBR green method (Table 5).

Primer mix	
SYBR green Master I mix [µL]	10
1 µM Primer forward [µL]	1
1 µM Primer reverse [µL]	1
Nuclease free water [µL]	2

Table 5: Primer mix for RT-PCR

Each quantitative PCR (final reaction volume 20 µL) included 6 µL cDNA (1:10 diluted with H_2O, for 18S rRNA diluted 1:100) and 14 µL Primer mix. Quantification was performed with the LightCylcer 480 Real-Time PCR system using the program listed below (Table 6).

Step	Temperature profile	Time	Function	
1	95˚C	5 min	pre-incubation	
2	95˚C	10 sec	amplification	
	55˚C	10 sec	amplification	
	72˚C	10 sec	elongation	50 cycles
3	95˚C	10 sec	melting curve	
	60˚C	1 min	melting curve	
	95˚C	10 sec	melting curve	

4	40˚C	30 sec	cooling

Table 6: Times and temperatures for a quantitative real-time PCR reaction.

Gene expression was normalized with respect to the endogenous housekeeping gene 18S rRNA, which was determined not to significantly change under different conditions.

5.5.4 Generation of ΔMKL1 mutants

The Q5 Site-Directed Mutagenesis Kit (New England Biolabs) was used for deletion mutant generation in a three-step manner. Step 1: Exponential amplification. Step 2: Kinase, Ligase and DpnI (KLD) treatment. Step 3: High efficiency transformation

Exponential Amplification Mix	Volume
Q5 Hot Start High Fidelity 2x Master Mix [µL]	12.5
Forward Primer 10 µM [µL]	1.25
Reverse Primer 10 µM [µL]	1.25
Template DNA 25 ng/µL [µL]	1
Nuclease-free water [µL]	9

Table 7: Step 1, Exponential amplification-Mix

Exponential Amplification Cycling Conditions	Temperature	Time
Initial denaturation	98˚C	30 s
	98˚C	10 s
25 cycles	50-72˚C	20 s
	72˚C	25 s/kb
Final extension	72˚C	120 s
Hold	4˚C	

Table 8: Step 1, Exponential amplification Cycling conditions

In step 2 Kinase, ligase and DpnI are added to the mix and incubated for 5 minutes at room temperature

KLD reaction	Volume
PCR product of step 1 [µL]	1
2 x KLD reaction buffer [µL]	5
10 x KLD enzyme mix [µL]	1
Nuclease-free water [µL]	3

Table 9: Step 2, KLD reaction

Finally, transformation is performed in step 3. Therefore, 5 µL of step 2-product are added to 50 µL of chemically-competent cells and incubated on ice for 30 minutes. Next, cells are heat-shocked at 42˚C for 30 seconds and incubated on ice for 5 minutes. 950 µL SOC medium is added and the mix is shaken at 37˚C for 1 h. 70 µL is spread onto appropriate selection plates and incubated over night at 37˚C followed by midi scale plasmid preparation.

5.5.5 Transformation into chemically competent *E.coli* DH5alpha bacteria cells

Aliquots of competent *E.coli* DH5alpha bacterial cells were stored at -80˚C. For each transformation, one aliquot including 15 µL bacteria suspension was thawed for 15 minutes. Afterwards 1 µL plasmid DNA was added and incubated on ice for 30 minutes. Next, the mix was heated at 42˚C for exactly 90 seconds and stored on ice for 2 minutes. 900 µL pre-warmed LB medium (without antibiotics) were added and the suspension was shaken at 150 rpm at 37˚C for one hour. 150 µL of the bacterial suspension was plated on pre-warmed agar plates containing the selection antibiotic and incubated overnight at 37˚C. Until further processing, the agar plate was sealed with Parafilm and stored at 4˚C.

5.5.6 Midi scale plasmid preparation

With the help of a sterile pipette tip, a single bacterial clone was picked and transferred in 50 mL LB medium containing the selection antibiotic and thereafter incubated for 16 h overnight while shaking at 300 rpm at 37˚C. Next day, bacterial cells were centrifuged at

3500 rpm for 10 minutes at 4˚C and the supernatant was discarded. Plasmid-DNA was extracted using the GenElute HP Plasmid Midiprep Kit. Thereafter DNA concentration and purity were determined by photometric measurement.

5.6 Luciferase reporter assay

Activation of a 5 x SRE reporter gen was measured with help of a dual luciferase reporter assay system. Cells of 60 % confluence were transfected in 6 well plates. Each transfection contained 500 ng of the 5 x SRE reporter plasmid and 250 ng of *Renilla* luciferase simian virus 40 reporter (SV40) reference reporter plasmid, which was used to normalize for transfection efficiency. 24 h post transfection the cells were lysed with the help of 1x passive lysis buffer and centrifuged at 13000 rpm after stored on ice for 15 minutes. Photoemisson and *firefly* luciferase activity was determined as the amount of converted luciferin into oxyluciferin.

5.7 Statistical analysis

Unless otherwise indicated, data were expressed as mean +/- standard deviation (SD). Statistical analysis among two groups was carried out using the Student's unpaired t-test. P-values are *p≤0.05, **p≤0.01, ***p≤0.001.

5.8 Software and databases

GraphPad Prism® (GraphPad Software, LaJolla, CA, USA) was used for calculations and statistical analysis. Research publications were obtained from the online database NCBI PubMed. Blots and microscopic images were procedded with ImageJ (Wayne Rasband, National Institute of Health, Bethesda, MD, USA).

6 Results

6.1 Identification of FLNA as a novel MKL1 interacting protein

Previously to this work, first evidence of an existing MKL1-FLNA interaction has been presented with the help of a yeast two-hybrid screening performed by Dr. S. Muehlich (Kircher P., Hermanns C. et al, 2015). Therefore, the initial part of this thesis aimed for a better understanding of the interaction's binding properties, or in other words, a revelation of the association and its surroundings in greater detail.

To open research on the MKL1-FLNA relationship, we selected well-established human melanoma cell lines (Cunningham CC., Gorlin JB. et al, 1992), consisting of the FLNA-deficient M2 and the matching stable FLNA-expressing A7 cell line (Fig. 1A). Both cell lines are predestined for researching FLNA and its environment, since they only differ in their FLNA expression status, while MKL1 levels and other biological properties remain untouched (Cunningham CC., 1995). To further expand our knowledge about the MKL1-FLNA association, especially under physiological conditions, we included alternative cell lines like primary human, mouse and 3T3 fibroblasts, HuH7 hepatocellular carcinoma, MDA-MB-468 mammary carcinoma, HLF hepatocellular carcinoma, and HEK-293 human embryonic kidney cells in the later stages of the work (Fig. 1B).

As described in *2.4.2,* the FLNA protein is susceptible to cleavage caused by calpain, a calcium dependent protease expressed ubiquitously, which the Human Genome Project recently revealed (Huang Y., Mather EL. et al., 2001). As shown in Fig. 1C, FLNA came into sight as a strong 280-kD band, representing unprocessed full-length FLNA. Furthermore, we observed two weaker 190-kD and 90-kD cleavage fragments. In addition, we were also able to restrain FLNA cleavage by incubating cells with a calpain inhibitor III (Fig. 1C). All following experiments in this work were performed with the full-length FLNA version, as indicated with the 280-kD mark in every relevant figure. Nevertheless, curiousness about FLNA

cleavage fragment presence remains, especially in context with a physical presence of MKL1, this way representing a topic of high value for future studies.

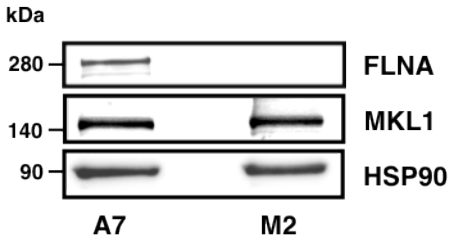

Figure 1A: Immunoblotting for FLNA, MKL1 and heat shock protein 90 (HSP90) as a loading control in lysates of A7 cells endogenously expressing FLNA and FLNA-deficient M2 cells.

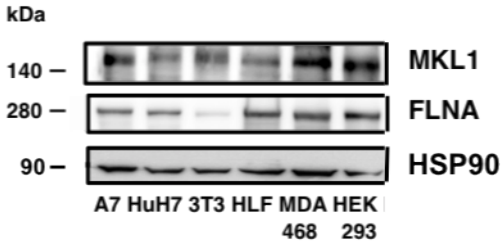

Figure 1B: endogenic MKL1 and FLNA levels in cells lysates, determined by immunoblotting. HSP90 as a loading control.

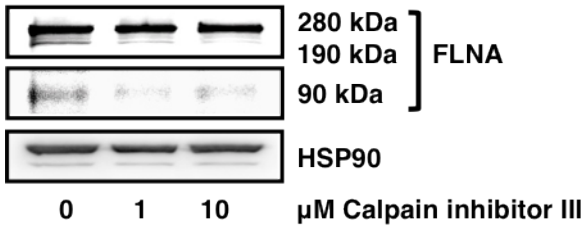

Figure 1C: Immunoblot analysis of FLNA, its calpain cleavage forms and HSP90 in A7 cells treated with the indicated amounts of Calpain inhibitor III.

Every performed experiment necessarily relied on a well-approved and established interaction of MKL1 and FLNA. Therefore, we were heavily interested in strengthening the original yeast two-hybrid findings by performing immunoprecipitations. This setup not only allowed us to support the primary findings by a second well respected biochemical method but also guaranteed insights under *in vivo* like environmental conditions.

We carried out immunoprecipitation experiments of A7 melanoma cells expressing FLAG-tagged MKL1. MKL1 was immediately detectable after immunoprecipitation of FLNA (Fig. 1D). This observation proves a direct interaction between MKL1 and FLNA, because only FLNA bound MKL1 is detectable after the process of precipitation.

This precipitation method includes A7 melanoma cell plating, MKL1 transfection, cell harvesting and lyse, addition of FLNA antibody for association with available MKL1, overnight rotation, beads incubation, which exclusively bind the before incubated (FLNA) antibody, washing and finally blotting with a second, this time FLAG-MKL1 antibody which is only able to detect MKL1 if a previous interaction with the FLNA antibody has taken place after cell lyse. To furthermore exclude a clonal difference in A7 cell nature, control experiments were carried out, using the same experimental setup in the FLNA-negative M2 cell line. As anticipated, FLNA and MKL1 were only recovered from FLNA immunoprecipitates when FLNA was re-expressed in M2 cells (Fig. 1E). Moreover, neither FLNA nor MKL1 was observed in immunoprecipitates with an unspecific primary antibody, further confirming the specificity of the MKL1-FLNA interaction (Fig. 1F).

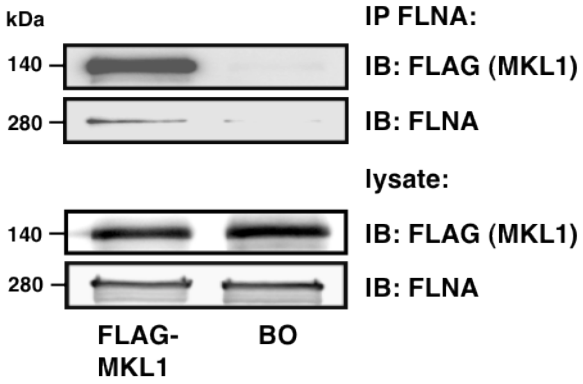

Figure 1D: Immunoprecipitation (IP) for FLNA and Western blot (IB) for MKL1 and FLNA in lysates from A7 cells transfected with FLAG-tagged MKL1. BO, Sepharose beads-only control, without antibody.

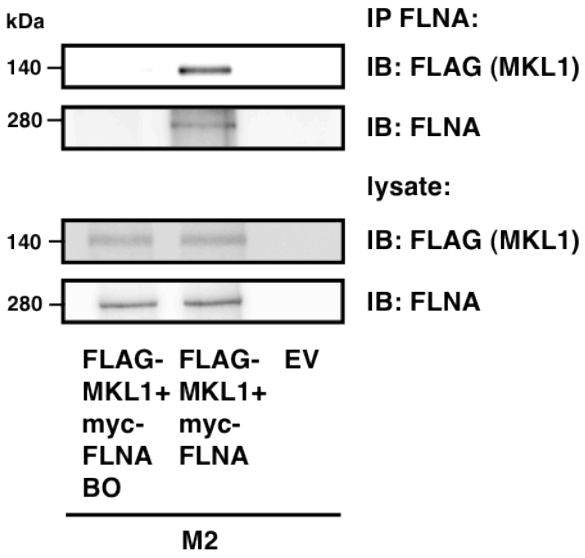

Figure 1E: Recovery of FLNA and MKL1 in immunoprecipitates with FLNA antibody upon reconstitution of FLNA in the FLNA-negative cell line M2, transfected with FLAG-MKL1 or EV. BO, Sepharose beads-only control, without antibody. EV, empty vector.

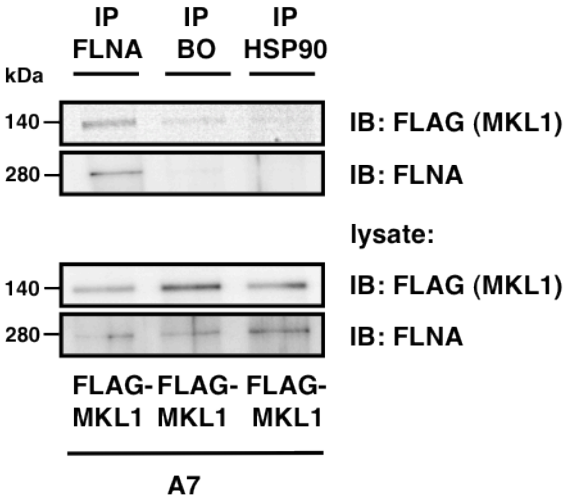

Figure 1F: Immunoprecipitation with HSP90 antibody as an unspecific primary antibody in A7 cells expressing FLAG-tagged MKL1 yielding no binding of FLNA and MKL1.

Next, we were wondering if it likewise would be possible to detect an endogenous MKL1-FLNA interaction besides the so far, in a certain way forced interaction based on transfection into the cell. Consequently, we expanded our cell library with mouse embryonic fibroblasts (MEFs) (Fig. 1G), HuH7 hepatocellular carcinoma cells (Fig. 1H), MDA-MB-468 mammary carcinoma cells (Fig. 1H), HLF hepatocellular cancer cells (Fig. 1I) and HEK-293 human embryonic kidney cells (Fig. 1I). MEF, HuH7 and MDA-MB-468 cell lines successfully

confirmed the data obtained in A7 cells (Fig 1G,H), while HLF and HEK-293 cells displayed no measurable interaction (Fig. 1I). Thus, we were able to majorly add to our knowledge that the MKL1-FLNA interaction takes place in a broad variety of non-cancer and cancer cell lines instead of just melanoma cells.

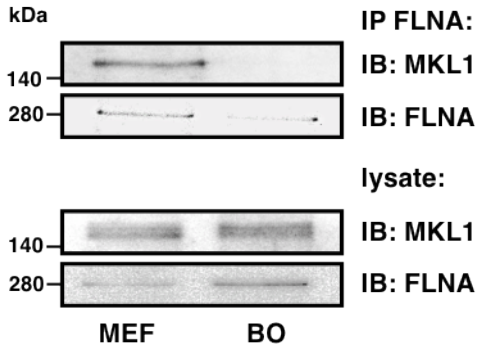

Figure 1G: IP for FLNA and IB for MKL1 and FLNA in lysates from MEFs. BO, without antibody.

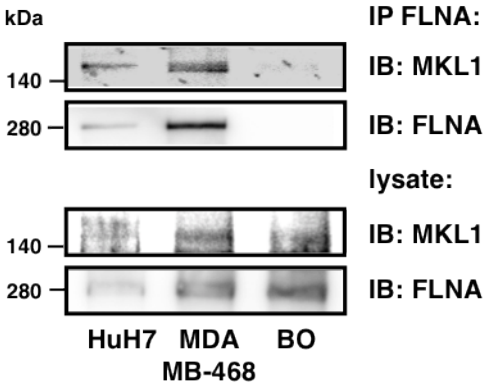

Figure 1H: IP for FLNA and IB for MKL1 and FLNA in lysates from HuH7 and MDA MB-468. BO, without antibody.

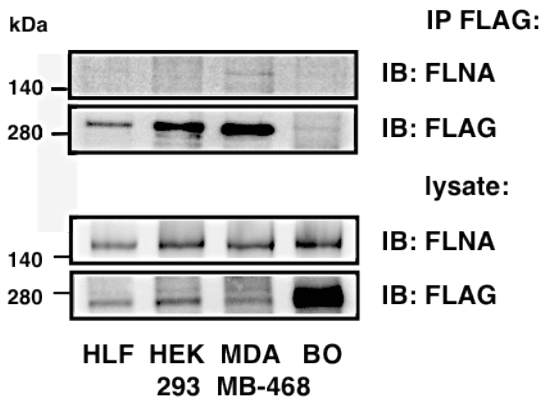

Figure 1I: IP for FLAG and IB for FLAG and FLNA in lysates from HLF, HEK293 and MDA MB-468. MDA MB-468 as a positive control. BO, without antibody.

After successfully stating the presence of a new interaction in a variety of cancer and non-cancer cell lines, questions were raised in which cell-compartment the interaction is taking place. Consistent with literature knowledge that MKL1 is regularly found in the nucleus of DLC1-defficient tumor cells (Muehlich S., Hampl V. et al, 2011), double immunofluorescence with differentially labeled antibodies specific for MKL1 and FLNA revealed that MKL1 and FLNA co-localized predominantly in the nucleus in A7 melanoma cells (Fig. 1J). Adding to our data that MKL1 accumulated in the nucleus of A7 melanoma cells, we demonstrated MKL1 relocation to the cytoplasm in FLNA-deficient M2 cells or A7 cells treated with FLNA siRNA (Fig. 1K). Untreated A7 cells displayed 70 % nuclear MKL1 localization, while FLNA depletion or experiments performed in M2 cells lead to a strong reduction of nuclear MKL1 appearance to around 20 % (Fig. 1K).

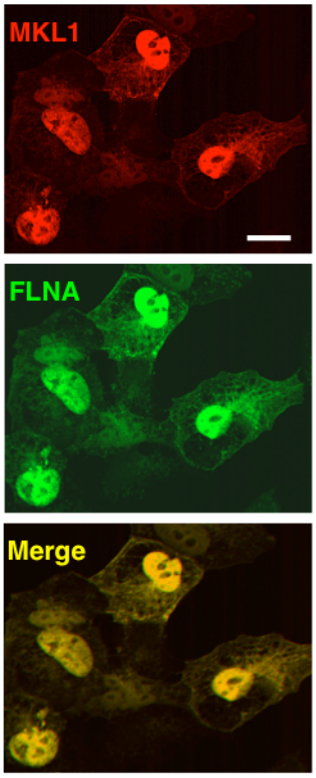

Figure 1J: Immunofluorescence analysis of MKL1 and FLNA in A7 cells. Scale bar, 20 µm. Representative images are shown.

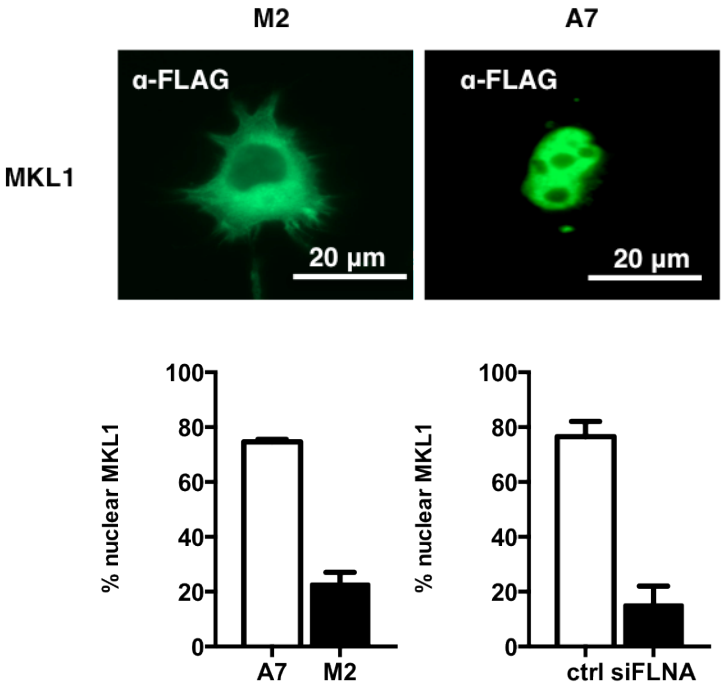

Figure 1K: Immunofluorescence analysis with anti-FLAG antibody of MKL1 in M2 and A7 cells (top and bottom left) and A7 cells treated with 50 nM siFLNA or 50nM negative control siRNA (ctrl) (bottom right). Data are means +/- SD (n=3 experiments). 100 cells counted each experiment. Representative images are shown. Scale bar, 20 µm

6.2 Mapping of MKL1-FLNA binding sites

After validating the interactions existence and further proving its location of appearance in the cell, we devoted to the upcoming question which MKL1 regions are indispensable for binding FLNA. To catch answers, we staked genetically engineered FLAG-tagged MKL1 mutants. More precisely, we used different MKL1 deletion variants, covering a certain span of amino acids to identify protein segments essential for FLNA interaction (Fig. 2A). Based on this model of step-by-step isolation of unnecessary MKL1 regions, we were able to narrow down the localization of the interaction to a region of 10 amino acids on the MKL1 protein (MKL1 301-310) (Fig. 2A and B).

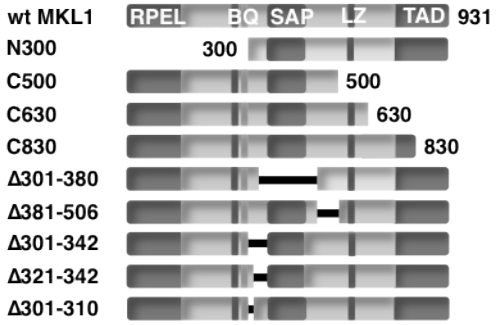

Figure 2A: Schematics oft the MKL1 derivatives used for mapping MKL1-FLNA binding sites. RPEL, conserved N-terminal domain; B, basic domain; Q, glutamine-rich domain; SAP, SAF-A/B-Acinus-PIAS domain; LZ, leucine zipper-like domain; TAD, transactivation domain.

	binding to FLNA		binding to FLNA
wt MKL1	+	Δ301-380	–
N300	+	Δ381-506	+
C500	+	Δ301-342	–
C630	+	Δ321-342	+
C830	+	Δ301-310	–

Figure 2B: Table of MKL1 derivatives indicating binding (+) or no binding (-) to FLNA.

Since one of MKL1s most important regulator and binding partner G-actin is facilitated via MKL1s N-terminal RPEL domain we thought about starting the investigation right here at the N-terminal site. Immunoprecipitation of cell extracts with an antibody against the FLAG-Tag and detection with FLNA antibodies showed that an N-terminal deletion construct of MKL1

lacking the first 300 amino acid residues (N300), this way also lacking the considered RPEL domain, was still able to bind FLNA (Fig. 2C). After eliminating the N-terminal domain as a possible interacting area, we shifted focus on the C-terminal protein end. However, C-terminal deletion constructs of MKL1 (C500, C630 and C830) likewise still interacted with FLNA, narrowing the possible field of interaction with FLNA down to amino acid MKL1 300-500 (Fig. 2D).

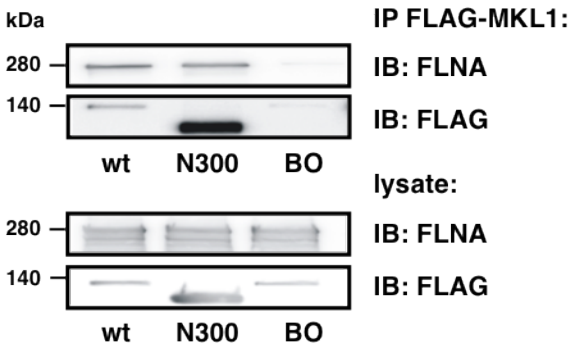

Figure 2C: Immunoprecipitation and Western blot as indicated in A7 cells transfected with FLAG-tagged wild-type (WT) MKL1 or the indicated MKL1 mutants. BO, Sepharose beads-only control. A portion of the cell lysate was also directly immunoblotted.

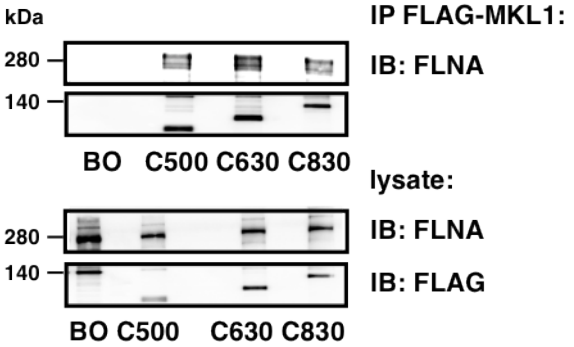

Figure 2D: Immunoprecipitation and Western blot as indicated in A7 cells transfected with FLAG-tagged wild-type (WT) MKL1 or the indicated MKL1 mutants. BO, Sepharose beads-only control. A portion of the cell lysate was also directly immunoblotted.

To further progress in cutting down the potential region of interaction, we next constructed internal deletions of amino acids 301 to 380 (Δ301-380) and amino acids 381 to 506 (Δ381-506), spanning the remaining 200 unexplored amino acids. Whereas MKL1 Δ381-506 still associated with FLNA, an interaction between MKL1 Δ301-380 and FLNA was hardly

detectable, no matter which antibody was used for pull-down efforts (FLNA or FLAG) (Fig. 2E).

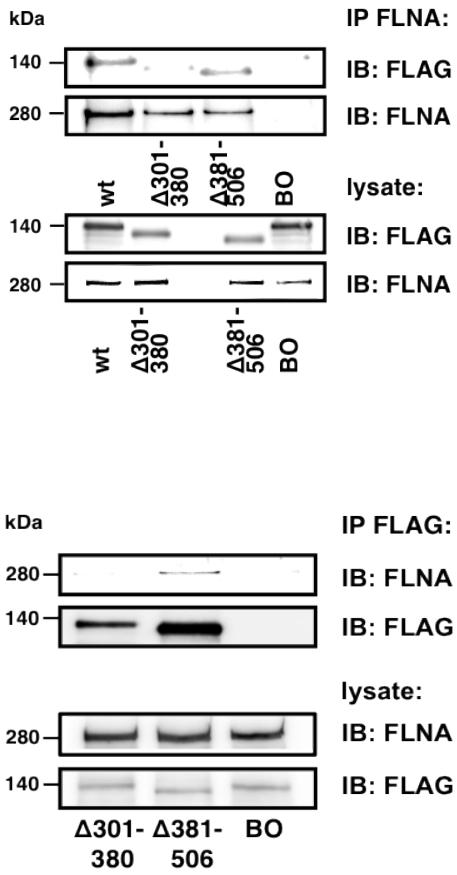

Figure 2E: Immunoprecipitation and Western blot as indicated in A7 cells transfected with FLAG-tagged wild-type (WT) MKL1 or the indicated MKL1 mutants. FLNA pulldown (top), FLAG pulldown (bottom). BO, Sepharose beads-only control. A portion of the cell lysate was also directly immunoblotted.

As described in *2.3.1* the SAP domain of MKL1 is supposed to be of certain importance regarding promoter activity. Moreover the domain lies between amino acids 343 and 378 in MKL1, which made us wondering about its contribution to the MKL1-FLNA interaction. However, FLNA still interacted with an MKL1 mutant lacking the SAP domain (Fig. 2F).

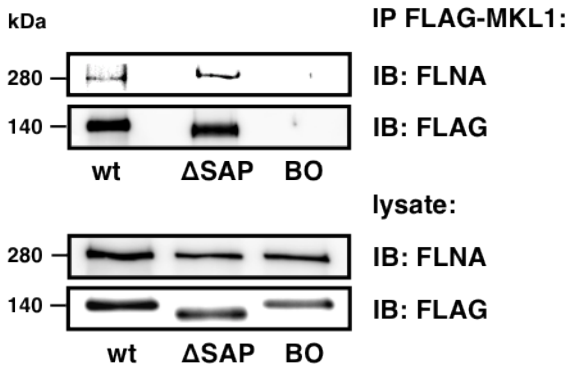

Figure 2F: Immunoprecipitation and Western blot as indicated in A7 cells transfected with FLAG-tagged wild-type (WT) MKL1 or the indicated MKL1 mutants. BO, Sepharose beads-only control. A portion of the cell lysate was also directly immunoblotted.

Following the result of this experiment we predicted that the FLNA binding site was located in a region spanning residues 301 to 342 in MKL1. Indeed, a Δ301-342 MKL1 construct displayed diminished FLNA binding in immunoprecipitation assays and binding further decreased with a mutant lacking amino acids 301 to 310, supporting our conclusion that these amino acids are required for FLNA binding (Fig. 2G and H). Concluding experiments were performed by addressing MKL1 amino acids 305 and 312. We chose these amino acids in particular because both of them provide targets for a possible phosphorylation, which plays a major role in MKL1 regulation and both are located in/next to the newly discovered interaction area. However, imunoprecipitation analysis including point mutants of MKL1 T305A and S312A showed no abolished FLNA interaction (Fig. 2I). In addition we took a look at the interaction of MKL2 with FLNA. MKL2 displayed a weaker association to FLNA than MKL1 did (Fig. 2J).

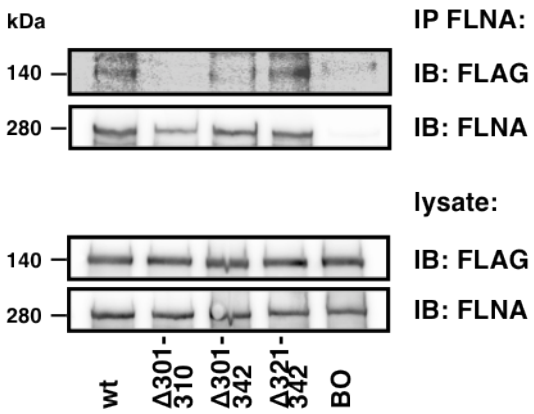

Figure 2G: Immunoprecipitation and Western blot as indicated in A7 cells transfected with FLAG-tagged wild-type (WT) MKL1 or the indicated MKL1 mutants. BO, Sepharose beads-only control. A portion of the cell lysate was also directly immunoblotted.

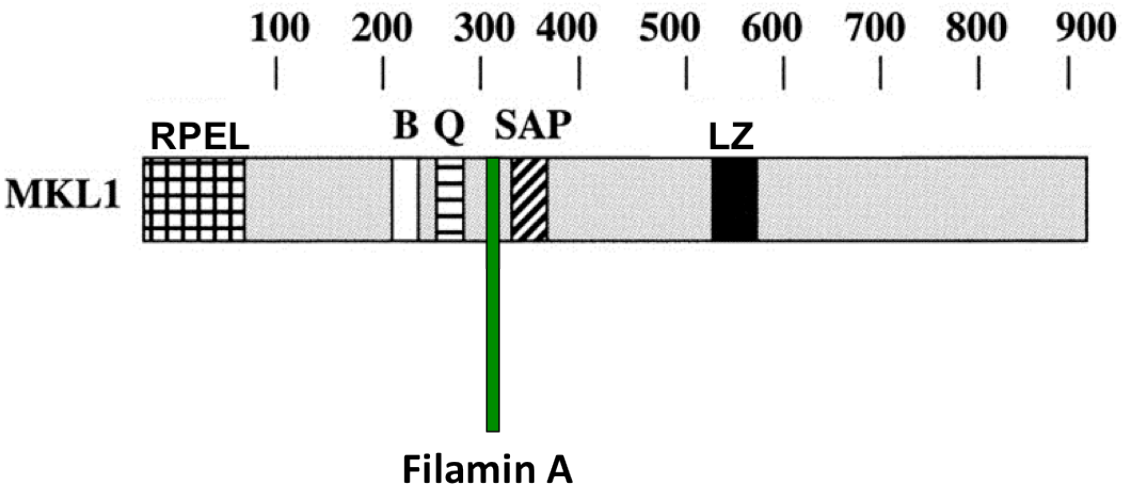

Figure 2H: Model of the MKL1-FLNA interaction happening at aa 301-310 on the MKL1 protein.

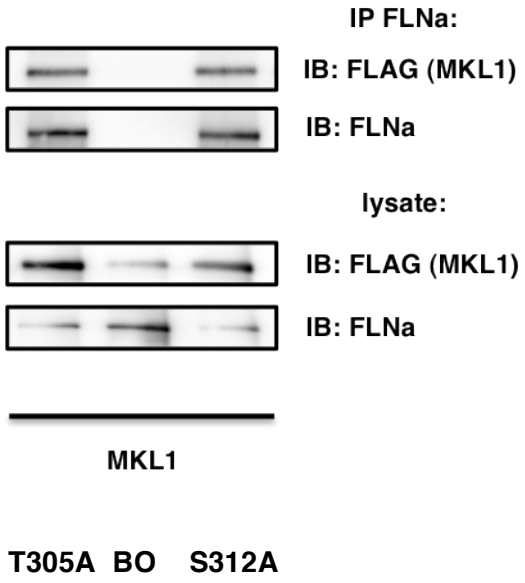

Figure 2I: Immunoprecipitation and Western blot as indicated in A7 cells transfected with FLAG-tagged wild-type (WT) MKL1 or the indicated MKL1 mutants. BO, Sepharose beads-only control. A portion of the cell lysate was also directly immunoblotted.

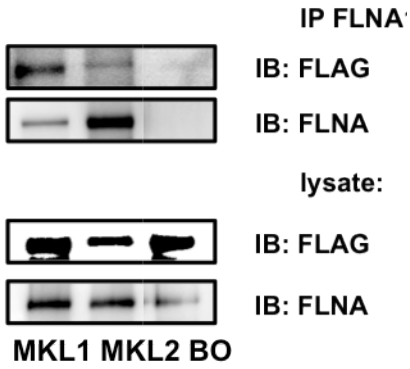

Figure 2J: Immunoprecipitation and Western blot as indicated in A7 cells transfected with FLAG-tagged wild-type (WT) MKL1 or MKL2. BO, Sepharose beads-only control. A portion of the cell lysate was also directly immunoblotted.

To onward expand our knowledge about MKL1-FLNA interaction, we set out to define protein segments of FLNA essential for the interaction with MKL1. FLNA offers a large variety of possible interaction sites for binding partners as already mentioned in *2.4.3*. It contains a filamentous F-actin binding domain at the N terminus and a rod segment consisting of 24 homologous repeats, separated into Rod1 (repeats 1 to 15) and Rod2 (repeats 16 to 23) by two hinge domains (Stossel TP., Condeelis J. et al, 2001). Therefore we transfected a series

of vectors expressing hemagglutinin (HA)-tagged FLNA fragments spanning the FLNA protein into A7 melanoma cells together with FLAG-MKL1 cDNA. Immunoprecipitation experiments revealed that FLNA amino acids 571 to 866 and amino acids 1779 to 2284 (corresponding to repeats 4 to 7 in the Rod1 domain and repeats 16 to 18 in the Rod2 domain) were essential for the interaction with MKL1, whereas other FLNA regions did not contribute to the interaction (Fig. 2K and L). Therefore we could show two possible interaction sites on FLNA, located on both, Rod1 and 2, suggesting a complex interaction occurring between multiple regions of FLNA and MKL1.

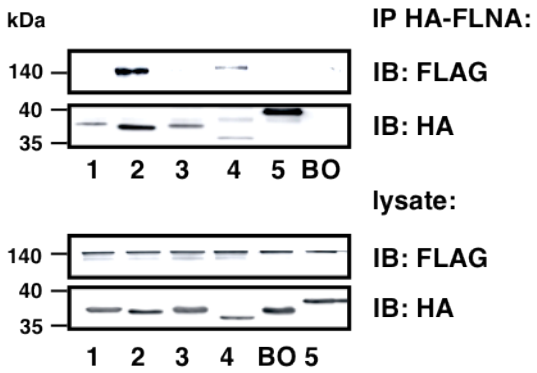

Figure 2K: Immunoprecipitation and immunoblotting as indicated in A7 cells co-transfected with a HA-tagged FLNA construct (1: FLNA amio acids 276 to 570; 2: FLNA amino acids 571 to 866; 3: FLNA amino acids 1155 to 1442; 4: FLNA amino acids 1779 to 2284; 5: FLNA amino acids 2285 to 2729) and FLAG-MKL1. BO, Sepharose beads-only control. A portion of the cell lysate was also directly immunoblotted.

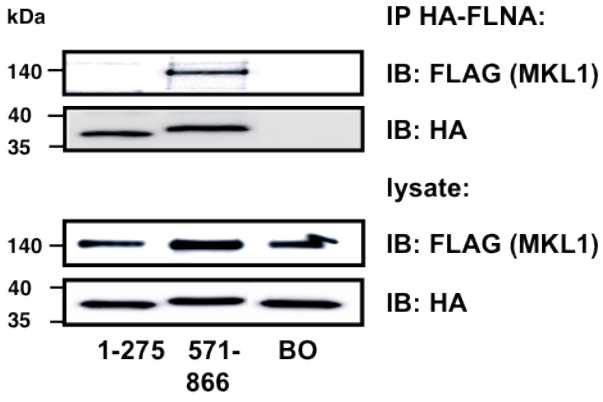

Figure 2L: Immunoprecipitation assay of A7 cells cotransfected with FLAG-MKL1 and HA-tagged FLNA fragments spanning FLNA aa 1-275 or 571-866 using antibodies against HA or FLAG. BO, Sepharose beads-only control. A portion of the cell lysate was also directly immunoblotted.

6.3 The dynamic MKL1-FLNA interaction, its correlation with the induction and repression of MKL1-SRF target genes and phosphorylation influence

After mapping the interaction in detail, our attention next focused on its condition under the influence of extracellular signals. Since activation of the Rho-actin cascade is known to have a significant effect on MKL1 activity *(2.2.1.2),* we first took a look at this particular pathway. In detail, we examined whether activation or inhibition of Rho-actin signaling alters the MKL1-FLNA association. Activation of Rho-actin signaling was achieved via treatment of primary human, 3T3 fibroblasts and HepG2 human liver cells with lysophosphatidic acid (LPA). LPA is a potent lipid mediator with actions on many cell types. One prominent cellular response induced by LPA is rearrangement of the actin cytoskeleton. LPA therefore forces actin polymerization by Rho activation, resulting in stress-fiber formation (Muehlich S., Schneider N. et al, 2004; Fukushima N., Ye X. et al, 2002).

Regarding IP-binding experiments, we found that LPA stimulation promotes the amount of endogenous MKL1 that co-immuoprecipitated with endogenous FLNA in both fibroblast cell lines (Fig. 3A) and HepG2 cells (Fig. 3B).

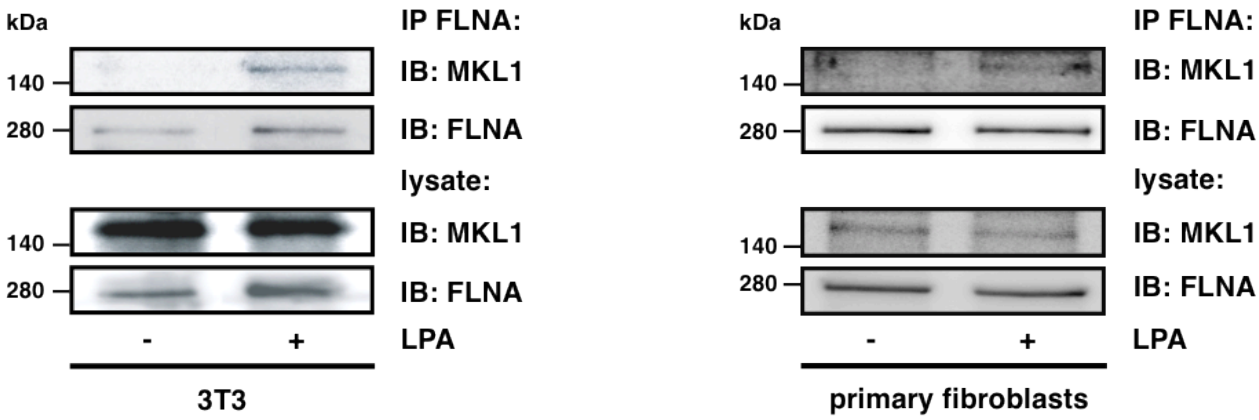

Figure 3A: Immuoprecipitation using FLNA antibody and Western blot for the indicated endogenous proteins in 3T3 fibroblasts (left) and primary human fibroblasts (right) incubated with or without 10 µM LPA for 2 hours. A portion of the cell lysate was also directly immunoblotted.

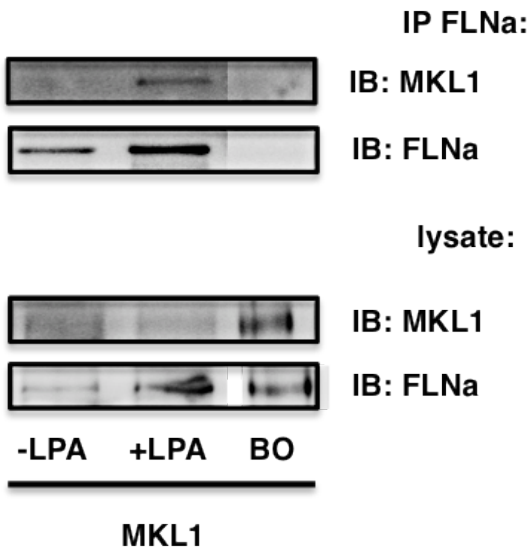

Figure 3B: Immuoprecipitation using FLNA antibody and Western blot for the indicated endogenous proteins in HepG2 cells incubated with or without 10 µM LPA for 2 hours. A portion of the cell lysate was also directly immunoblotted.

To further investigate on this phenomenon, we once again examined MKL1 localization. As anticipated, MKL1 relocated into the nucleus of primary and 3T3 fibroblasts when incubated with LPA in comparison to cytoplasmic MKL1 rest without LPA treatment (Fig. 3C). Again, this fits well with the immunoprecipitation data obtained in 3T3 and primary human fibroblasts (Fig. 3A), showing no or only little signs of interaction prior LPA treatment. Apparently, these findings also differ from the IP-binding data we obtained in cancer cells, like for instance A7 (Fig. 1D), HuH7 (Fig. 1H) or MDA MB-468 (Fig. 1H). Interestingly these cancer cells neither had to be activated to achieve MKL1-FLNA association, nor has it been necessary to force MKL1 relocation into the nucleus by prior drug treatment in A7 cells (Fig. 1J and K).

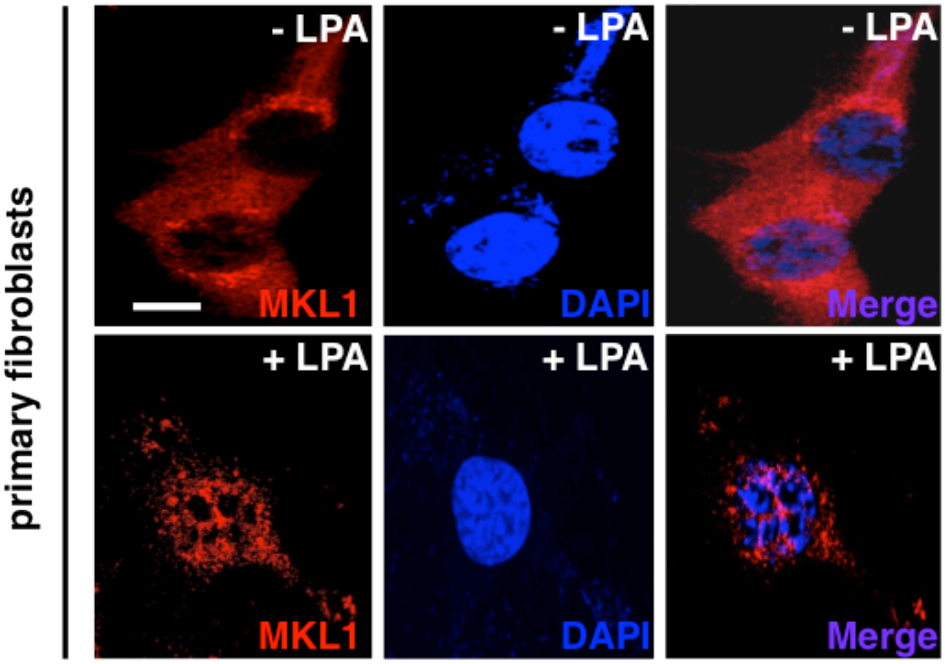

Figure 3C: Immunofluorescence analysis of MKL1 in primary fibroblasts treated with or without LPA. 4',6-Diamidino-2-phenylindole (DAPI) (blue) as nuclear counterstain. Scale bar, 200µm.

In addition, MKL1 also accumulated in the nucleus of LPA-treated, post knockdown FLNA-depleted fibroblasts, suggesting that the actual MKL1 nuclear translocation process upon LPA addition is not essentially dependent on a FLNA binding in fibroblasts (Fig. 3D).

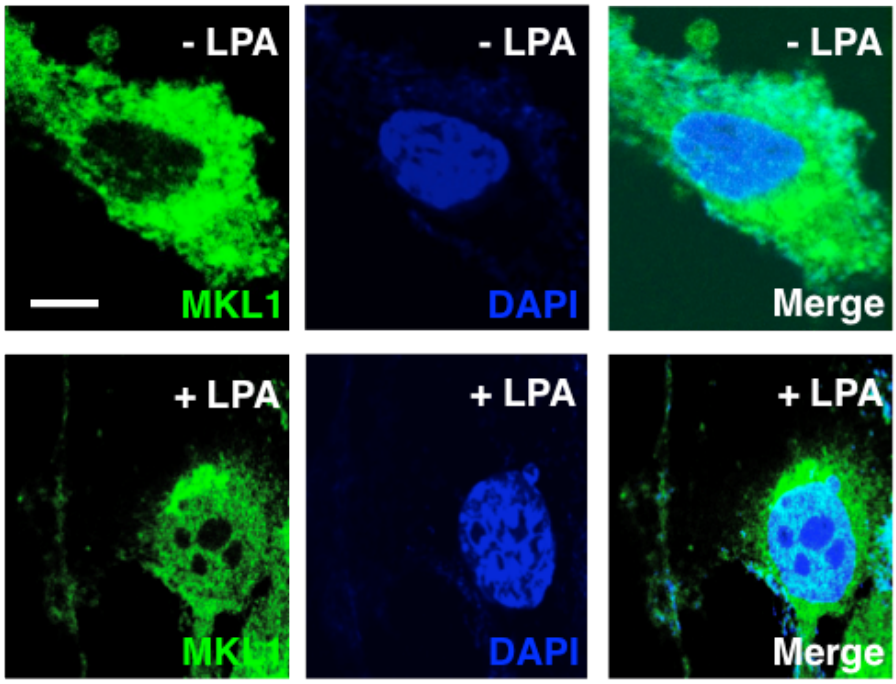

Figure 3D: Immunofluorescence with an antibody specific for MKL1 (and counterstained with DAPI) to assess the translocation of MKL1 to the nucleus upon LPA treatment in 3T3 fibroblasts expressing 50 nM FLNA siRNA. Scale bar, 200µm.

Next, we explored the functional effects implicated by the MKL1-FLNA interaction. Therefore we addressed qRT-PCR analysis. Interestingly, we found that association of endogenous MKL1 and FLNA upon LPA treatment was accompanied by the induction of the well-established MKL1 target genes *SM22, CTGF, ITGA5* and *CNN1* in primary fibroblasts (Fig. 3E).

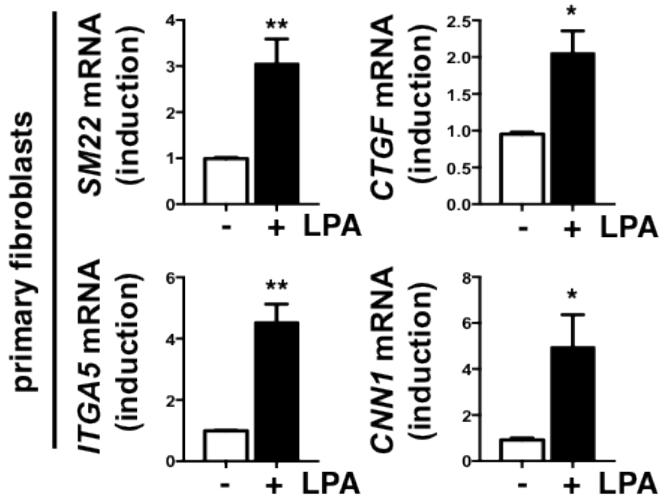

Figure 3E: Quantitative real-time polymerase chain reaction (qRT-PCR) analysis of the mRNA expression of *SM22, CTGF, ITGA5* and *CNN1* in primary human fibroblasts after 2 hours of LPA stimulation compared with controls. Data are means +/- SD (n=3 experiments). *P < 0.05, **P < 0.01, unpaired Student's t test.

After picturing the correlation between Rho-actin/LPA activation and MKL1-FLNA association we next investigated on its biological counterpart: Suppression of the interaction via utilization of an actin polymerization inhibitor. Treatment with latrunculin B (LatB) effectively blocked complex formation between MKL1 and FLNA in A7 melanoma cells and led to redistribution of MKL1 into the cytoplasm, therefore showing fibroblast-like characteristics (Fig. 3F). Strengthening our findings about cytoplasmic MKL1 re-localization, performed qRT-PCR analysis revealed an inhibitory effect by LatB incubation on the characteristic MKL1 target gene *SRF* in A7 cells (Fig. 3G). As expected, FLNA-depleted M2 cells showed no discrepancy by treatment with LatB compared to no LatB incubation. Their *SRF* levels remained low in either approach (Fig. 3G). These observations are also meshing very well with the previously achieved oppositional effect on target gene activation by LPA treatment (Fig. 3E). Additionally executed SRF reporter gene assays confirmed this data once again by delivering similar results as obtained in qRT-PCR investigations (Fig. 3H).

On a mechanistic viewpoint, LatB binds actin monomers in a one to one stoichiometry, thereby efficiently blocking binding to adenosintriphosphat (ATP), preventing actin polymerization (Yarmola E., Somasundaram T. et al, 2000). Only while bound to ATP, G-actin is able to polymerize into filamentous F-actin, this way LatB disrupts F-actin cytoskeleton formation and particularly important, forces MKL1 localization into the cytoplasm.

To sum it up, the MKL1-FLNA interaction displays a highly dynamic form of interaction which consequences in divergent levels of visible association and MKL1 localization. Moreover, it pinpoints a clear correlation between the intensity of the MKL1-FLNA interaction and the amplitude of MKL1-SRF target gene induction (Illustrated by the usage of actin drugs LPA and LatB).

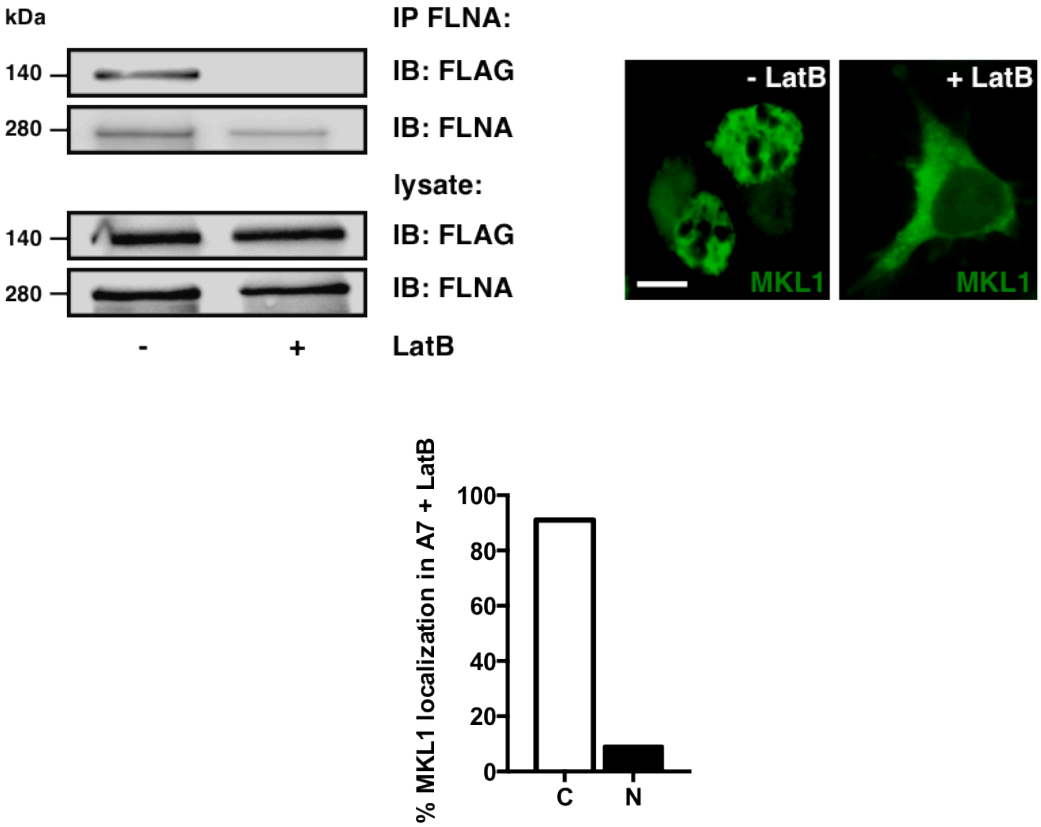

Figure 3F: (Top left) Immunoprecipitation and Western Blot as in (A) in A7 cells expressing FLAG-tagged MKL1 treated with or without 0.3 µM LatB for 45 min. (Top right) Immunofluorescence analysis of MKL1 in cells treated as in top left. Scale bar 200 µm. (Bottom) Statistical analysis of (Top right), 100 cells counted.

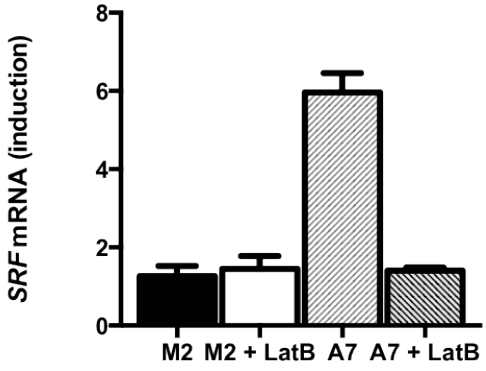

Figure 3G: A7 and M2 cells were subjected to qRT-PCR using *SRF* primers. Data are means +/- SD (n = 2). rel, relative to 18S rRNA.

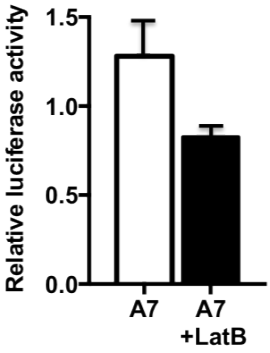

Figure 3H: Luciferase assays for 5xSRE reporter activity in A7 cells transfected with a 5xSRE reporter gene and a *Renilla* luciferase internal control vector (pRL-SV40P) and treated with or without 0.3 µM LatB for 45 min.

Work from our laboratory revealed that MKL1 phosphorylation by the kinase ERK 1/2 enhances G-actin binding to MKL1, thus leading to a significant higher rate of nuclear export (Muehlich S., Wang R. et al, 2008). For that reason we wondered weather there is a link between FLNA binding to MKL1 and a thereby forced switch from the repressive MKL1-G-actin to a MKL1-F-actin complex due to alteration of MKL1 phosphorylation status by FLNA. Phosphorylated MKL1 finds itself shifted to a slower-migrating form in SDS gels, plus it is well detectable by an antibody that specifically recognizes phosphorylated MKL1. Under experimental conditions we observed the change in mobility caused by MKL1 phosphorylation and could detect p-MKL1 in FLNA-deficient M2. In FLNA-expressing A7 cells however, no p-MKL1 signal was observable (Fig. 3I). To provide further evidence, we knocked down FLNA in A7 cells, creating a M2 cell-like environment. Consistent with the previous obtained results, the p-MKL1 signal became visible after treatment with FLNA siRNA (Fig. 3I). Taken together, these experiments provide evidence that FLNA inhibits MKL1 phosphorylation and may this way counteract the repressive MKL-G-actin complex by blocking nuclear export, thus retaining active MKL1 in the nucleus.

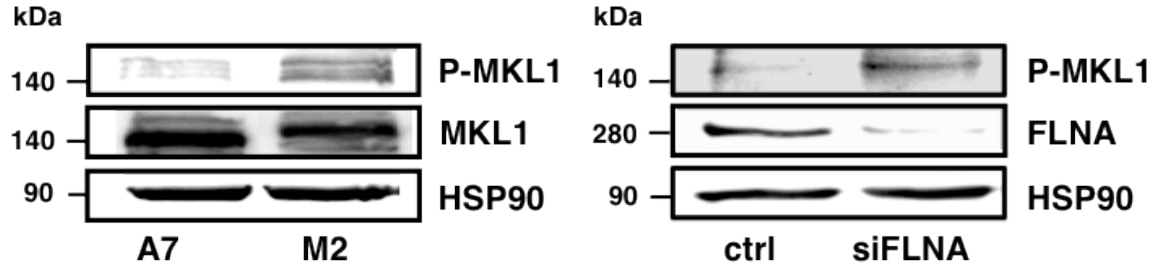

Figure 3I: Immunoblotting for the indicated proteins in A7 and M2 cells (left) and A7 cells expressing 50nM FLNA siRNA (siFLNA) (right). P-MKL1, phosphorylated MKL1.

6.4 Identification of FLNA as a transducer of actin polymerization to SRF activity

Since the MKL1-FLNA complex formation appeared to be highly dynamic on the one hand and also relied to actin dynamics on the other, we thought about examining if there is a mechanistic link between actin polymerization, FLNA and MKL1. Being a member of the actin-binding-protein class, FLNA has a compelling role in linking actin in the process of cytoskeleton dynamics (*2.4.3*). Therefore it did not come by surprise that FLNA bound an actin mutant, which does favor actin polymerization (S14C-actin). In contrast no observable interaction between FLNA and a non-polymerizing actin mutant (R62D-actin) was determined in melanoma and hepatocellular cancer cells (Fig. 4A).

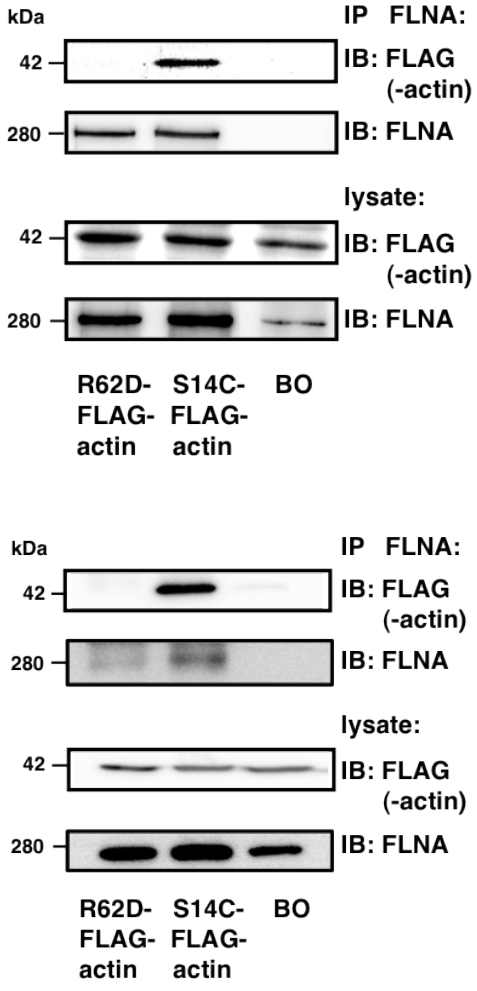

Figure 4A: Immunoprecipitation using FLNA antibody and Western Blot for the indicated proteins in A7 cells (top) and HuH7 cells (bottom) transfected with FLAG-tagged R62D-actin or S14C-actin. A portion of the cell lysate (bottom) was immunoblotted. BO, beads only.

Next, we expressed MKL1 and the indicated actin mutant. Remarkably, we found that FLNA was required for an association between the actin mutant favoring actin polymerization (S14C-actin) and MKL1. We were able to co-immunoprecipitate S14C-actin with MKL1 in FLNA-expressing A7 cells, but however not in FLNA-deficient M2 cells (Fig. 4B). As expected, binding of the non-polymerizable actin mutant (R62D-actin) to MKL1 was detectable in both FLNA-expressing and FLNA-deficient cells (Fig. 4B). To strengthen the achieved results, we went on and reintroduced FLNA into FLNA-deficient M2 cells. As a result, rescuing of the S14C-actin-MKL1 binding was obtained (Fig. 4B), which further marked the specificity of the effect. Endogenic complex analysis in LPA stimulated 3T3 fibroblasts revealed similar results by displaying complex formation of FLNA, MKL1 and S14C-actin in contrast to monomeric R62D-actin transfection, where no such interaction was observable (Fig. 4C). To further address MKL1-FLNA-actin forming complex issues and in particular FLNAs role, we designed an experiment comparing wt-MKL1 and MKL1 Δ301-380 binding to GFP-actin, which comprises monomeric G-actin and polymerized F-actin. Interestingly, MKL1 Δ301-380, which is not able to bind FLNA, displayed weaker GFP-actin binding patterns then wt-MKL1 did (Fig. 4D).

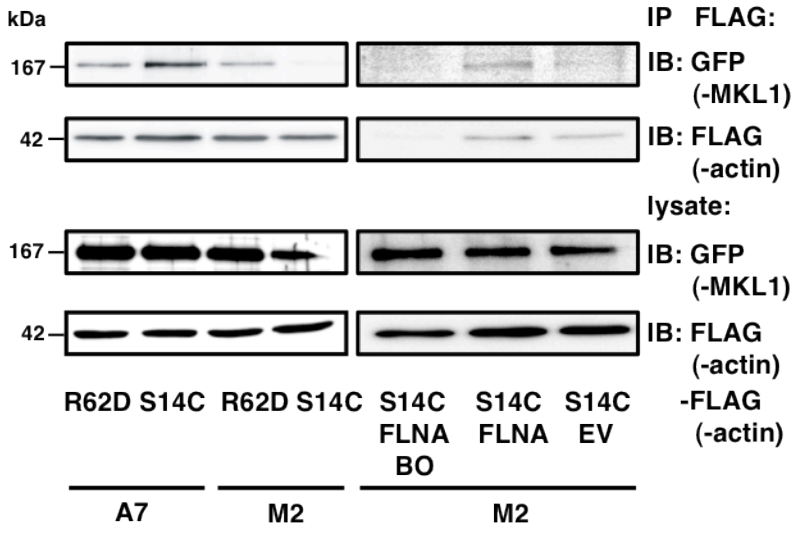

Figure 4B: Immunoprecipitation and Western Blot as in (A) in A7 and M2 cells transfected with GFP-MKL1 and FLAG-R62D-actin or FLAG-S14C-actin. Separate cultures of M2 cells transfected as described were reconstituted with myc-tagged FLNA or an empty vector (EV).

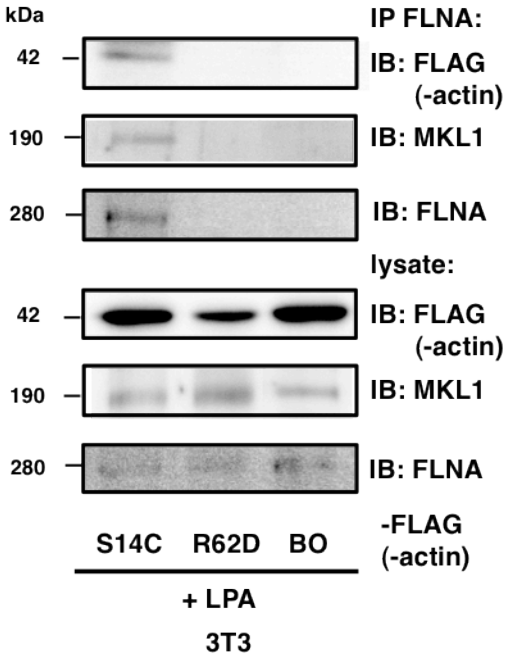

Figure 4C: Immunoprecipitation and Western Blot as in (A) in LPA stimulated (2h) 3T3 fibroblast cells, transfected with FLAG-R62D-actin or FLAG-S14C-actin.

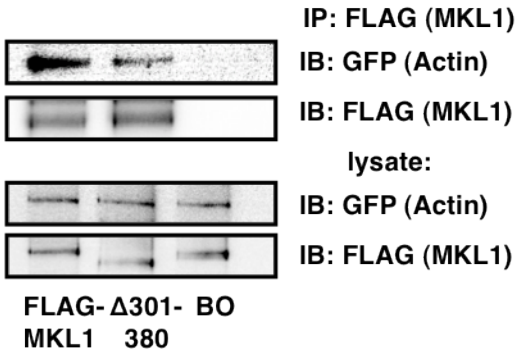

Figure 4D: Immunoprecipitation and Western Blot as in (A) in A7 cells transfected with GFP-actin and FLAG-MKL1.

To put this data in context, we hypothesized FLNA as a transducer, which efficiently converts the signal of polymerized actin into SRF activation by mediating an association between polymerized actin and MKL1. To further investigate this concept, we performed reporter gene assays with 5 x SRE reporter gene and the F-actin-formation-favoring S14C-actin mutant and secondly screened the effective polymerization ability of this mutant by submitting it to immunocytochemistry. We chose a 5 x SRE, which SRF is connecting to, this way presenting an excellent option to measure its activity. Flag-tagged S14C-actin enabled

the identification of transfected cells using microscopy with FLAG antibody and phalloidin, which specifically binds F-actin. As a result, compared to surrounding un-transfected cells, A7 cells transfected with S14C-actin displayed enhanced actin polymerization (Fig. 4E).

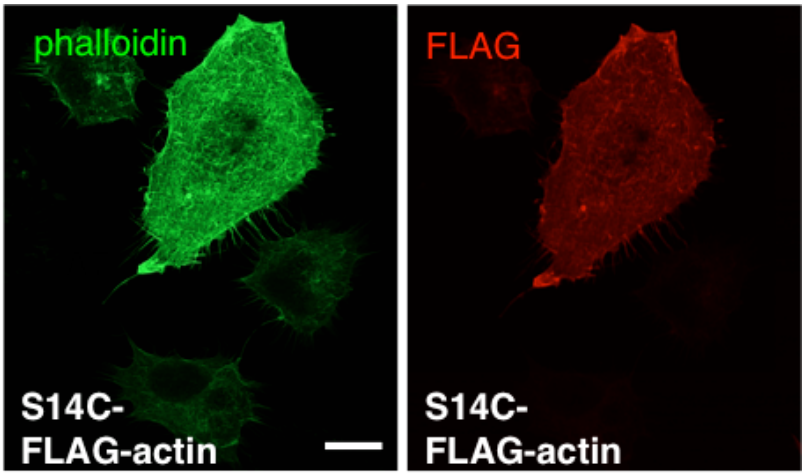

Figure 4E: Immunofluorescence analysis of phalloidin or FLAG in A7 cells transfected with FLAG-S14C-actin. Scale bar, 200 µm.

Regarding reporter gene assay results we experienced a 13-fold induction of luciferase activity in S14C-actin and FLNA expressing cells compared to the only slight increase in luciferase expression in S14C-actin-expressing but FLNA-deficient cells (Fig. 4F).

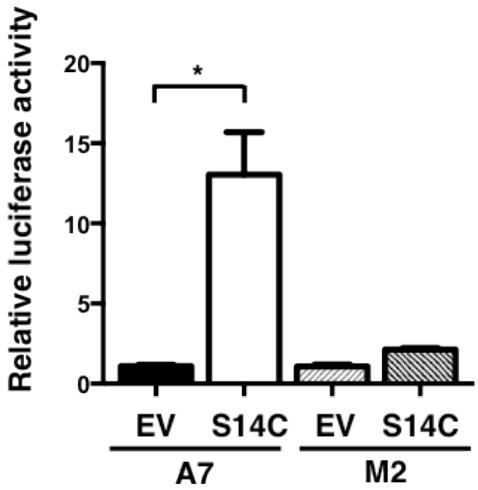

Figure 4F: Luciferase assays for 5xSRE reporter activity in A7 or M2 cells transfected with FLAG-S14C-actin or EV along with a 5xSRE reporter gene and a *Renilla* luciferase internal control vector (pRL-SV40P). Data are means +/- SD (n=3). *P < 0.05, unpaired Student's t test.

This data provides first evidence that FLNA plays an important role in actin-dependent SRF activation. To reinforce these results, we performed the same assay setup including Jasplakinolide, a substance originally isolated by marine sponge, to force actin polymerization. Jasplakinolide causes F-actin stabilization and stimulation of actin filament nucleation, this way decreasing cellular G-actin pool quantity. It furthermore differs from other actin stabilizers by showing exceptional cell permeability (Bubb R., Spector I. et al, 2000). As a result, Jasplakinolide treatment led to an enhanced luciferase activity in A7 cells, but not in FLNA depleted M2 cells, similar to the data obtained in Fig. 4F (Fig. 4G). Moreover, and to once again prove the dynamic nature of the occurring process, we reconstituted M2 cells with different amounts of FLNA, which led to a step-by-step restoration of SRF activity (Fig. 4H). In general and consistent with the previous obtained data, reporter gene assays revealed a 5-fold induction difference in untreated A7 versus M2 cells (Fig. 4I). After proving the sensitive impact available FLNA quantity has on SRF activity, we addressed questions regarding similar fine dosing effects caused by MKL1 involvement. In context with the results achieved by FLNA, 5 x SRE activity raised when melanoma cells where treated with increasing amounts of MKL1 in a step-by-step manner (Fig. 4J)

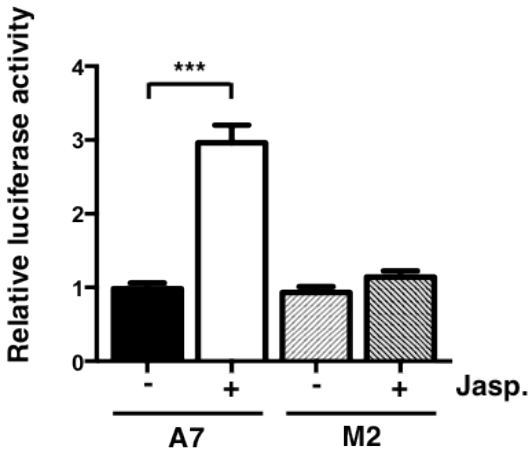

Figure 4G: Luciferase assay performed as in (F) in A7 and M2 cells treated with or without 0.5 µM Jasplakinolide (Jasp.) for 7 hours. *** P < 0.001, unpaired Student's t test.

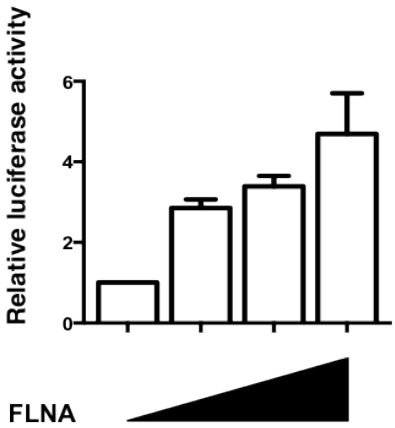

Figure 4H: Luciferase assays performed as in (F) in M2 cells expressing increasing amounts of FLNA expressing vector and a 5xSRE reporter gene.

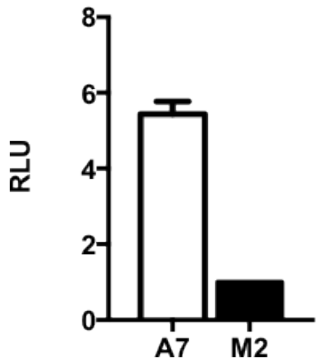

Figure 4I: Luciferase assays performed as in (F) in M2 and A7 cells

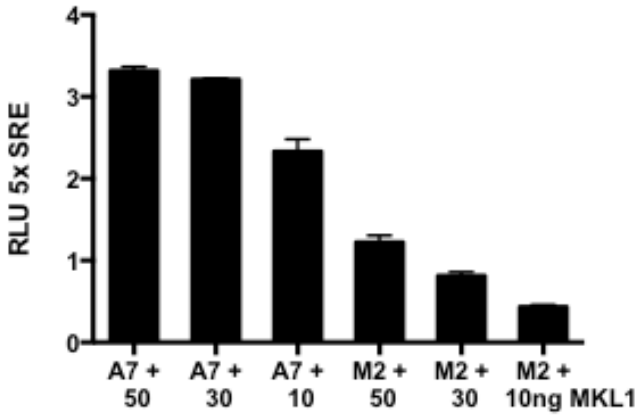

Figure 4J: Luciferase assays performed as in (F) in M2 and A7 cells expressing increasing amounts of MKL1.

Compared to the fine-meshed actin network construct in A7 cells, achieved by S14C-Flag-actin transfection, no network formation was detectable in FLNA-deficient M2 cells post transfection (Fig. 4K). Together with the other results displayed in chis chapter, these findings support the theory that actin polymerization requires FLNA.

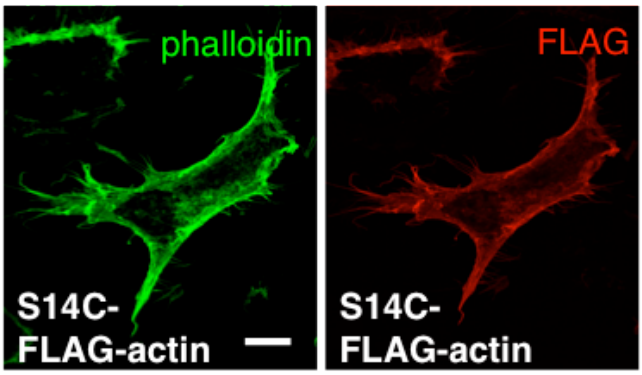

Figure 4K: Immunofluorescence analysis using phalloidin or FLAG antibody in M2 cells transfected with S14C-FLAG-actin. Scale bar, 200µm.

On a further note, Baarlink C. et al (2013) showed that MKL1-SRF activation is in need of nuclear actin polymerization, driven by the formin mDia. To additional increase our knowledge about actin network formation and to clarify weather nuclear actin polymerization requires FLNA, we expressed a constitutively active version of mDia1 (Dia1ct) that displays predominant nuclear localization and causes increased nuclear actin assembly. Interestingly, only FLNA-expressing A7 cells reacted with a 8-fold increase in SRF-dependent transcriptional activity when compared to mock transfections (Fig. 4L), further suggesting that nuclear actin polymerization requires FLNA for MKL1 activation. Together these results are compatible with the concept that FLNA couples actin polymerization to MKL1-SRF transcriptional activity.

After investigating nuclear F-actins role, we analyzed its monomeric counterpart, G-actin. We performed SRF reporter gene assays including NLS-R62D-actin, a R62D-actin mutant that constitutively localizes to the nucleus The NLS-R62D-actin dose was increased in a step-by-step manner, which led to an expected reduction of SRF reporter activity in FLNA expressing melanoma cells (Fig. 4M and N). Next, we extended the assay setup by introducing mDia-ct, a constitutively nuclear active mDia mutant or mDia-NES, causing increased cytoplasmic actin assembly to the experiment. Nuclear formin was able to counteract the repressive nuclear G-actin effect in a certain manner, this way retaining luciferase activity on higher

levels (Fig. 4M) in contrast to treatment with cytoplasmic formin in FLNA expressing melanoma cells, where luciferase activity remained on a lower level (Fig. 4N). FLNA depleted M2 melanoma cells remained at minor-level reporter gene activity throughout the experiment (Fig 4M and N).

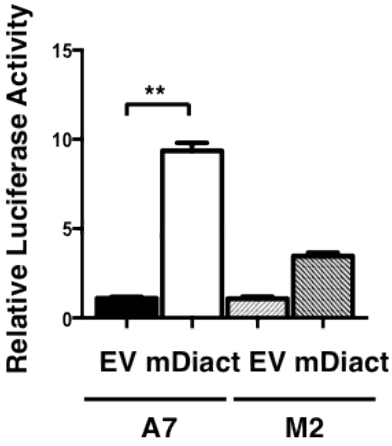

Figure 4L: mDiact expression vector (mDiact) or empty vector (EV) were transfected into A7 and M2 cells and luciferase assays carried out as described before.

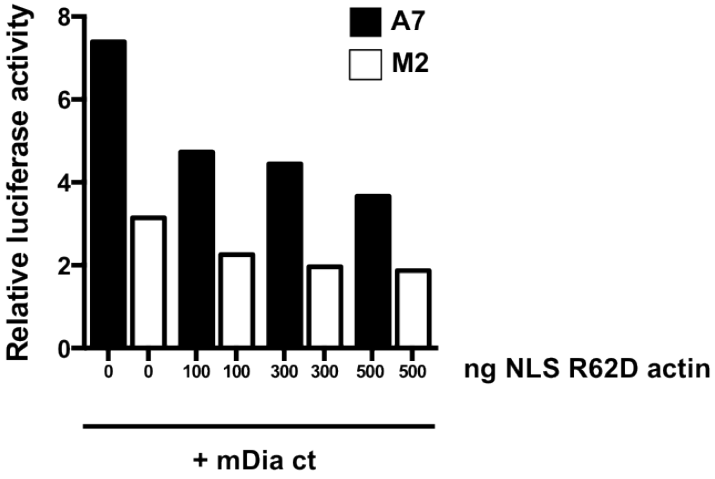

Figure 4M: mDiact expression vector and the stated amount of NLS R62D actin were transfected into A7 and M2 cells and luciferase assays carried out as described before.

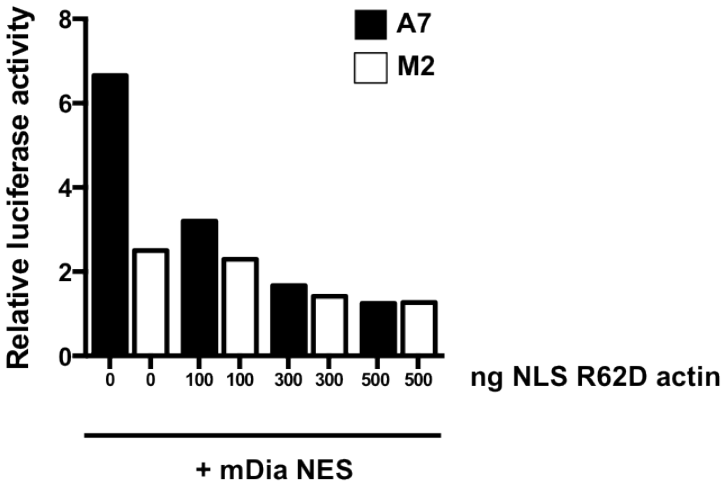

Figure 4N: mDia NES expression vector and the stated amount of NLS R62D actin were transfected into A7 and M2 cells and luciferase assays carried out as described before.

6.5 Interaction of FLNA and MKL1 in cell migration and invasion

Both, MKL1 and its new binding partner FLNA are known for their tremendous and autonomous influence in the broad field of migrating procedures (*2.2, 2.4.3*). This obviously raises the question if FLNA plays a valuable role in MKL1 mediated cellular functions, such as the above-mentioned migration. To address this issue in an experimental way, we first chose a setup devoting RNA interference (RNAi) and therefore the effect of MKL1 and FLNA depletion on cell migration. Expression of MKL1 and FLNA at the protein level was reduced by 90 % post knockdown (Fig. 5A).

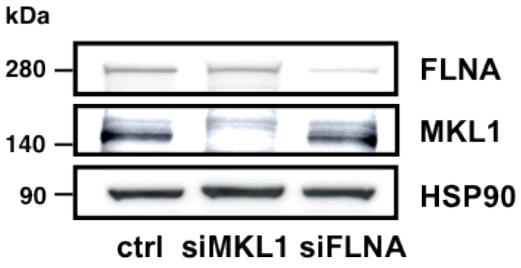

Figure 5A: Knockdown efficiencies. Cell migration (assessed by a culture scratch-wound assay) by A7 cells transfected with 50nM negative control siRNA (ctrl), 50 nM FLNA siRNA (siFLNA), or 50 nM MKL1 siRNA (siMKL1).

As described in *2.4.3*, filopodia hold a crucial role in terms of cell mobility. This tempted us to take a closer look at the appearance of these slender projections composed of cross-linked actin bundles by FLNA. Interestingly, filopodia presence in A7 melanoma cells was reduced up to 30 % after MKL1 and FLNA knockdown in comparison to the control (Fig. 5B and C).

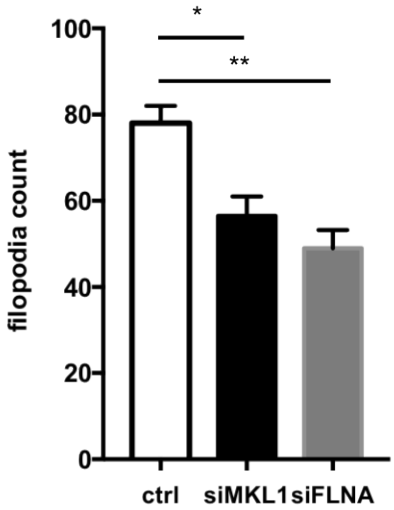

Figure 5B: Filopodia appearance in A7 cells. Cells transfected with 50nM negative control siRNA (ctrl), 50 nM FLNA siRNA (siFLNA), or 50 nM MKL1 siRNA (siMKL1). n=3 experiments, 100 cells counted.

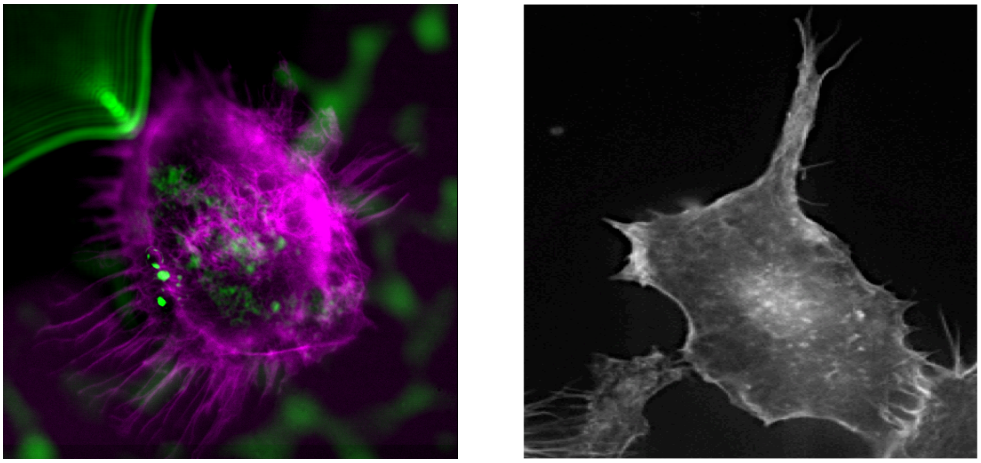

Figure 5C: Filopodia appearance in A7 cells. Immunofluorescence analysis using phalloidin. Cells transfected with (left) 50nM negative control siRNA (ctrl) or (right) 50nM FLNA siRNA (siFLNA), n=3 experiments, 100 cells counted. Representative picture

To investigate cell migration in detail, we took advantage of wound-healing-scratch assays. 24 hours post scratch creation, control cells succeeded in closing the wound gap entirely while siMKL1 and siFLNA treated cells clearly were not (Fig. 5D).

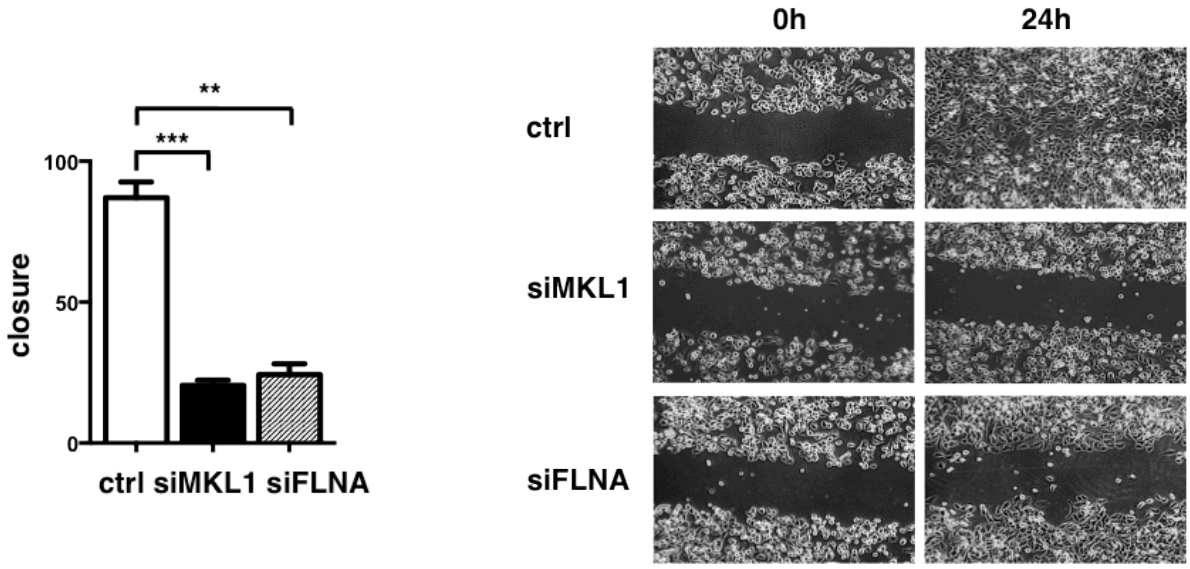

Figure 5D: Cell migration (assessed by a culture scratch-wound assay) by A7 cells transfected with 50nM negative control siRNA (ctrl), 50 nM FLNA siRNA (siFLNA), or 50 nM MKL1 siRNA (siMKL1). Data are means +/- SD (n=3 experiments). ** P < 0.01, *** P < 0.001. (Right) Representative images.

Next, we shifted focus on a possible synergetic effect of MKL1 and FLNA regarding migratory events. Interestingly, reintroduction of siRNA-resistant wild-type MKL1, but not siRNA-resistant mutant MKL1 Δ301-380 or Δ301-342, which are unable to interact with FLNA, partly restored the migrating ability of A7 melanoma cells depleted of endogenous MKL1 (Fig. 5E). Identically results were obtained from HuH7 hepatocellular carcinoma cells (Fig. 5E) and are displayed as a representative example for A7 cells including wild-type-MKL1, MKL1 Δ301-380 and an empty vector as control (Fig. 5F). These data suggests that MKL1 orchestrates cell migration in concert with FLNA.

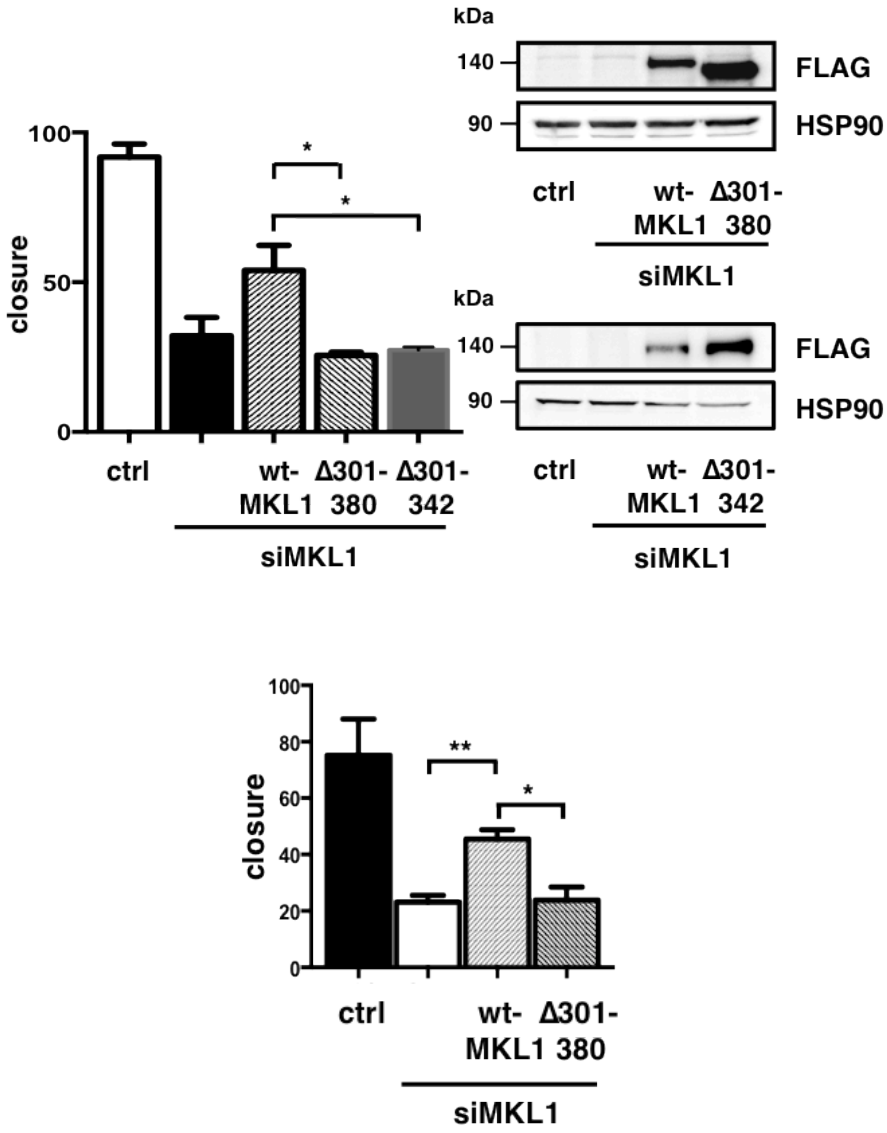

Figure 5E: Cell migration assessed as in (D) by A7 cells (top) and HuH7 cells (bottom) transfected with 50 nM negative control siRNA (ctrl) or 50 nM MKL1 siRNA (siMKL1) and reconstituted with FLAG-tagged WT MKL1, MKL1 Δ301-380 or Δ301-342, confirmed by Western Blot. Data are means +/- SD (n= 3). *P < 0.05, ** P < 0.01.

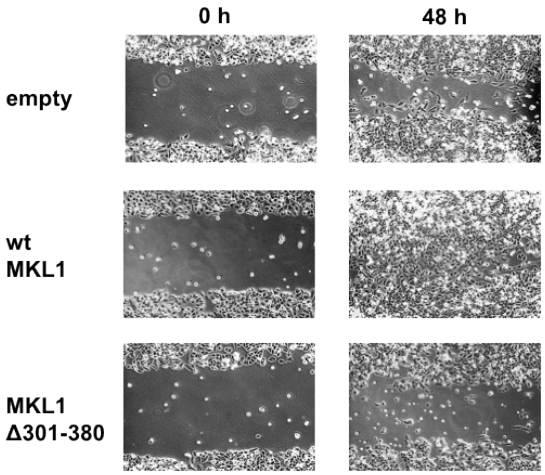

Figure 5F: Cell migration assessed as described in 5E. Representative images from A7 cells are shown.

Together with the fact that migration and invasion share a descent amount of specific characteristics we wanted to know about possible effects of the FLNA-MKL1 interaction on invasive cell migration. For that reason we introduced Transwell invasion assays. A7 melanoma cells were allowed to penetrate through a three-dimensional Matrigel propelled by a cell medium gradient. As a result, invasive migration of A7 cells was strongly reduced in the absence of MKL1 (Fig. 5G). Even more important and in match with our previously obtained results in scratch-wound assays, reconstitution with siRNA-resistant wild-type MKL1 enhanced the invasive nature of MKL1 siRNA-expressing A7 cells, while on the other hand invasive cell migration remained nearly unchanged upon reconstitution with siRNA-resistant MKL1 Δ301-380, proving once again that FLNA promotes MKL1-dependent cell motility (Fig. 5G).

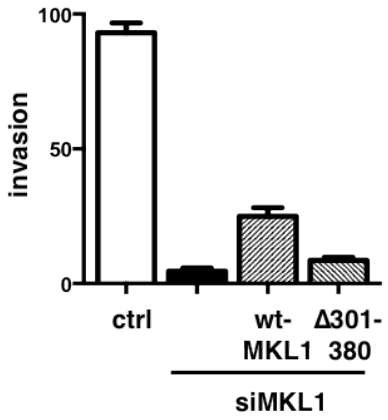

Figure 5G: Cell invasion, assessed by a three-dimensional Matrigel invasion assay, by A7 cells transfected with 50 nM negative control siRNA (ctrl) or 50 nM MKL1 siRNA (siMKL1) and reconstituted with FLAG-tagged WT or mutant MKL1.

6.6 Interaction of FLNA and MKL1 in the expression of MKL1 target genes

Besides its large variety of influences on biological functionality, MKL1's core task is operating transcriptional activity. Therefore with the introduction of a new interaction partner, it was key to us to tie the knot on our research by having a more in detail look on the impact of the FLNA-MKL1 interaction on the transcriptional activity of MKL1. We first investigated the effect of FLNA on the expression of established MKL1 target genes, such as *SRF, CTGF, SM22*, *ITGA5, FHL2* and *TGF-beta* (Schmidt L., Duncan K. et al, 2012; Elberg G., Chen L., et al, 2008; Cheng X., Yang Y., et al 2015) by once again turning to FLNA expressing A7 cells and FLNA deficient M2 cells. Expression of *SRF, CTGF, SM22, ITGA5, FHL2* and *TGF-beta* was strongly inhibited in M2 cells lacking FLNA (Fig. 6A).

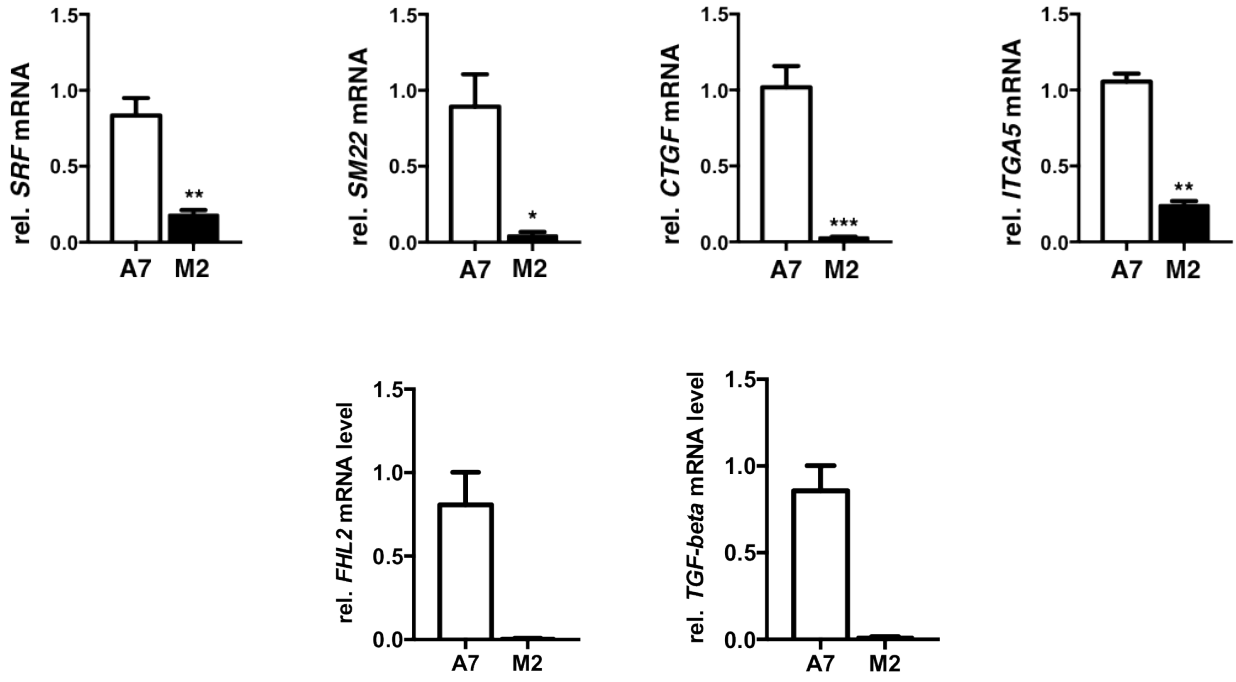

Figure 6A: A7 and M2 cells were subjected to qRT-PCR using *SRF, CTGF, SM22*, *ITGA5, FHL2 and TGF-beta* primers. Data are means +/- SD (n = 3 experiments*, FHL2* and *TGF-beta* n = 2). * P < 0.05, ** P < 0.01, *** P < 0.001. rel, relative to 18S rRNA.

To further support these findings that FLNA deficiency accounts for impaired MKL1-dependent target gene expression we silenced FLNA in MEFs (Fig. 6B) and A7 cells (Fig. 6C) using RNA interference. In line with the data obtained from A7 and M2 cells, silencing of

FLNA expression in MEFs and A7 resulted in a strong reduction of *FLNA*, *SRF, SM22, CTGF*, *ITGA5, TGF-beta* and *FHL2* expression (Fig. 6B and C). To underline the observed results we continued addressing MKL1 target gene expression by looking at protein levels. Western Blot analysis revealed a strong abolishment of *SM22* protein levels after again silencing FLNA (Fig. 6D). Drexler M. and Nossek M achieved similar results investigating on *CTGF* and *ITGA5* (Kircher P., Hermanns C. et al, 2015). Additionally, after MKL1 knockdown, SRF protein levels were decreased and totally revoked after a combined MKL1 and FLNA knockdown in A7 cells hinting at a synergetic effect of MKL1 and FLNA regarding target gene expression (Fig. 6E).

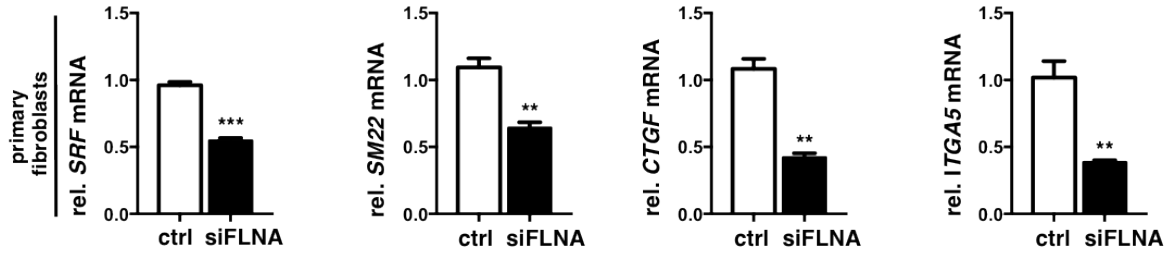

Figure 6B: MEF cells were subjected to qRT-PCR using *SRF, CTGF, SM22* and *ITGA5* primers. Transfection with negative control siRNA (ctrl) or 50 nM FLNA siRNA (siFLNA). Data are means + / - SD (n=3). ** P < 0.01, *** P < 0.001. rel, relative to 18S rRNA.

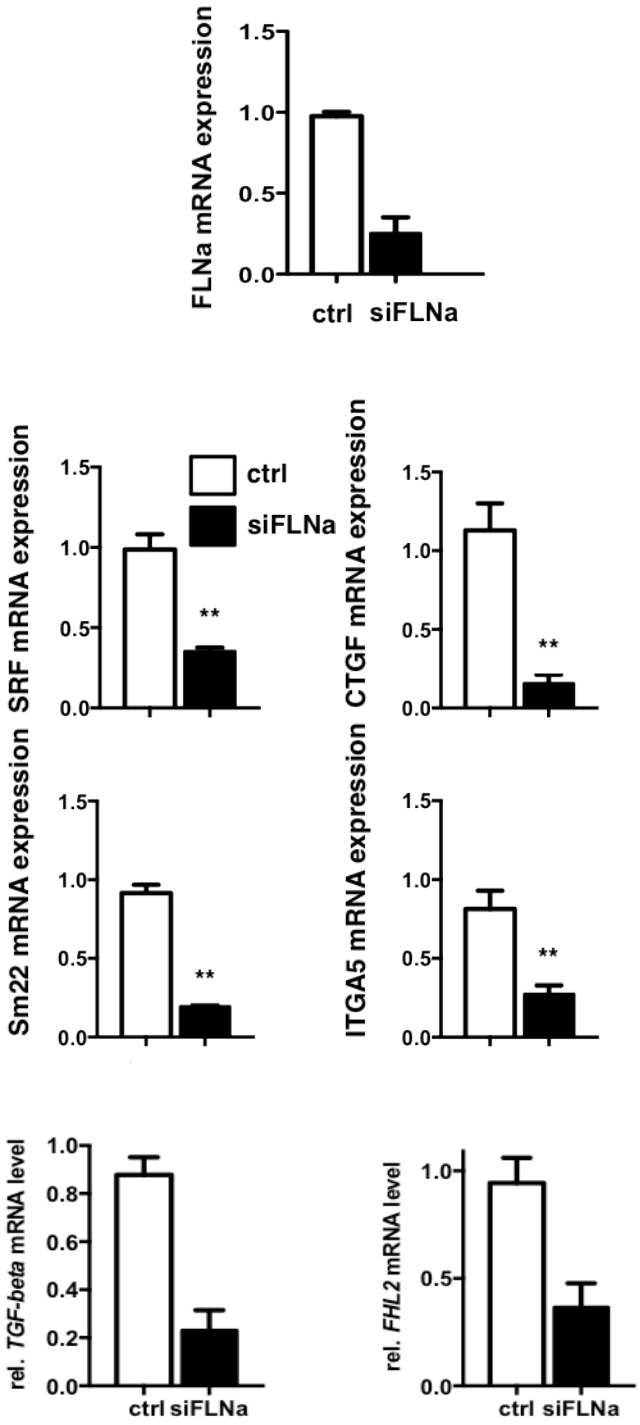

Figure 6C: A7 cells were subjected to qRT-PCR using *FLNA*, *SRF, CTGF, SM22, ITGA5, TGF-beta and FHL2* primers. Transfection with negative control siRNA (ctrl) or 50 nM FLNA siRNA (siFLNA). Data are means + / - SD (n=3, *TGF-beta* and *FHL2* n = 2). ** P < 0.01. rel, relative to 18S rRNA.

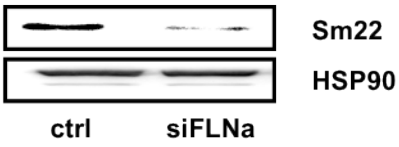

Figure 6D: A7 cells were subjected to Western Blot analysis. Transfection with negative control siRNA (ctrl) or 50 nM FLNA siRNA (siFLNA)

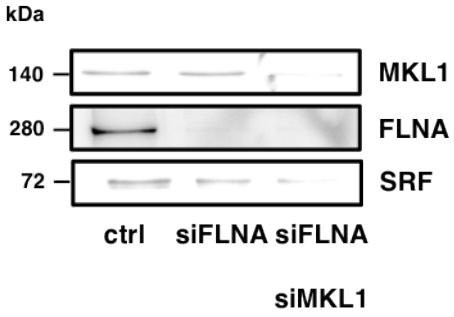

Figure 6E: A7 cells were subjected to Western Blot analysis. Transfection with negative control siRNA (ctrl) or 50 nM FLNA siRNA (siFLNA) or 50 nM MKL1 siRNA (siMKL1).

To further validate that FLNA deficiency directly accounts for the impaired MKL/SRF expression, we depleted FLNA expression in A7 melanoma cells in a step-by-step manner. When increasing amounts of FLNA siRNA were transfected, SRF expression decreased simultaneously, further confirming a straightforward correlation between FLNA and SRF expression (Fig. 6F).

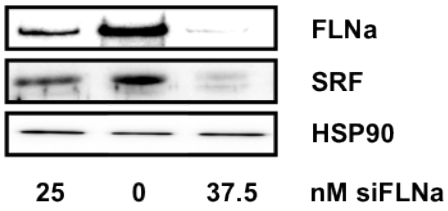

Figure 6F: A7 cells were subjected to Western Blot analysis. Transfection with 50 nM FLNA siRNA (siFLNA).

Hermanns C. found that *GLIPR1* and *CNN1* represent novel MKL1-dependent target genes because of their notably reduced expression upon MKL1 depletion (Kircher P., Hermanns C. et al, 2015). Similar observations as in Fig. 6B were made for primary human and 3T3 fibroblasts as well as for HuH7 hepatocellular carcinoma cells depleted of FLNA (Fig. 6G).

Hermanns C. added data for HepG2 hepatocellular carcinoma cells, 3T3 fibroblasts and MDA-MB-468 mammary carcinoma (Kircher P., Hermanns C. et al, 2015).

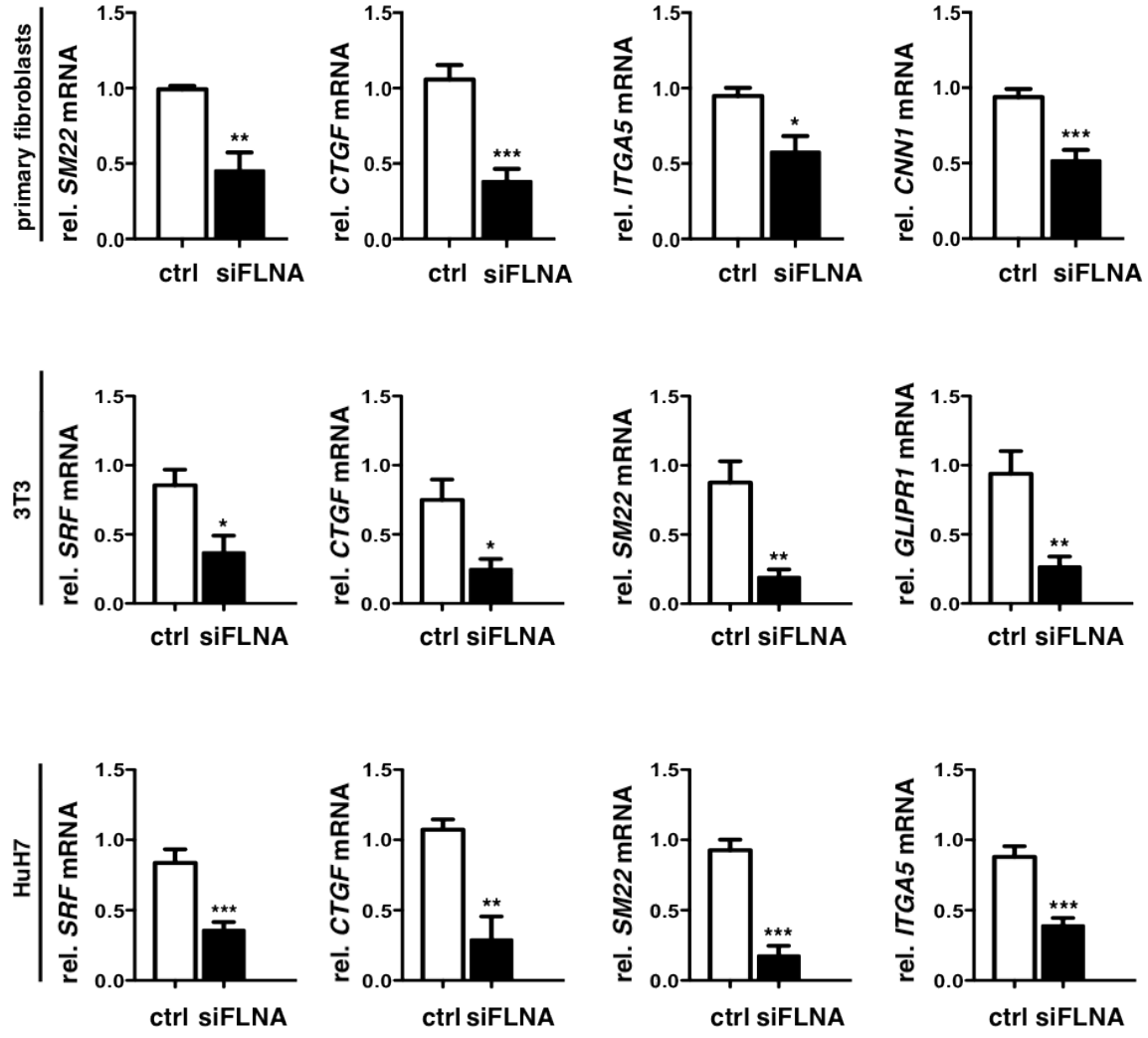

Figure 6G: Primary human, 3T3 fibroblasts and HuH7 cells were subjected to qRT-PCR using *SRF, CTGF, SM22*, *ITGA5* and *GLIPR1* primers. Transfection with negative control siRNA (ctrl) or 50 nM FLNA siRNA (siFLNA). Data are means +/- SD (n=3). * P < 0.05, ** P < 0.01, *** P < 0.001. rel, relative to 18S rRNA.

Since all these findings caused by FLNA silencing primary aim on a repressive effect, we wanted to know whether FLNA introduction in turn induces MKL1-SRF dependent target gene expression. FLNA overexpression strongly activated the expression of MKL1-SRF target genes, which was prevented by knocking down SRF or MKL1 (Fig. 6H). These results demonstrate the SRF and MKL1 dependency of FLNA-induced target gene expression.

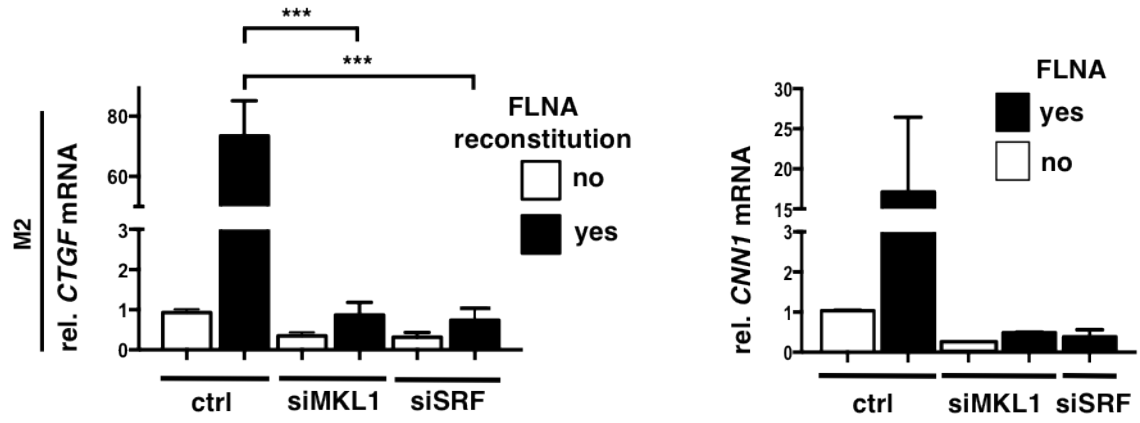

Figure 6H: CTGF (left) and CNN1 (right) mRNA expression, determined by qRT-PCR as in (A), in M2 cells expressing negative control siRNA (ctrl), 50 nM MKL1 siRNA (siMKL1), or 50 nM SRF siRNA (siSRF) and reconstituted with myc-FLNA. Data are means +/- SD (n=3). *** P < 0.001.

Investigations with the help of reporter gene assays with 5 x SRE reporter gene including constitutively active MKL1 (MKL1 N100) led to similar results. Luciferase activity proved to be FLNA-dependent because it was strongly reduced in FLNA-deficient cells compared to FLNA-expressing cells (Fig. 6I). Hermanns C. fortified the data by qRT-PCR experiments (Kircher P., Hermanns C. et al, 2015).

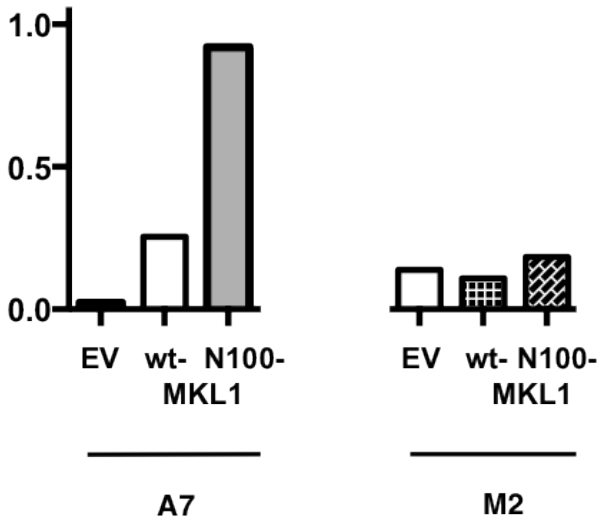

Figure 6I: Luciferase assays for 5 x SRE reporter activity in A7 or M2 cells transfected with FLAG-wt-MKL1, FLAG-N100-MKL1 or EV along with a 5 x SRE reporter gene and a *Renilla* luciferase internal control vector (pRL-SV40P).

To ultimately reach our goal, linking FLNA-MKL1 symbiosis to MKL1 target gene expression, we last but not least tested whether introduction of the MKL1 mutants unable to bind FLNA would also affect the transcription of MKL1 target genes. Indeed, expression of *SM22* and *CTGF* mRNA was clearly reduced in the presence of the MKL1 mutants Δ301-380, Δ301-342 and Δ301-310 (Fig. 6J).

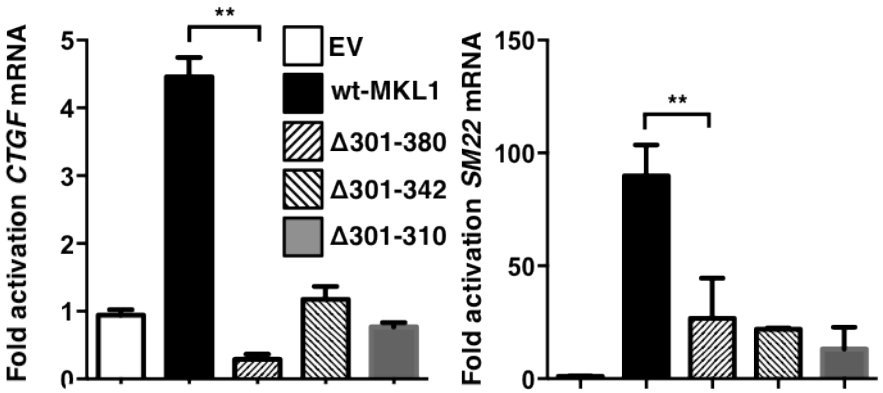

Figure 6J: The abundance of CTGF and SM22 mRNA in A7 cells transfected with FLAG-MKL1, MKL1 Δ301-380, MKL1 Δ301-342 and MKL1 Δ301-310 or EV for 48 hours, as analysed by qRT-PCR. Data are means +/- SD (n=3). ** P < 0.01.

7 Discussion

7.1 Identification of a novel MKL1 interacting protein: Impact of the new MKL1-FLNA interaction on cellular functions

7.1.1 Consequences and biological effects of the MKL1-FLNA binding

The goal of this thesis was to shed light on the interaction between the co-activator MKL1 and the actin-binding protein FLNA and furthermore to examine the biological effects of this association in order to reveal its linked physiological and pathophysiological function. We found a new mechanism of MKL1 activation that is mediated through its binding to FLNA. The interaction is required for the expression of MKL1 target genes and MKL1-dependent cell motility. Cells expressing a MKL1 mutant unable to bind FLNA exhibited impaired cell migration and invasion along with reduced MKL1 target gene expression. Increased or decreased MKL1-FLNA interaction correlated with induction and repression of MKL1 target genes, and protein levels respectively. Therefore, we provide evidence that the association not only is strictly sensitive to the available amounts of MKL1 and FLNA, but moreover we are able to define the interaction as highly dynamic (Kircher P., Hermanns C. et al, 2015).

We were able to present a somewhat weaker interaction between MKL2 and FLNA as well. This discrepancy between MKL1 and 2 regarding binding properties could be a result of MKL2 consisting of three RPEL domains in contrast to the two of MKL1 (Cen B., Selvaraj A. et al, 2003). We hypothesize that the extra RPEL domain provides additional affinity for G-actin to successfully interact with MKL2, this way stronger inhibiting nuclear entrance and association with FLNA.

Furthermore, after confirming the interaction between MKL1 and FLNA, we identified the necessary binding zones on both proteins, picturing a complex pattern of interaction, which involves multiple regions. We investigated the association between MKL1 and FLNA in different physiological and cancer cell lines. In total we used melanoma, hepatocellular carcinoma, mammary carcinoma as well as primary murine, primary human and 3T3 fibroblast cell lines as physiological cell representatives to highlight the interactions

existence and its broad significance for the first time (Kircher P., Hermanns C. et al, 2015). For the sake of completeness one has to mention that not all examined cell lines fortified a functioning interaction. We discovered that hepatocellular cancer cells (HLF) and human embryonic kidney cells (HEK-293) witnessed no or only a rather weak detectable interaction. It is possible that the respectively low amounts of total MKL1 or FLNA expressed in these cells affect the MKL1-FLNA interaction in this scenario. Still, the possibility of an actual interaction occurring in these cell lines might not be totally ruled out under certain circumstances (eg cellular stress, diseases).

7.1.2 Localization of the MKL1-FLNA binding and potential DLC1 influence

We found that MKL1 and FLNA co-localized predominantly in the nucleus in A7 melanoma cells as well as in fibroblasts after LPA stimulation, while FLNA-depleted M2 melanoma cells and FLNA knockdown treated A7 cells displayed cytoplasmic MKL1 localization. This hints at FLNA maybe holding MKL1 in the nucleus, which will be discussed in greater detail in the later paragraphs of this chapter. Nuclear MKL1 localization is especially important, since co-activator functionality and cellular localization are tightly connected (Miralles F., Posern G. et al, 2003). The transcriptional machinery is in desperate need of a nuclear-based co-activator before getting started. This demand for a catalyser is perfectly fulfilled by MKL1 in its active nuclear condition.

Regarding FLNA localization these findings likewise fit well with literature knowledge, since a large amount of nuclear FLNA in A7 melanoma cells has been described previously (Berry F., O'Neill M. et al, 2005). In an additional manner, prior studies of our group revealed nuclear localization of MKL1 in tumor cells lacking the tumor suppressor DLC1, while DLC1 expressing cells display MKL1 in the cytoplasm (Hampl V., Martin C. et al, 2013; Muehlich S., Hampl V. et al, 2012). Consistent with our novel findings of no observable interaction of MKL1 and FLNA in DLC1-expressing cells, like HLF cells, these results offer room for speculation about an exclusive nuclear MKL1-FLNA complex formation in absence of DLC1. The interaction of the transcription factor FOXC1 with FLNA, which also exclusively takes place in the nucleus strengthens this theory (Berry F., O'Neill M. et al, 2005). Hampl V. and colleagues furthermore linked DLC1 depletion to a strong formation of F-actin network and MKL1 activity (2013). This leads to a theory about connectivity of DLC1 loss and increased FLNA activity. Furthermore, restoration of DLC1 in DLC1-deficient cells resulted in

suppression of *CTGF* expression (Hampl V., Martin C. et al, 2013), similar to the data obtained in the present work through FLNA knockdown. It is tempting to speculate that FLNA works as an antagonist to regular DLC1 activity. Nevertheless, future investigations will definitely be necessary to deliver the missing piece of a possible FLNA-DLC1 connection. Since we were able to figure out that FLNA is also representing a direct target gene of MKL1, one proposal for further analysis concerning that topic would be the usage of DLC1 knockdown experiments followed by measurements on FLNA expression levels. If our thoughts are correct, DLC1 knockdown should lead to up-regulated FLNA levels.

7.1.3 MKL1 shuttling affected by FLNA?

MKL1-shutteling in and out of the nucleus is known to be governed by actin treadmilling, phosphorylation status, RhoA activity, DLC1 expression, appearance of external stimulation signals, cellular stress or diseases and last but not least sources in two totally different cell environments, notably the nucleus and the cytoplasm (Muehlich S., Wang R. et al, 2008; Cen B., Selvaraj A. et al, 2004; Vartiainen M., Guettler S. et al, 2007; Posern G., Treisman R. 2006). As one can obviously sense, a fairly high number of parameters are in charge for operating this complex program.

Our investigations hint at yet another factor coming into play. We suggest a link between FLNA appearance and MKL1-shutteling and localization, since both proteins are heavily affected by actin dynamics, FLNA represents a F-actin binding protein while F-actin-bound MKL1 is kept nuclear (Baarlink C. et al, 2013). Our very own results complement these finding by providing a necessity of FLNA appearance for MKL1-F-actin association. Furthermore, we are providing evidence that FLNA interferes with MKL1 phosphorylation. MKL1 phosphorylation leads to export out of the nucleus into the cytoplasm (Muehlich S., Wang R. et al, 2008). Thus it is tempting to speculate to name FLNA a catalyzer of MKL1 activation, in this case by conducting MKL1s cellular localization. Further studies will definitely be necessary to judge clearly on this theory, but nevertheless even referring to our current knowledge we are able to postulate that FLNA seems to have at least some kind of supportive influence on MKL1 shuttle mechanism by its impact on actin and phosphorylation.

If speculating about a collective MKL1-FLNA entrance into the nucleus, one has to remember that the MKL1-FLNA complex represents a, without question, very large macromolecule

(Nakamura F., Stossel T. et al, 2011). In contrast to small molecules that enter the nucleus without further regulation procedures, these types of large proteins, and even MKL1 on its own, require association with transport factors like importins. Importins bind nuclear localization signals (NLS) located on the protein, for example as on MKL1, this way allowing the Importin-NLS-MKL1 complex to interact with the nuclear pore and successfully pass through its channel (Depping R., Jelkmann W. et al, 2015). Based on the stated arguments of size and pore restrictions, a collective MKL1-full-length-FLNA entrance into the nucleus is highly doubtful, however a translocation of FLNA fragments together with the transcription factor androgen receptor has been demonstrated (Loy C., Sim K. et al, 2003). Future studies laying focus on MKL1s condition during nuclear entrance or exit might be of great interest, especially regarding its FLNA binding status during that process.

MKL1 is inactive and rests in the cytoplasm when bound to monomeric G-actin, however signals that activate RhoA cause actin polymerization and MKL1 dissociation from G-actin, followed by nuclear entrance (Vartiainen M., Guettler S. et al, 2007). We hypothesize that nuclear FLNA impairs MKL1 phosphorylation and facilitates actin networking, thereby probably holding MKL1 in the nucleus. Regardless the matter of fact that our work is setting its focus on MKL1s meaningful nuclear actions while bound to FLNA, this shuttle-scenario is a prime example for MKL1s ability to rapidly influence its surroundings, serving as an immediate on-off switch depending on its current position with valuable impact on genes and cell mobility on the one hand, but also playing a significant role in disease progression on the other.

7.1.4 RhoA-actin signaling activating and inhibiting drugs and its functional effects on the MKL1-FLNA interaction

RhoA induction through LPA in primary human and 3T3 fibroblasts promoted the association of endogenous MKL1 with FLNA and increased MKL1 target gene expression, whereas exposure to an actin polymerization inhibitor dissociated MKL1 from FLNA and decreased MKL1 target gene expression in cancer cells. These results involve a relocation of MKL1 to the nucleus with LPA and to the cytoplasm under LatB treatment (Scharenberg M., Pippenger B. et al, 2014; Vartiainen M., Guettler S. et al, 2007). These observations also reveal first signs of different MKL1-FLNA complex role, regarding the cell model one keeps track on examining. Expanding this thought, one can postulate that MKL1-FLNA interaction

takes place at least in part in the nucleus under pathophysiological or at least stressful conditions, which often involves growth factor or serum release, comparable to the LPA-activation model in the present chapter. Consistent with our findings about impaired MKL1 phosphorylation in the presence of FLNA, we investigated that administration of LatB leads to cytoplasmic MKL1 redistribution due to its phosphorylation. LatB causes MKL1-G-actin complex formation including phosphorylated MKL1.

We explored the functional effects implicated by the MKL1-FLNA interaction. Therefore we addressed qRT-PCR analysis. Interestingly, we found that association of endogenous MKL1 and FLNA upon LPA treatment in primary fibroblasts was accompanied by the induction of the well-established MKL1 target genes *SM22, CTGF, ITGA5* and *CNN1* (Smith E., Teixeira A. et al, 2013; Medjkane S., Perez-Sanchez C. et al, 2008; Muehlich S., Hampl V. et al, 2012). This is particularly fascinating since similar results were obtained in FLNA expressing A7 cancer cell, compared to a relatively low level of target gene expression in FLNA-depleted M2 cells. Furthermore we were able to reduce target gene expression in A7 cells by FLNA siRNA or LatB treatment. Therefore, comparison of the A7, A7 siFLNA and M2 data with results obtained in fibroblasts with LPA or no LPA incubation makes sense. One now could assume that LPA treated fibroblast cells behave in a certain way like a hepatocellular carcinoma cell with nuclear active MKL1, concerning their biological properties such as target gene expression (Muehlich S., Hampl V. et al, 2012). This is suiting well, as stress-stimulated fibroblasts cells may operate in a similar way as cancer cells.

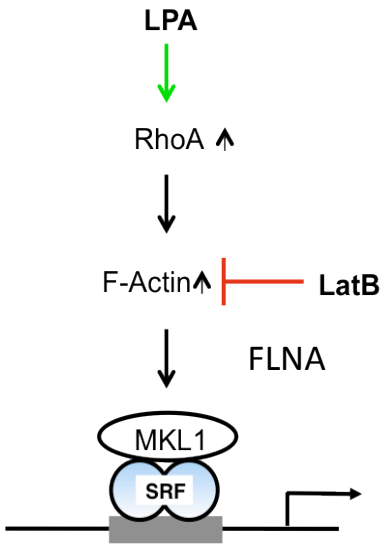

Figure 9: Model of activating LPA and inhibitory LatB affecting MKL1/SRF activation. Adapted from Miralles F., Posern G., 2003

7.2 Rounding the puzzle: Where do MKL1 and FLNA gear?

Besides its task as a gelation factor, stabilizer and director for actin networks, helping the cell to save and position actin, FLNA has a known reputation for being a binding partner for an extensive amount of other proteins (Savoy M., Ghosh M. et al, 2013; Nakamura F., Stossel P. et al, 2011). To date, the transcription factor FOXC1, the androgen receptor AR, Smad proteins and many more have been described to be regulated by FLNA (Berry F., O'Neil M. et al, 2005; Sasaki A., Masuda Y. et al, 2001; Loy C., Sim K. et al, 2003). We introduce the co-activator MKL1 as the newest member of the FLNA binding partner family. Surprisingly, in terms of binding patterns (FOXC1, AR) or phosphorylation status (Smad), similarities to the MKL1-FLNA interaction are detectable. It has been discovered that these dynamic interactions involving FLNA have positive and negative influences on transcriptional processes, which sounds reasonable in reference to the large variety of FLNA binding partner proteins including their different origins and duties (Berry F., O'Neill M. et al, 2004; Brandt T., Baarlink C. et al, 2009; Loy C., Sim K. et al, 2003; Sasaki A., Masuda Y. et al, 2001). We are expanding the FLNA paradigm by announcing MKL1 as a protein, which benefits in a strong way of the FLNA interaction, ultimately resulting in high rates of transcriptional activity and gene expression.

7.2.1 MKL1-interacting region on FLNA

Since FLNA is a rather large molecule, it holds the role of a scaffold, simplifying MKL1 docking and binding processes. Besides the N-terminal actin association domain, most protein interactions take place at one of the two Rod segments of FLNA, containing so-called repeats which adopt an immunoglobulin-like fold (Nakamura F., Stossel T. et al, 2011). Because of the major similarity between these repeats, proteins can bind at multiple sites (Nakamura F., Stossel T. et al, 2011). In our case, mapping of the FLNA protein revealed that repeats 4 to 7 on Rod1 and repeats 16 to 18 on Rod2 (amino acids 571 to 866 and 1779 to 2284, respectively) are essential for the interaction with MKL1, suggesting a complex interaction occurring between multiple regions of MKL1 and FLNA.

This is stunning since another transcription factor called FOXC1 associates with FLNA in the exact same way (Berry F., O'Neill M, et al, 2004). Interestingly, following elevated levels of nuclear FLNA, FOXC1 is unable to activate transcription by being transported to

transcriptionally inactive regions of the nucleus. The targeting of FOXC1 to these regions might prevent it from accessing the required co-activators necessary for transcriptional activation (Berry F., O'Neill M. et al, 2004). Consistent with the findings of Berry F. and colleagues, we speculate on FLNA holding MKL1 to a particular cell region, in our case the nucleus. This opposed role of activating and inhibiting, depending on its interaction-partners utilized, demonstrates a prime example for FLNAs mechanistic multi-functionality. Its origin duty of crosslinking actin filaments has been supplemented by various additional tasks in the process of evolution. In this particular case FLNA is working as transcriptional barrier or catalyst, since in contrast to our findings it has the opposite effect on FOXC1 then on MKL1.

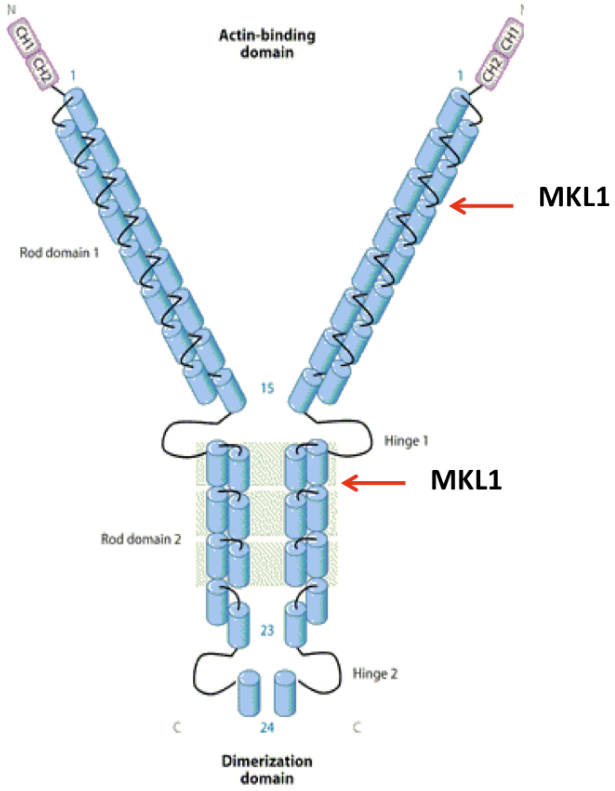

Figure 10: Model of the FLNA-MKL1 interaction taking place at Rod1 and 2 on the FLNA protein.

Another nuclear transcription factor linked to FLNA is the androgen receptor (AR), which is not only mediating male sexual differentiation but its limitless activity is associated to prostate cancer (Loy C., Sim K. et al, 2003). Interestingly and consistent with our findings, AR interacted with FLNA in the same area MKL1 does (repeat 16 to 18 on Rod2). The interaction resulted in a repression of androgen signaling, measured by an androgen-regulated control protein widely used as a marker for prostate cancer progression (Loy C., Sim K. et al, 2003). Together with our results about FLNAs nuclear activity in terms of MKL1, regulation of the

androgen receptor is an additional example about nuclear processes controlled by a formerly, primarily for its cytoplasmic presence known FLNA. In contrast to our findings using full length FLNA during all performed investigations, Loy C. and colleagues specifically address cleaved FLNA. They postulate an interaction of AR with the shorter, cleaved C-terminal 100 kDa fragment of FLNA. This is particularly appealing since smaller FLNA fragments probably have less trouble to enter the nucleus then the large full-length macromolecule. It is more likely that a complex of fragmented FLNA and AR handles the shuttle procedure with success than the massive full-length FLNA-MKL1 complex. In addition to the thoughts stated in the previous chapter, this strengthens the theory about a FLNA independent MKL1 shuttling. Nevertheless, nuclear entrance of FLNA is still controversial and very little is known about the exact shuttle operation. Our experiments confirm the existence of two shorter FLNA fragments (190 kDa and 90 kDa), however at the present we do not know how both of them differ in their biological functions and localization. Further investigations respective full length FLNA movement and experiments regarding a possible connectivity with smaller FLNA fragments and MKL1 will be necessary to judge clearly on this topic.

Smad proteins are involved in the transforming growth factor (TGF-beta) signaling pathway (Sasaki A., Masuda Y. et al, 2001). Before they enter the nucleus, Smads are getting phosphorylated and afterwards participate in target gene transcription. Recently, Sasaki A. and colleagues identified FLNA as a Smad binding partner along with stating that TGF-beta signaling was defective in FLNA-deficient melanoma M2 cells, compared to strong signal in the FLNA-expressing A7 cells. In contrast to our investigations where FLNA impairs MKL1 phosphorylation, it might be possible that in this case, FLNA is essential for effective Smad phosphorylation (Sasaki A., Masuda Y. et al, 2001). It is a known fact that MKL1-phosphorylation heavily impacts MKL1-shutteling out of the nucleus (Muehlich S., Wang R. et al, 2008). As a consequence of ERK 1/2 phosphorylation, G-actin binding to MKL1 is simplified. We were able to demonstrate that MKL1-phosphorylation processes were suppressed by FLNA, therefore possibly restraining the MKL1-FLNA complex in the nucleus. This scenario might offer a potentially interesting target for future drug treatment investigations, namely inhibitors of the MKL1-FLNA interaction. Blocking of FLNA would lead to enhanced MKL1 phosphorylation, decreased nuclear MKL1 levels and therefore reduction of MKL1 provoked tumorigenic events, including migration, invasion and target gene

overexpression which is supported by the studies of Hampl V. and colleagues and their findings of abolished hepatocellular carcinoma (HCC) xenograft growth after MKL1/2 depletion (2013).

7.2.2 FLNAs unique structure-properties simplifying MKL1 association?

Speculations arising about the particular interaction area of MKL1 at the beginning on both FLNA rods (repeat 4 and 16) might be addressed if one takes a more in detail look at FLNAs unique structure. FLNAs vast variety of cellular tasks starts and ends with its structural flexibility. Two hinges grant the flexibility for the protein itself and the connected actin networks (Popowicz G., Schleicher M. et al, 2006). This high degree of elasticity not only allows an easier formation of complex actin structures but also could help to enable interaction partners an association with FLNA by simplifying the docking process, this way making it more accessible then a rigid skeleton. This theory is strengthened by the fact that filamins in higher organisms showcase a weaker, less rigid form of dimerization as a result of evolution (Popowicz G., Schleicher M. et al, 2006). Furthermore, filamins in higher organisms share a greater amount of interaction partners then the ones in lower organisms. Popowicz G. and colleagues moreover revealed that single repeats have the ability to unfold if exposed to force. The occurring force also enhances the repeats length, this way probably granting straightforward access for binding candidates. It also has been postulated that sudden unfolding of the filamin rod during stressful cytoskeletal situations might work as a method to protect the structure from being damaged or leading to prevention from fatal breaking issues (Popowicz G., Schleicher M. et al, 2006).

Fascinatingly, especially repeat 4, which associates with MKL1, unfolds easily on the one hand but also has a stable folding intermediate on the other (Popowicz G., Schleicher M. et al, 2006). Thus, repeat 4 seems to be an excellent choice for MKL1 to bind since it is flexible, able to absorb and withstand force and stress. These circumstances allow simplification of the act of docking due to unfolding and formation of a stable intermediate state.

Since FLNA is known to generate and connect a fine meshed and large network of polymerized F-actin in an orthogonal manner (Nakamura F., Stossel T. et al, 2011) and furthermore represents a rather huge molecule by itself, questions arise about possible spots for MKL1 to enter the network and perform the docking process, in particular viewed from a steric perspective. As it has been said before, the extraordinary qualities of FLNA

repeat number 4 in terms of elasticity and unfolding should provide help for MKL1 to find its estimated binding area. Since both interacting repeats lay quiet close to one of the hinge regions, it might be tempting to guess about these hinge regions generating space in case of an incoming MKL1 interaction by using their unique flexibility attributes. Further geometric investigations will be necessary to solve this riddle in particular.

7.2.3 Force, mechanical stress and a potential influence on MKL1 binding nature

Mechanical stress might be another factor coming into play. It is defined as the distribution of forces applied on a solid or fluid body, which is deformed as a result of these external loads (Noguerira M., Moreira J. et al, 2015). These forces not only lead to deformation, they furthermore are changing the relative locations of molecules within a body. An intuitive comparison would be pressure. This is correct if we speak of vertical forces. Parallel forces however are considered shear stress (Noguerira M., Moreira J. et al, 2015). Thus, mechanical stress holds the ability to unfold the FLNA repeat together with dissociation and association of binding partners like MKL1.

Force furthermore is able to activate MKL1 through RhoA stimulation (Zhao X., Laschinger C., et al, 2007). During pressure situations, myocardium growth is linked to myofibroblast differentiation, an event where cardiac fibroblasts express smooth muscle actin (SMA), thereby enhancing the ability to increase cell contractility. Force application induced nuclear MKL1 translocation as a follow up of Rho activation and actin assembly (Zhao X., Laschinger C. et al, 2007), with MKL1 also being an important determinant of SMA expression (Wang DZ., Li S. et al, 2002). If we think one step ahead, a released or newly FLNA-bound MKL1 protein this way could be a useful cellular sensor for mechanical forces taking influence on the cell. In addition, mechanical stress is a critical factor in cancer as many solid tumors show increased fluid pressure, building a barrier for transcapillary transport (Noguerira M., Moreira J. et al, 2015). These barriers often provide problems for therapeutic schemes, since agent uptake is inefficient. Physicians try to detect these increased pressures when doing clinical exams, but measuring methods still lag satisfying reproducibility. Interestingly, increased pressure is also responsible for cancer invasion. Invasive cells prefer soft tissues like muscle rather then bone (Noguerira M., Moreira J. et al, 2015). Cells are also able to escape easier and reach blood vessels to form distant metastasis under pressure. Protein

quantification, like MKL1 might be the future key for sensing force and pressure parameters and moreover would offer a much saver, easier and accurate approach.

7.2.4 FLNA-interacting region on MKL1

Regarding mapping from MKL1s perspective view, mutational analysis revealed that amino acids 301 to 310 on MKL1 are required for the interaction with FLNA. To reach this amino acid span, we used deletion variants of MKL1, step by step narrowing down the possible region responsible for interaction procedures. One has to keep in mind that the actual area of interaction might surpass the ten described amino acids by a certain amount, potentially looming into regions up- or downstream 301 to 310, since it is not possible to exclude a somehow more compact way of interaction by mutation analysis. To sum it up, we have identified a previously unrecognized region between MKL1 amino acids 301 and 310 that balances the interaction with FLNA. Curiously, none of MKL1s essential domains is getting affected by binding events in this area. The SAP domain lays a little bit further upstream at amino acids 343 to 378 representing the closest one.

Our group generated data, significantly showing that FLNA enhances MKL1 activity. This being said, it appears odd to question these strong results at first. Still, one has to be cautious and ask self-critical about possible divergent issues happening under certain circumstances. First of all, almost all of our results hint in the direction of a strong MKL1-FLNA complex formation under pathophysiological conditions (growth factors, wound healing, invasion, diseases, cancer cells with impaired tumor suppressor), so what about physiological scenarios? Searching for a reason to answer that question, once again actin availability and status comes to our mind at first.

7.3 Actin in control. Role of actin in the FilaminA-MKL1 machinery

We hypothesize about FLNA functioning as a positive cellular transducer, linking actin polymerization to MKL1 activity and counteracting the known repressive complex of MKL1 and monomeric actin. SRF reporter gene assays revealed a 13-fold induction of luciferase activity in F-actin, FLNA and MKL1 expressing cells compared to only a slight induction when no FLNA was available. Similar results were achieved in FLNA-expressing cells versus FLNA-depleted cells by treating cells with or without actin stabilizer Jasplakinolide. Furthermore, this data was strengthened by Immunofluoresence investigations, examining actin network formation. Experiments in FLNA-depleted cells revealed that only very little network building was achieved if FLNA was not available, compared to strong actin-network formation in FLNA-expressing cells. Taken together, these results provide evidence for FLNA working as a positive cellular transducer, resulting in MKL1 activity through actin polymerization.

No MKL1-F-actin interaction was observable in FLNA depleted melanoma cells, in contrast to a clear measurable association in FLNA expressing ones. This data hints at a potential complex formation scenario of MKL1, FLNA and F-actin in tumor cells.

7.3.1 Possible formation of a trimeric MKL1-FLNA-F-actin complex

Now, speculating about the existence of a trimeric-complex of MKL1-FLNA-F-actin, we carefully have to embrace steric thoughts. First of all, we have to state that we do not hold any information in which fashion MKL1-FLNA-F-actin possibly do interact. Do we know MKL1 interacts FLNA? That is the key part of this work and presented in great detail. Is there any available data about FLNA-F-actin binding? This is verified in numerous publications as well (Nakamura F., Stossel T. et al, 2011; Cunningham C., Gorlin J. et al, 1992). What about MKL1s association to F-actin? We provided evidence of this association taking place in FLNA expressing A7 cells, while no such interaction was visible in FLNA depleted M2 cells, hinting at a crucial necessity of FLNA for a putative MKL1-FLNA-F-actin complex.

A speculative setting with FLNA as a core protein, flanked by MKL1 at repeat 4 and 16 on the one side and F-actin bond to FLNAs actin binding domain on the other might sound most suitable (Fig. 13). Viewed from MKL1s perspective, FLNA is binding MKL1 at aa 301-310, however we do not know where the MKL1-F-actin interaction takes place yet. Interestingly, an immunoprecipitaion setup comparing MKL1 Δ301-380 and wt-MKL1 binding patterns to

actin displayed a weaker MKL1 Δ301-380-Actin association versus wt-MKL1-Actin, which also hints at trimeric complex formation since MKL1 Δ301-380 is not able to bind FLNA anymore. Nevertheless this has to be investigated in greater detail, since the examined GFP-Actin displays F-actin as well as the monomeric G-actin, making it difficult to credit the effect to polymerized F-actin alone.

Since immunoprecipitation analysis, in terms of searching for an answer on these complicated complex formations are slowly reaching their limits, alternative binding assays will be necessary to shade light on this “complex” topic.

7.3.2 G-actin terminating MKL1-FLNA machinery?

To round up formation theories, one should also consider G-actin. Since FLNA is such a huge molecule, it might be arguable that its long and voluminous rod domains deliver steric trouble for G-actin to reach MKL1s RPEL domain. This would bring us to a competitive model between FLNA and G-actin competing for a MKL1 association. Consistent with this idea, it is known that actin sterically occludes the NLS region on MKL1 by binding the RPEL domain, this way blocking nuclear import in a competitive manner by blocking importin signaling (Mouilleron S., Langer C. et al, 2011; Pawlowski R., Rajakylä EK. et al, 2010). In contrast to competing theories, RNA export factor Ddx19 which is facilitating MKL1 nuclear entrance does not compete with actin for MKL1 binding (Rajakylä EK., Viita T. et al, 2015). To shade light on this topic we designed a reporter gene assay setup using NLS-R62D-actin, a constitutive cytoplasmic mutant of actin. We increased the NLS-R62D-actin dose in a step-by-step manner, which led to a reduction of SRF reporter activity in FLNA expressing and FLNA depleted melanoma cells because MKL1 is getting shuttled back into the cytoplasm. We moved forward by introducing mDia-ct, a constitutive nuclear mutant of the formin mDia and secondly fusing a NES signal to mDia, which thereby enables cytoplasmic formin localization (Baarlink C., Wang H. et al, 2013). Fascinatingly, nuclear formin was able to counteract the repressive nuclear G-actin effect, this way retaining luciferase activity on higher levels in contrast to treatment with cytoplasmic formin, where luciferase levels dropped heavily. FLNA depleted melanoma cells remained at low-level reporter gene activity throughout the entire experiment, no matter how much G-actin or formin was introduced.

We suggest a model in which nuclear G-actin terminates the highly active MKL1-FLNA machinery by dismissing MKL1 from FLNA, binding MKL1 by itself and exporting it out of the

nucleus in a concentration dependent manner. The hypothesis is furthermore strengthened by our results that FLNA displays no interaction with the monomeric R62D-actin mutant. However, one has to put in perspective that this model may only hold a secondary role under biological circumstances. The available G-actin pool is rather small under predominant, high F-actin levels and active MKL1 conditions in the nucleus (Vartiainen MK., Guettler S. et al, 2007), which we consider the case in our experiments. Nevertheless this competing scenario could still exist and might be used to terminate transcriptional activity.

7.3.3 Linking actin dynamics to state of the art drug development

Individual cells steadily undergo physical changes in appearance, shape and position during embryonic development as well as in the state of functional components of mature multicellular organisms (Olson E., Nordheim A., 2010). These physical changes demand cellular motile functionality, which is regulated by physiological and pathophysiological stimuli. The physical properties for cellular motility rest upon macromolecular assemblies, like actin filaments (Olson E., Nordheim A., 2010). Actin filaments heavily rely on FLNA as a gelation factor and networking scaffold on the one hand but are also the key activator for MKL1. We are linking actin polymerization to MKL1-FLNA activity for the first time. Recent publications provide evidence that nuclear and cytoplasmic actin pools communicate in a dynamic way (Vartiainen M., Guettler S. et al, 2007; Grosse R., Vartiainen MK., 2013). Therefore it is key to take a more precise look at cytoskeletal reorganization. Cytoskeletal actin dynamics are controlled by different membrane receptors like Receptor Tyr kinase, Integrins and TGF-beta, which modulate the activity of Rho GTPases through Rho guanine nucleotide exchange factors (GEFs) (Olson E., Nordheim A., 2010). Receptor Tyr kinases include insulin and epidermal growth factor (EGF) receptors. Interestingly, insufficient EGF receptor signaling is associated to similar neurodegenerative diseases as caused by FLNA mutations (Bublil E., Yarden Y., 2007). On the other hand, excessive EGF signaling is linked to a wide variety of tumor formation (Lee MY., Chou CY. et al, 2008; Lo HW., Hsu SC. et al, 2007). This led to development of EGFR inhibitors including Gefitinib® for lung- and Cetuximab® for colon cancer. Downstream effects of EGF activation result in high-level amounts of cytoplasmic F-actin (Mouneimne G., Soon L. et al, 2004; Olson E., Nordheim A. 2010) leading to MKL1 target gene activity in the nucleus. Thus, current state-of-the art EGF inhibitor agents represent a valuable example how there are already indirect MKL1 influencing drugs successfully used in cancer treatment.

7.3.4 The formin mDia as the missing key in launching MKL1-FLNA-F-actin complex activity?

Still, several actin related questions remain. Is nuclear actin actively responding to cytoplasmic alterations? Do the two pools freely exchange? Does nuclear actin assemble into F-actin the same way as their cytoplasmic counterpart and how does it influence the MKL1-FLNA complex? Taken together, functions and existence of nuclear actin have been a mystery for many years. We found that FLNA is required for an association between F-actin and MKL1, which suggests that FLNA may mediate an association between polymerized actin and MKL1, thereby transduces the signal of polymerized actin to SRF activation. Since the MKL1-FLNA complex is formed in the nucleus in melanoma cells, nuclear actin characteristics are of great interest for our research. To further address questions about nuclear actin, Baarlink and colleagues investigated MKL1 regulation in the nucleus. Evidence was provided that serum stimulation is able to rapidly and transiently induce formation of F-actin structures in a fibroblast nucleus (Baarlink C. et al, 2013). These findings mesh excellent with our data of an essential role of F-actin for the FLNA-MKL1 interaction. However, and this is crucial, Baarlinks group needed a stimulation agent for their nuclear F-actin outburst the same way we needed LPA for MKL1-FLNA complex formation in the equivalent fibroblast cell line. According to Baarlink C. and colleagues the nuclear F-actin structures are dependent to the formin mDia. The Rho family of GTPases orchestrates fundamental cell processes through remodeling of the cytoskeleton after being activated by external stimuli like LPA. The largest family of Rho-GTPase effectors are formins (Jegou A., Carlier MF. et al, 2013). mDia1 is regulating myosin activity through feedback mechanisms, while mDia2 is stimulating the production of filopodia. They are able to stimulate nuclear actin filament polymerization, accelerate the elongation and last but not least stabilize them (Baarlink C., Grosse R., 2014)

Since our results demonstrate that FLNA expressing melanoma cells lead to significant longer formation and higher number of filopodia then their FLNA deficient counterpart, a result that is also obtained through mDia2 activity, nuclear F-actin composition driven by formins might be the missing but plausible explanation for the new MKL1-FLNA intense activity. This is strengthened by our very own observations that only a very weak actin network was visible in FLNA depleted melanoma cells. Consistent with that, luciferase activity rose

significantly when mDia and FLNA were available, in particular compared to a setup with no FLNA presence.

7.3.5 Mechanistic summary of the MKL1-FLNA association

In conclusion, we identified FLNA as a MKL1 interacting protein and an important participant in MKL1-SRF-mediated transcription. The novel interaction is required for MKL1 dependent gene expression, cell migration and invasion. Therefore, binding to FLNA represents a newly identified mechanism that positively regulates MKL1 activity, thus opposing the known repressive complex of MKL1 and G-actin (Fig. 11).

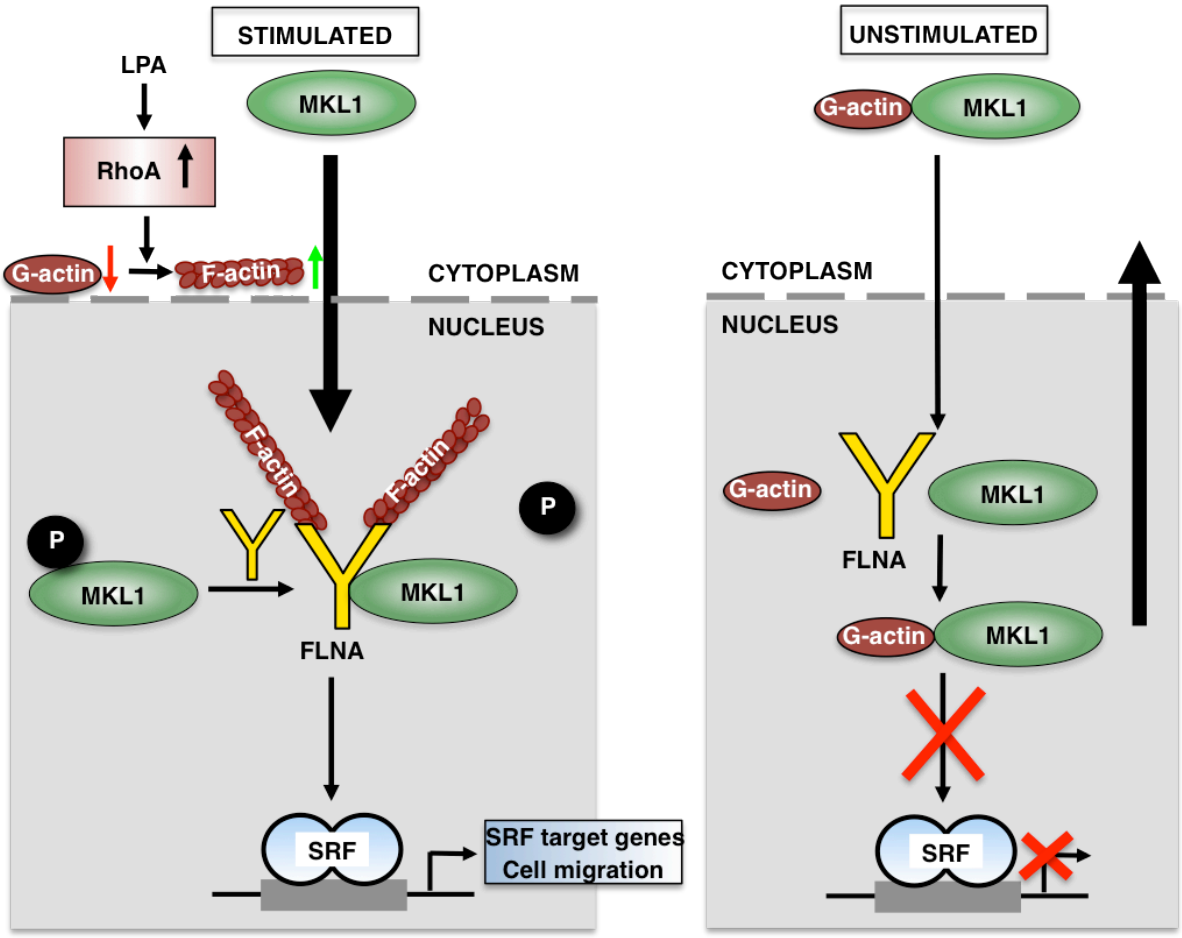

Figure 11: Model of the MKL1-FLNA interaction in LPA stimulated fibroblasts (left) and the unstimulated counterpart (right). MKL1 exists in a repressive G-actin complex (right) or an activating FLNA complex (left). FLNA impairs MKL1-phosphorylation, which is a prerequisite for G-actin binding, thereby switching the repressive MKL1-G-actin structure to a MKL1-FLNA complex that transduces actin polymerization into SRF activity. Adapted from Kircher P., Hermmans C., 2015.

7.4 MKL1 and FLNA: A highly dynamic duo leading to cancer?

MKL1s original naming as megakaryoblastic leukemia 1 already reveals a bond to neoplastic cancer events. Following chromosomal translocation the emerging protein of MKL1 and a fusion partner is strictly nuclear localized because it is not subject to G-actin mediated nuclear export anymore (Mercher T., Busson-Le Coniat M. et al, 2001; Descot A., Rex-Haffner M. et al, 2008). As a result, SRF transcriptional activity is strongly and permanently activated.

Consistent with MKL1s pioneer discovery, our investigations revealed that the interaction of MKL1 and FLNA regulates MKL1 gene expression. This idea is supported by the strong induction of proven MKL1 target genes like *SM22, CTGF, ITGA5, CNN1, MYH9, GLIPR1, TGF-beta* and *FHL2* (Schmidt L., Duncan K. et al, 2012; Elberg G., Chen L., et al, 2008; Cheng X., Yang Y., et al 2015) in FLNA expressing melanoma cells and their correlated low expression levels in FLNA-depleted cells. The synergetic effect of an available MKL1-FLNA complex was not only demonstrated by addressing a variety of target genes, but also could be shown by reporter gene experiments which revealed a tight and sensitive connection between the amount of present MKL1, FLNA and the measured SRF reporter activity. A step-by-step increase of siFLNA concentration led to lower levels of SRF protein levels and double knockdown of MKL1 and FLNA reduced SRF protein levels even more then just single knockdown of one of the two proteins. qRT-PCR experiments which used a setup in FLNA-depleted melanoma cells with FLNA rescue combined with MKL1 knockdown, provided more evidence for a synergetic effect by displaying the highest levels of gene expression when FLNA and MKL1 were bot available. Furthermore, we were able to demonstrate that MKL1 deletion mutants that are unable to bind FLNA heavily decreased the expression of MKL1 target genes.

Melanoma is an aggressive skin malignancy, which is able to spread into other organs of the body, including more than 230000 new cases and 55000 deaths per year (Eggermont et al., 2014). It is developing from the pigment-containing melanocytes and mostly occurs on the legs in women while men are affected on the back at a high percentage (World Cancer Report., 2014, Chapter 5.14, WHO). The primary cause of melanoma is exposure to ultraviolet light, influencing especially people with low levels of skin pigment and corrupting our genetic information (Kanavy HE, Gerstenblith MR et al., 2011). Highly energetic and most dangerous UVC lights are absorbed by the ozone layer, while the longer UV wavelengths

UVA and UVB however do pass the atmosphere. Wavelengths of the intermediate UVB light are long enough to pass through the ozone layer but still energetic enough to attack DNA (Goodsell D., 2001). Each melanocyte experiences up to 100 of these reactions during every second of sunlight exposure (Goodsell D., 2001), however most of them are corrected right away. If the damage does not get eliminated, the genetic information may be permanently mutated, resulting in transformation of regular melanocyte stem cells into cancer cells.

Previous studies have illustrated that FLNA interacts with many proteins related to cancer progression (Kim H., McCulloch CA., 2010; Leung R., Wang Y. et al, 2010), a circumstance that involves growth, motility and invasive properties. Interestingly Zhang K. and colleagues found that reduction of FLNA expression inhibited the ability of melanoma cells to form colonies. They also postulated that knockdown of FLNA correlated with reduced melanoma growth in tumor xenograft (Zhang K., Zhu T. el al, 2014). This way, appropriate FLNA levels seem to be essential in tumor cells for motility and invasive purposes, to resist mechanical stress and attachment to extracellular matrix (ECM) to form metastases.

Per definition, benign, non-cancerous tumors in contrast to malignant ones are self-limited in its growth, which means they are not capable of invading into close-by tissues. As one can imagine, this invasive cell properties are of great interest in the field of today's cancer research. We found that the interaction between MKL1 and FLNA controls MKL1 dependent cell motility and invasion. Similar to gen expression experiments, the MKL1 deletion mutant unable to bind FLNA exhibited strongly reduced motile and invasive properties in comparison to wild-type MKL1. Furthermore MKL1 and FLNA knockdown led to a decreased number of filopodia formation. Filopodia are known to be crucial for motility procedures (Kim MC., Whisler J. et al, 2015). These investigations confirm that the interaction with FLNA is needed for MKL1 to execute its motile functions and invasive role in a synergetic way. It delivers yet another important value that the MKL1-FLNA interaction is essential for tumor progression. Literature provides evidence that knockdown of MKL1 in a variety of cancer cells led to impaired cell migration (Muehlich S., Hampl V. et al, 2012; Medjkane S., Perez-Sanchez C, et al, 2009). Based on our own new results in melanoma and hepatocellular carcinoma cells, we propose a synergetic model, where the interaction of MKL1 and FLNA results in a strong increase of motility events, compared to a condition where no MKL1-FLNA interaction is taking place, resulting in reduced cell mobility. Consistent with our data, Liao X.

and colleagues recently postulated similar results in terms of migration by the interaction between MKL1 and the transcription factor, signal transducers and activators of transcription (STAT3). The association also led to a synergetic increased wound healing in breast cancer cells (Liao X., Wang N. et al, 2014).

Another interesting topic regarding FLNA and cancer development is DNA damage response. It has been reported that FLNA holds a nuclear function by interacting with BRCA2, a critical tumor suppressor protein involved in DNA damage repair (Yuan Y., Shen Z. et al, 2001). Evidence was given that inhibition of FLNA led to reduction of DNA double strand break repair in cancer cells, resulting in sensitization of cells to ionizing radiation. Furthermore chemotherapy effectiveness improved through sensitizing cancer cells to cis-platin and bleomycin drug treatment in low level FLNA cancer cells by delaying the repair of DNA double strand breaks. Bleomycin causes mainly double strand breaks, while cis-platin binds with DNA to form different types of platinium-DNA adducts. These results indicate that FLNA not only plays a significant role in repair of a variety of DNA damage but also that lack of FLNA is a marker for a better outcome after DNA damage based treatment. In other words, FLNA can be inhibited to sensitize FLNA positive cancer to therapeutic DNA damage. This way, FLNA can be used as a biomarker and a target for DNA damage based cancer therapy (Yue J., Lu H. et al, 2011).

As stated in the beginning, this thesis experiments were performed with full-length-FLNA interacting MKL1 in the nucleus, which afterwards releases its cancer progressing potential. Therefore it is tempting to speculate that cleaved FLNA might not be able to induce MKL1 target gene expression, migration and invasion. It also has been postulated that that FLNA cleavages comes in hand with reduced metastasis (Bedolla RG., Wang Y. et al, 2009). This way and in addition to simply inhibiting FLNA expression, an alternative strategy to disrupt the FLNA function could be induction of FLNA cleavage. Recently Planaguma J. and colleagues provided a novel optical tool for tracking the cellular functions of FLNA in real time (Planaguma J., Minsaas L. et al, 2012). The group developed a fluorescent FLNA-EGFP construct by inserting the EGFP-tag inside the flexible hinge 1 region of FLNA between two calpain cleavage sites. Therefore, this tool might be promising as an instrument for stating FLNA as a future biomarker and presenting optical data of FLNA cleavage activity.

Fascinatingly, and similar to FLNA knockdown effects, depletion of MKL1 reduced cell adhesion, invasion and motility, all typical Rho-dependent cytoskeletal processes, in melanoma and breast cancer cells (Medjkane S., Perez-Sanchez C. et al, 2009). Moreover, depletion of MKL1 target genes *MYH9* and *MYL9,* which have been related to invasive tumor presence previously, resulted in significantly reduced invasiveness, impaired lung colonization and reduced formation of lung tumors, delivering evidence that MKL1 target genes have at least some influence on tumor progression (Medjkane S., Perez-Sanchez C. et al, 2009).

Another interesting approach, which links MKL1 to cancer development, is suppressor of cancer cell invasion (SCAI), a newly found protein that regulates invasive cell migration (Brandt T., Baarlink C. et al, 2009). Similar to MKL1, SCAI is primary located nuclear in cancer cells where it forms a complex with MKL1 and SRF, this way effectively blocking MKL1 activity. Fittingly, lower SCAI levels are tightly correlated with increased invasive cell migration and SCAI is down-regulated in several human tumors. Brandt T. and colleagues further stated that the integrin beta-1 is strongly up-regulated after suppression of SCAI, which correlates well with our very own findings about elevated integrin alpha-5 levels when MKL1 and FLNA both were available. This is even more interesting, since one of integrins major task as a cell surface receptor is the mediation of adhesive interactions. Therefore integrins have recently been suggested crucial for invasive cell migration and tumor progression (DeMali K., Wannerberg K. et al, 2003; Brakebusch C., Fassler R. et al, 2002).

The present chapter gives an example about the similar roles of MKL1 and FLNA in the field of cancer development and especially metastasis. They both display strong impacts on motility, invasion and oncogenic target gene expression with their respective appearance. We conclude that activation of MKL1/FLNA signaling in tumor cells provide oncogenic properties, similar to the effect obtained from a fusion protein consisting of MKL1 and RBM15 in megakaryoblastic leukemia cells (Mercher T., Busson-Le Coniat M. et al, 2001; Descot A., Rex-Haffner M. et al, 2008): Constitutive nuclear localization combined with strong induction of MKL1 target genes, accompanied with tumor progression.

Around 90% of all cancer deaths emerge from the metastatic spread of primary tumors (Christofori G., 2006), but of all mechanisms involved in carcinogenesis, areal invasion and metastasis formation are clinically most relevant, however sadly least understood.

Expanding the current knowledge, we for the first time provide evidence that the MKL1-FLNA complex performs a symbiotic effect, which surpasses the one, each of the two interaction partner showcases in singularity. This way, the MKL1-FLNA complex might be an extraordinary target for future pharmacotherapeutic approaches. A possible idea to suppress the complex would be dummy binding agents which target aa 301-310 on MKL1, respectively repeat 4 or 16 on FLNA, thus inhibiting successfully complex formation. Our experiments reveal a nuclear complex localization and it might be tempting to speculate about reduced cancerogenic properties if the complex is relocated to the cytoplasm or drugs even blocking a complex formation, thus modeling the MKL1 pathway in a therapeutic way.

7.5 The many faces of MKL1 and FLNA: Final thoughts and a link to neuronal diseases

The present work showcases data of a novel complex, formed of two proteins, which are both heavily involved in cellular motility procedures and target gene expression when active. All carried out investigations, which resulted in a visible interaction, soaring levels of target gene activation, reporter gene activity, cellular migration and invasion required a matching high concentration of MKL1 and FLNA.

This increased MKL1/SRF activity was not measurable under physiological conditions in un-stimulated 3T3 fibroblast cells, which led to our theory about complex formation under pathophysiological conditions like in melanoma and hepatocellular carcinoma cells or during wound healing, where strong MKL1-dependent motility and overexpression of MKL1/SRF target genes were detectable. This oncogenic potential of MKL1-FLNA already being discussed in detail, we now want to have a look at FLNA and MKL1 mutations.

Consistent with our experiments stating a synergetic reduction of migratory courses when MKL1 and FLNA are both depleted, it is known that FLNA mutations prevent neuronal migration during fetal development and cause human periventricular nodular heterotopia (PVNH) due to FLNA depletion (Zhou A., Hartwig J. et al, 2010). Diversity and elasticity, which is provided by FLNA as a gelation factor and orthogonal actin cross-linker, is required for modulating cell shape, which again is key for complex movement and crawling. In cortex

development, most neurons essentially travel from the ventricular zone to the cortical plate. FLNA is precisely regulated in the ventricular zone what appears to orchestra neuronal migration (Yagi H., Oka Y. et al, 2016). FLNA on its own is conducted by FLNA-interacting protein (FILIP), which induces FLNA degradation thus clipping neurons in the ventricular zone, preventing their journey and leading to abnormal appearance, which is the case in PVNH. Clinical symptoms are epileptic seizures and vascular complications (Zhou A., Hartwig J. et al, 2010).

Fascinatingly, MKL1 respectively SRF mutations led to similar observations (Knöll B, Nordheim A., 2009). SRF and its co-activator MKL1 regulate neuronal cell migration, guide axons development, synapse function and last but not least, performance in learning and memory. MKL1-deletion resulted in aberrant brain development. In contrast to wild-type axons with multiple finger-like filopodia structures consisting of bundled F-actin, MKL1-deficient axons develop fewer filopodia (Knöll B, Nordheim A., 2009).

Similar to their potential as pharmacological targets in cancer treatment, neurological disorders represent a field for therapeutic MKL1-FLNA modulation. In contrast to cancer treatment where complex formation blocking seems logical, MKL1 or FLNA stimulation might be the method of choice in this neuronal case, granting for example re-growth of lesioned axons. On the other hand, enhanced SRF and FLNA activity might also accelerate disease: in Alzheimers disease, SRF led to speeded up progression of cerebral amyloid plagues (Bell R., et al, 2009) and FLNA was identified as a requirement for amyloid toxic signaling (Wang H., Bakshi K. et al, 2012). Furthermore our very own findings state that MKL1 and FLNA in advanced levels do push tumor metastasis. In conclusion, interfering with MKL1 and FLNA activity, in this case in brain pathology, might be a double-edged sword, potentially resulting in either beneficial or harmful effects. Can not live with (too much of) it, can not live without it.

8 Figures

9 Tables

10 Abbreviation index

µg	micro gram
µL	micro Liter
µM	micro Molar
aa	amino acids
AB	AntiBody
ABP	Actin Binding Protein
AMKL	Acute Mega Karyoblastic Leukemia
APS	AmmoniumPeroxodiSulfate
bp	base pairs
BRCA1/2	BReast CAncer 1/2
BSA	Bovine Serum Albumin
cDNA	copy DNA
CTGF	Connective Tissue Growth Factor
DAPI	4`, 6-DiAmindino-2-PhenylIndole
DLC1	Deleted in Liver Cancer 1
DMEM	Dulbecco`s Modified Eagle Medium
DNA	Deoxyribo Nucleic Acid
E.coli	*Escherichia coli*
ECM	ExtraCellular Matrix
ERK	Extracellular signal-Regulated Kinase
F-actin	Filamentous actin
FCS	Fetal Calf Serum
FLNA	FiLamiN A

FOXC1	FOrkhead boX C1
G-actin	Globular actin
GDP	GuanosinDiPhosphat
GEF	Guanosin Exchange Factor
GPCR	G Protein-Coupled Receptor
GTP	GuanosinTriPhosphat
h	hour(s)
HA	HemAgglutine
HSP90	Heat Shock Protein 90
IB	ImmunoBlot
IF	ImmunoFluorescence
IP	ImmunoPrecipitation
ITGA5	InTeGrin Alpha 5
kDa	kilo Dalton
LPA	LysoPhospatidic Acid
M	Molar
mA	milli Ampere
MEM	Minimal essential Medium
mg	milli gramm
min	minute(s)
MKL1	MegaKaryoblastic Leukemia protein1
MKL2	MegaKaryoblastic Leukemia protein2
mL	milliLiter
mm	millimeter
mRNA	messenger RNA
MRTF	Myocardin-Related Transcription Factor
NES	Nuclear Export Signal

nm	nao meter
P-MKL1	phosphorylated MKL1
PAGE	PolyAcrylamide Gel Electrophoresis
PBS	Phosphate Buffered Saline
PCR	Polymerase Chain Reaction
PI	complete Protease Inhibitor cocktail
PVDF	PolyVinyliDene Fluoride
RNA	RiboNucleic Acid
rpm	rounds per minute
RT	Room Temperature
RT-PCR	Real-Time Polymerase Chain Reaction
s	seconds
SDS	Sodium Dodecyl Sulfate
siRNA	small-interfering RiboNucleic Acid
SRE	Serum Response Element
SRF	Serum Response Factor
TBST	Tris-Buffered Saline Tween 20
TCF	Ternary Complex Factors
TEMED	TEtraMethylEthylethyleneDiamine
TRIS	TRIS(hyrdoxymethyl)aminomethane
WT	WildType

11 References

Ahronian LG, Zhu LJ, Chen YW, Chu HC, Klimstra DS, Lewis BC (2016) A novel KLF6-Rho GTPase axis regulates hepatocellular carcinoma cell migration and dissemination. *Oncogene.* doi: 10.1038/onc.2016.2.

Amaral LA (2008) A truer measure of our ignorance. *Proc Natl Acad Sci U S A*. 105(19):6795-6.

Aravind L, Koonin EV (2000) SAP - a putative DNA-binding motif involved in chromosomal organization. *Trends Biochem Sci*. (3):112-4.

Arosio D, Casagrande C, Manzoni L (2012) Integrin-mediated drug delivery in cancer and cardiovascular diseases with peptide-functionalized nanoparticles. *Curr Med Chem*. (19):3128-51.

Arsenian S, Weinhold B, Oelgeschläger M, Rüther U, Nordheim A (1998) Serum response factor is essential for mesoderm formation during mouse embryogenesis. *EMBO J*. 17(21):6289-99.

Arwert EN, Hoste E, Watt FM (2012) Epithelial stem cells, wound healing and cancer. *Nat Rev Cancer*. 12(3):170-80.

Baarlink C, Grosse R (2014) Formin' actin in the nucleus. *Nucleus.* 5(1):15-20.

Baarlink C, Wang H, Grosse R (2013) Nuclear actin network assembly by formins regulates the SRF coactivator MAL. *Science.* 340(6134):864-7.

Bachmann AS, Howard JP, Vogel CW (2006) Actin-binding protein filamin A is displayed on the surface of human neuroblastoma cells. *Cancer Sci.* 97(12):1359-65.

Bedolla RG, Wang Y, Asuncion A, Chamie K, Siddiqui S, Mudryj MM, Prihoda TJ, Siddiqui J, Chinnaiyan AM, Mehra R, de Vere White RW, Ghosh PM (2009) Nuclear versus cytoplasmic localization of filamin A in prostate cancer: immunohistochemical correlation with metastases. *Clin Cancer Res.* 15(3):788-96.

Bell RD, Deane R, Chow N, Long X, Sagare A, Singh I, Streb JW, Guo H, Rubio A, Van Nostrand W, Miano JM, Zlokovic BV (2009) SRF and myocardin regulate LRP-mediated amyloid-beta clearance in brain vascular cells. *Nat Cell Biol*. 11(2):143-53.

Bennewith KL, Huang X, Ham CM, Graves EE, Erler JT, Kambham N, Feazell J, Yang GP, Koong A, Giaccia AJ (2009) The role of tumor cell-derived connective tissue growth factor (CTGF/CCN2) in pancreatic tumor growth. *Cancer Res*. 69(3):775-84.

Berry FB, O'Neill MA, Coca-Prados M, Walter MA (2005) FOXC1 transcriptional regulatory activity is impaired by PBX1 in a filamin A-mediated manner. *Mol Cell Biol*. (4):1415-24.

Brakebusch C, Fässler R (2002) The integrin-actin connection, an eternal love affair. *EMBO J.* 22(10):2324-33.

Brandt DT, Baarlink C, Kitzing TM, Kremmer E, Ivaska J, Nollau P, Grosse R (2009) SCAI acts as a suppressor of cancer cell invasion through the transcriptional control of beta1-integrin. *Nat Cell Biol.* 11(5):557-68.

Bubb MR, Spector I, Beyer BB, Fosen KM (2000) Effects of jasplakinolide on the kinetics of actin polymerization. An explanation for certain in vivo observations. *J Biol Chem*. 275(7):5163-70.

Bublil EM, Yarden Y (2007) The EGF receptor family: spearheading a merger of signaling and therapeutics. *Curr Opin Cell Biol.* 19(2):124-34.

Carlsson L, Nyström LE, Sundkvist I, Markey F, Lindberg U (1977) Actin polymerizability is influenced by profilin, a low molecular weight protein in non-muscle cells. *J Mol Biol*. 115(3):465-83.

Cen B, Selvaraj A, Burgess RC, Hitzler JK, Ma Z, Morris SW, Prywes R (2003) Megakaryoblastic leukemia 1, a potent transcriptional coactivator for serum response factor (SRF), is required for serum induction of SRF target genes. *Mol Cell Biol*. (18):6597-608.

Cen B, Selvaraj A, Prywes R (2004) Myocardin/MKL family of SRF coactivators: key regulators of immediate early and muscle specific gene expression. *J Cell Biochem.* 93(1):74-82.

Chang PS, Li L, McAnally J, Olson EN (2001) Muscle specificity encoded by specific serum response factor-binding sites. *J Biol Chem*. 276(20):17206-12.

Chen CC, Lau LF (2009) Functions and mechanisms of action of CCN matricellular proteins. *Int J Biochem Cell Biol.* (4):771-83.

Cheng X, Yang Y, Fan Z, Yu L, Bai H, Zhou B, Wu X, Xu H, Fang M, Shen A, Chen Q, Xu Y (2015) MKL1 potentiates lung cancer cell migration and invasion by epigenetically activating MMP9 transcription. *Oncogene.* 34(44):5570-81.

Christofori G (2006) New signals from the invasive front. *Nature*. 441(7092):444-50.

Cohen AW, Park DS, Woodman SE, Williams TM, Chandra M, Shirani J, Pereira de Souza A, Kitsis RN, Russell RG, Weiss LM, Tang B, Jelicks LA, Factor SM, Shtutin V, Tanowitz HB, Lisanti MP (2002) Caveolin-1 null mice develop cardiac hypertrophy with hyperactivation of p42/44 MAP kinase in cardiac fibroblasts. *Am J Physiol Cell Physiol*. 284(2):C457-74.

Cunningham CC (1995) Actin polymerization and intracellular solvent flow in cell surface blebbing. *J Cell Biol.* 129(6):1589-99.

Cunningham CC, Gorlin JB, Kwiatkowski DJ, Hartwig JH, Janmey PA, Byers HR, Stossel TP (1992) Actin-binding protein requirement for cortical stability and efficient locomotion. *Science.* 255(5042):325-7.

Cunningham CC, Vegners R, Bucki R, Funaki M, Korde N, Hartwig JH, Stossel TP, Janmey PA (2001) Cell permeant polyphosphoinositide-binding peptides that block cell motility and actin assembly. *J Biol Chem.* 276(46):43390-9.

da Costa LF (2001) Return of de-differentiation: why cancer is a developmental disease*. Curr Opin Oncol.* 13(1):58-62.

DeMali KA, Wennerberg K, Burridge K (2003) Integrin signaling to the actin cytoskeleton. *Curr Opin Cell Biol.* 15(5):572-82.

Depping R, Jelkmann W, Kosyna FK (2015) Nuclear-cytoplasmatic shuttling of proteins in control of cellular oxygen sensing. *J Mol Med*. 93(6):599-608.

Descot A, Rex-Haffner M, Courtois G, Bluteau D, Menssen A, Mercher T, Bernard OA, Treisman R, Posern G (2008) OTT-MAL is a deregulated activator of serum response factor-dependent gene expression*. Mol Cell Biol.* 28(20):6171-81.

Domazetovska A, Ilkovski B, Cooper ST, Ghoddusi M, Hardeman EC, Minamide LS, Gunning PW, Bamburg JR, North KN (2007) Mechanisms underlying intranuclear rod formation. *Brain.* 130(Pt 12):3275-84.

Dominguez R (2004) Actin-binding proteins--a unifying hypothesis. *Trends Biochem Sci.* (11):572-8.

Dominguez R, Holmes KC (2011) Actin structure and function. *Annu Rev Biophys.* 40:169-86.

Dopie J, Skarp KP, Rajakylä EK, Tanhuanpää K, Vartiainen MK (2012) Active maintenance of nuclear actin by importin 9 supports transcription. *Proc Natl Acad Sci U S A*. 109(9):E544-52.

Elberg G, Chen L, Elberg D, Chan MD, Logan CJ, Turman MA (2008) MKL1 mediates TGF-beta1-induced alpha-smooth muscle actin expression in human renal epithelial cells. *Am J Physiol Renal Physiol.* 294(5):F1116-28.

Feng Y, Chen MH, Moskowitz IP, Mendonza AM, Vidali L, Nakamura F, Kwiatkowski DJ, Walsh CA (2006) Filamin A (FLNA) is required for cell-cell contact in vascular development and cardiac morphogenesis. *Proc Natl Acad Sci U S A*. 103(52):19836-41.

Feng Y, Walsh CA (2004) The many faces of filamin: a versatile molecular scaffold for cell motility and signaling. *Nat Cell Biol.* 6(11):1034-8.

Flanagan LA, Chou J, Falet H, Neujahr R, Hartwig JH, Stossel TP (2001) Filamin A, the Arp2/3 complex, and the morphology and function of cortical actin filaments in human melanoma cells. *J Cell Biol.* 155(4):511-7.

Fox JW, Lamperti ED, Ekşioğlu YZ, Hong SE, Feng Y, Graham DA, Scheffer IE, Dobyns WB, Hirsch BA, Radtke RA, Berkovic SF, Huttenlocher PR, Walsh CA (1998) Mutations in filamin 1 prevent migration of cerebral cortical neurons in human periventricular heterotopia. *Neuron*. (6):1315-25.

Fukushima N, Ye X, Chun J (2002) Neurobiology of lysophosphatidic acid signaling. *Neuroscientist*. 8(6):540-50.

Galkin VE, Orlova A, Egelman EH (2012) Actin filaments as tension sensors. *Curr Biol*. 22(3):R96-101.

Gardel ML, Nakamura F, Hartwig JH, Crocker JC, Stossel TP, Weitz DA (2006) Prestressed F-actin networks cross-linked by hinged filamins replicate mechanical properties of cells. *Proc Natl Acad Sci U S A*. 103(6):1762-7.

Goodsell DS (2001) The molecular perspective: ultraviolet light and pyrimidine dimers. *Stem Cells*. (4):348-9.

Gorlin JB, Yamin R, Egan S, Stewart M, Stossel TP, Kwiatkowski DJ, Hartwig JH (1990) Human endothelial actin-binding protein (ABP-280, nonmuscle filamin): a molecular leaf spring. *J Cell Biol.* 111(3):1089-105.

Grosse R, Vartiainen MK (2013) To be or not to be assembled: progressing into nuclear actin filaments. *Nat Rev Mol Cell Biol.*(11):693-7.

Guan M, Zhou X, Soulitzis N, Spandidos DA, Popescu NC (2006) Aberrant methylation and deacetylation of deleted in liver cancer-1 gene in prostate cancer: potential clinical applications. *Clin Cancer Res*. 12(5):1412-9.

Hampl V, Martin C, Aigner A, Hoebel S, Singer S, Frank N, Sarikas A, Ebert O, Prywes R, Gudermann T, Muehlich S (2013) Depletion of the transcriptional coactivators megakaryoblastic leukaemia 1 and 2 abolishes hepatocellular carcinoma xenograft growth by inducing oncogene-induced senescence. *EMBO Mol Med.* 5(9):1367-82.

Hanahan D, Weinberg RA (2000) Hallmarks of cancer: the next generation. *Cell.* 144(5):646-74.

Hill CS, Wynne J, Treisman R (1994) Serum-regulated transcription by serum response factor (SRF): a novel role for the DNA binding domain. *EMBO J*. 13(22):5421-32.

Hill CS, Wynne J, Treisman R (1995) The Rho family GTPases RhoA, Rac1, and CDC42Hs regulate transcriptional activation by SRF. *Cell.* 81(7):1159-70.

Hinkel R, Trenkwalder T, Petersen B, Husada W, Gesenhues F, Lee S, Hannappel E, Bock-Marquette I, Theisen D, Leitner L, Boekstegers P, Cierniewski C, Müller OJ, le Noble F, Adams RH, Weinl C, Nordheim A, Reichart B, Weber C, Olson E, Posern G, Deindl E, Niemann H, Kupatt C (2014) MRTF-A controls vessel growth and maturation by increasing the expression of CCN1 and CCN2. *Nat Commun*. 5:3970.

Holmes KC, Popp D, Gebhard W, Kabsch W. (1990) Atomic model of the actin filament. *Nature*. 347(6288):44-9.

Huang Y, Mather EL, Bell JL, Madou M (2001) MEMS-based sample preparation for molecular diagnostics. *Anal Bioanal Chem*. 372(1):49-65.

Jaffe AB, Hall A (2005) Rho GTPases: biochemistry and biology. *Annu Rev Cell Dev Biol.* 21:247-69.

Jégou A, Carlier MF, Romet-Lemonne G (2013) Formin mDia1 senses and generates mechanical forces on actin filaments. *Nat Commun*. 4:1883.

Johansen FE, Prywes R (1995) Serum response factor: transcriptional regulation of genes induced by growth factors and differentiation. *Biochim Biophys Acta*. 1242(1):1-10.

Kanavy HE, Gerstenblith MR (2011) Ultraviolet radiation and melanoma. *Semin Cutan Med Surg.* (4):222-8.

Kim H, McCulloch CA (2010) Filamin A mediates interactions between cytoskeletal proteins that control cell adhesion. *FEBS Lett*. 585(1):18-22.

Kim H, Nakamura F, Lee W, Shifrin Y, Arora P, McCulloch CA (2010) Filamin A is required for vimentin-mediated cell adhesion and spreading. *Am J Physiol Cell Physiol.* 298(2):C221-36.

Kim MC, Whisler J, Silberberg YR, Kamm RD, Asada HH (2015) Cell Invasion Dynamics into a Three Dimensional Extracellular Matrix Fibre Network. *PLoS Comput Biol.* 11(10):e1004535.

Kim TY, Jong HS, Song SH, Dimtchev A, Jeong SJ, Lee JW, Kim TY, Kim NK, Jung M, Bang YJ (2003) Transcriptional silencing of the DLC-1 tumor suppressor gene by epigenetic mechanism in gastric cancer cells. *Oncogene*. 22(25):3943-51.

Kircher P, Hermanns C, Nossek M, Drexler MK, Grosse R, Fischer M, Sarikas A, Penkava J, Lewis T, Prywes R, Gudermann T, Muehlich S (2015) Filamin A interacts with the coactivator MKL1 to promote the activity of the transcription factor SRF and cell migration. *Sci Signal*. 8(402):ra112

Knöll B, Nordheim A (2009) Functional versatility of transcription factors in the nervous system: the SRF paradigm. *Trends Neurosci.* 32(8):432-42.

Kokai E, Beck H, Weissbach J, Arnold F, Sinske D, Sebert U, Gaiselmann G, Schmidt V, Walther P, Münch J, Posern G, Knöll B (2013) Analysis of nuclear actin by overexpression of wild-type and actin mutant proteins. *Histochem Cell Biol*. 141(2):123-35.

Kress H, Stelzer EH, Holzer D, Buss F, Griffiths G, Rohrbach A (2007) Filopodia act as phagocytic tentacles and pull with discrete steps and a load-dependent velocity. *Proc Natl Acad Sci U S A.* 104(28):11633-8.

Kümper S, Mardakheh FK, McCarthy A, Yeo M, Stamp GW, Paul A, Worboys J, Sadok A, Jørgensen C, Guichard S, Marshall CJ (2016) Rho-associated kinase (ROCK) function is essential for cell cycle progression, senescence and tumorigenesis. *Elife*. doi: 10.7554/eLife.12203.

Larriba MJ, Martín-Villar E, García JM, Pereira F, Peña C, de Herreros AG, Bonilla F, Muñoz A (2009) Snail2 cooperates with Snail1 in the repression of vitamin D receptor in colon cancer. *Carcinogenesis*. (8):1459-68.

Lee MY, Chou CY, Tang MJ, Shen MR (2008) Epithelial-mesenchymal transition in cervical cancer: correlation with tumor progression, epidermal growth factor receptor overexpression, and snail up-regulation. *Clin Cancer Res.* 14(15):4743-50.

Lehmann MJ, Sherer NM, Marks CB, Pypaert M, Mothes W (2005) Actin- and myosin-driven movement of viruses along filopodia precedes their entry into cells. *J Cell Biol.* 170(2):317-25.

Leung R, Wang Y, Cuddy K, Sun C, Magalhaes J, Grynpas M, Glogauer M (2010) Filamin A regulates monocyte migration through Rho small GTPases during osteoclastogenesis. *J Bone Miner Res*. (5):1077-91.

Li N, Zhang J, Liang Y, Shao J, Peng F, Sun M, Xu N, Li X, Wang R, Liu S, Lu Y (2007) A controversial tumor marker: is SM22 a proper biomarker for gastric cancer cells*? J Proteome Res.* (8):3304-12.

Liao XH, Wang N, Liu LY, Zheng L, Xing WJ, Zhao DW, Sun XG, Hu P, Dong J, Zhang TC (2014) MRTF-A and STAT3 synergistically promote breast cancer cell migration. *Cell Signal*. 26(11):2370-80.

Lin Y, Buckhaults PJ, Lee JR, Xiong H, Farrell C, Podolsky RH, Schade RR, Dynan WS (2009) Association of the actin-binding protein transgelin with lymph node metastasis in human colorectal cancer*. Neoplasia.* (9):864-73.

Lo HW, Hsu SC, Xia W, Cao X, Shih JY, Wei Y, Abbruzzese JL, Hortobagyi GN, Hung MC (2007) Epidermal growth factor receptor cooperates with signal transducer and activator of transcription 3 to induce epithelial-mesenchymal transition in cancer cells via up-regulation of TWIST gene expression. *Cancer Res*. 67(19):9066-76.

Loy CJ, Sim KS, Yong EL (2003) Filamin-A fragment localizes to the nucleus to regulate androgen receptor and coactivator functions. *Proc Natl Acad Sci U S A.* 100(8):4562-7.

Medjkane S, Perez-Sanchez C, Gaggioli C, Sahai E, Treisman R (2009) Myocardin-related transcription factors and SRF are required for cytoskeletal dynamics and experimental metastasis. *Nat Cell Biol.* 11(3):257-68.

Mercher T, Coniat MB, Monni R, Mauchauffe M, Nguyen Khac F, Gressin L, Mugneret F, Leblanc T, Dastugue N, Berger R, Bernard OA (2001) Involvement of a human gene related to the Drosophila spen gene in the recurrent t(1;22) translocation of acute megakaryocytic leukemia. *Proc Natl Acad Sci*. 98(10):5776-9.

Miralles F, Posern G, Zaromytidou AI, Treisman R (2003) Actin dynamics control SRF activity by regulation of its coactivator MAL*. Cell.* 113(3):329-42.

Mokalled MH, Johnson A, Kim Y, Oh J, Olson EN (2010) Myocardin-related transcription factors regulate the Cdk5/Pctaire1 kinase cascade to control neurite outgrowth, neuronal migration and brain development. *Development.* 137(14):2365-74.

Mouilleron S, Langer CA, Guettler S, McDonald NQ, Treisman R (2011) Structure of a pentavalent G-actin*MRTF-A complex reveals how G-actin controls nucleocytoplasmic shuttling of a transcriptional coactivator. *Sci Signal*. 4(177):ra40.

Mouneimne G, Soon L, DesMarais V, Sidani M, Song X, Yip SC, Ghosh M, Eddy R, Backer JM, Condeelis J (2004) Phospholipase C and cofilin are required for carcinoma cell directionality in response to EGF stimulation. *J Cell Biol*. 166(5):697-708.

Muehlich S, Cicha I, Garlichs CD, Krueger B, Posern G, Goppelt-Struebe M (2007) Actin-dependent regulation of connective tissue growth factor. *Am J Physiol Cell Physiol*. 292(5):C1732-8.

Muehlich S, Hampl V, Khalid S, Singer S, Frank N, Breuhahn K, Gudermann T, Prywes R (2012) The transcriptional coactivators megakaryoblastic leukemia 1/2 mediate the effects of loss of the tumor suppressor deleted in liver cancer 1*. Oncogene.* 31(35):3913-23.

Muehlich S, Schneider N, Hinkmann F, Garlichs CD, Goppelt-Struebe M (2004) Induction of connective tissue growth factor (CTGF) in human endothelial cells by lysophosphatidic acid, sphingosine-1-phosphate, and platelets*. Atherosclerosis.* 175(2):261-8.

Muehlich S, Wang R, Lee SM, Lewis TC, Dai C, Prywes R (2008) Serum-induced phosphorylation of the serum response factor coactivator MKL1 by the extracellular signal-regulated kinase 1/2 pathway inhibits its nuclear localization. *Mol Cell Biol*. (20):6302-13.

Nakamura F, Stossel TP, Hartwig JH (2011) The filamins: organizers of cell structure and function. *Cell Adh Migr.* 5(2):160-9.

Niemann H, Kupatt C (2014) MRTF-A controls vessel growth and maturation by increasing the expression of CCN1 and CCN2. *Nat Commun*. 5:3970.

O'Connell MP, Fiori JL, Baugher KM, Indig FE, French AD, Camilli TC, Frank BP, Earley R, Hoek KS, Hasskamp JH, Elias EG, Taub DD, Bernier M, Weeraratna AT (2009) Wnt5A activates the calpain-mediated cleavage of filamin A. *J Invest Dermatol*. 129(7):1782-9.

Olson EN, Nordheim A (2010) Linking actin dynamics and gene transcription to drive cellular motile functions. *Nat Rev Mol Cell Biol*. (5):353-65.

Ozanne DM, Brady ME, Cook S, Gaughan L, Neal DE, Robson CN (2000) Androgen receptor nuclear translocation is facilitated by the f-actin cross-linking protein filamin. *Mol Endocrinol.* (10):1618-26.

Pawłowski R, Rajakylä EK, Vartiainen MK, Treisman R (2010) An actin-regulated importin α/β-dependent extended bipartite NLS directs nuclear import of MRTF-A. *EMBO J.* 29(20):3448-58.

Pellegrini L, Tan S, Richmond TJ (1995) Structure of serum response factor core bound to DNA. *Nature*. 376(6540):490-8.

Planagumà J, Minsaas L, Pons M, Myhren L, Garrido G, Aragay AM (2012) Filamin A-hinge region 1-EGFP: a novel tool for tracking the cellular functions of filamin A in real-time*. PLoS One.* 7(8):e40864.

Popowicz GM, Schleicher M, Noegel AA, Holak TA (2006) Filamins: promiscuous organizers of the cytoskeleton. *Trends Biochem Sci*. 31(7):411-9.

Posern G, Miralles F, Guettler S, Treisman R (2004) Mutant actins that stabilise F-actin use distinct mechanisms to activate the SRF coactivator MAL. *EMBO J.* 23(20):3973-83.

Posern G, Sotiropoulos A, Treisman R (2002) Mutant actins demonstrate a role for unpolymerized actin in control of transcription by serum response factor. *Mol Biol Cell*. (12):4167-78.

Posern G, Treisman R (2006) Actin' together: serum response factor, its cofactors and the link to signal transduction. *Trends Cell Biol*. 16(11):588-96.

Rajakylä EK, Viita T, Kyheröinen S, Huet G, Treisman R, Vartiainen MK (2015) RNA export factor Ddx19 is required for nuclear import of the SRF coactivator MKL1. *Nat Commun*. 6:5978.

Roberts KL, Baines JD (2011) Actin in herpesvirus infection. *Viruses.* (4):336-46.

Sahai E, Marshall CJ (2002) ROCK and Dia have opposing effects on adherens junctions downstream of Rho. *Nat Cell Biol*. 4(6):408-15.

Sasaki A, Masuda Y, Ohta Y, Ikeda K, Watanabe K (2001) Filamin associates with Smads and regulates transforming growth factor-beta signaling. *J Biol Chem.* 276(21):17871-7.

Savoy RM, Ghosh PM (2013) The dual role of filamin A in cancer: can't live with (too much of) it, can't live without it. *Endocr Relat Cancer*. 20(6):R341-56.

Sayar N, Karahan G, Konu O, Bozkurt B, Bozdogan O, Yulug IG (2015) Transgelin gene is frequently downregulated by promoter DNA hypermethylation in breast cancer. *Clin Epigenetics*. 7:104.

Scharenberg MA, Pippenger BE, Sack R, Zingg D, Ferralli J, Schenk S, Martin I, Chiquet-Ehrismann R (2014) TGF-β-induced differentiation into myofibroblasts involves specific regulation of two MKL1 isoforms. *J Cell Sci.* 127(Pt 5):1079-91.

Schmidt LJ, Duncan K, Yadav N, Regan KM, Verone AR, Lohse CM, Pop EA, Attwood K, Wilding G, Mohler JL, Sebo TJ, Tindall DJ, Heemers HV (2012) RhoA as a mediator of clinically relevant androgen action in prostate cancer cells. *Mol Endocrinol*. 26(5):716-35.

Selvaraj A, Prywes R (2003) Megakaryoblastic leukemia-1/2, a transcriptional co-activator of serum response factor, is required for skeletal myogenic differentiation. *J Biol Chem*. 278(43):41977-87.

Seng TJ, Low JS, Li H, Cui Y, Goh HK, Wong ML, Srivastava G, Sidransky D, Califano J, Steenbergen RD, Rha SY, Tan J, Hsieh WS, Ambinder RF, Lin X, Chan AT, Tao Q (2007) The major 8p22 tumor suppressor DLC1 is frequently silenced by methylation in both endemic

and sporadic nasopharyngeal, esophageal, and cervical carcinomas, and inhibits tumor cell colony formation. *Oncogene*. 26(6):934-44.

Sharrocks AD (2001) The ETS-domain transcription factor family. *Nat Rev Mol Cell Biol*. (11):827-37.

Shimo T, Nakanishi T, Nishida T, Asano M, Sasaki A, Kanyama M, Kuboki T, Matsumura T, Takigawa M (2001) Involvement of CTGF, a hypertrophic chondrocyte-specific gene product, in tumor angiogenesis. *Oncology*. (4):315-22.

Small JV, Stradal T, Vignal E, Rottner K (2002) The lamellipodium: where motility begins. *Trends Cell Biol.* 12(3):112-20.

Smith EC, Teixeira AM, Chen RC, Wang L, Gao Y, Hahn KL, Krause DS (2013) Induction of megakaryocyte differentiation drives nuclear accumulation and transcriptional function of MKL1 via actin polymerization and RhoA activation. *Blood.* 121(7):1094-101.

Sotiropoulos A, Gineitis D, Copeland J, Treisman R (1999) Signal-regulated activation of serum response factor is mediated by changes in actin dynamics. *Cell*. 16(3):250-2.

Spiegelman BM, Heinrich R (2004) Biological control through regulated transcriptional coactivators. *Cell.* 119(2):157-67.

Stossel TP, Condeelis J, Cooley L, Hartwig JH, Noegel A, Schleicher M, Shapiro SS (2001) Filamins as integrators of cell mechanics and signalling. *Nat Rev Mol Cell Biol*. (2):138-45.

Stumpf MP, Kelly WP, Thorne T, Wiuf C (2007) Evolution at the system level: the natural history of protein interaction networks. *Trends Ecol Evol.* (7):366-73.

Tian HM, Liu XH, Han W, Zhao LL, Yuan B, Yuan CJ (2013) Differential expression of filamin A and its clinical significance in breast cancer. *Oncol Lett*. 6(3):681-686.

Treisman R (1986) Identification of a protein-binding site that mediates transcriptional response of the c-fos gene to serum factors. *Cell.* 46(4):567-74.

Treisman R (1995) DNA-binding proteins. Inside the MADS box. *Nature*. 376(6540):468-9.

Turcotte S, Desrosiers RR, Béliveau R (2003) HIF-1alpha mRNA and protein upregulation involves Rho GTPase expression during hypoxia in renal cell carcinoma. *J Cell Sci*. 116(Pt 11):2247-60.

Uramoto H, Akyürek LM, Hanagiri T (2010) A positive relationship between filamin and VEGF in patients with lung cancer. *Anticancer Res.* 30(10):3939-44.

van der Flier A, Sonnenberg A (2001) Structural and functional aspects of filamins. *Biochim Biophys Acta.* 1538(2-3):99-117.

Van Troys M, Vandekerckhove J, Ampe C (1999) Structural modules in actin-binding proteins: towards a new classification*. Biochim Biophys Acta.* 1448(3):323-48.

Vartiainen MK, Guettler S, Larijani B, Treisman R (2007) Nuclear actin regulates dynamic subcellular localization and activity of the SRF cofactor MAL. *Science*. 316(5832):1749-52.

Wang D, Chang PS, Wang Z, Sutherland L, Richardson JA, Small E, Krieg PA, Olson EN (2001) Activation of cardiac gene expression by myocardin, a transcriptional cofactor for serum response factor*. Cell.* 105(7):851-62.

Wang DZ, Li S, Hockemeyer D, Sutherland L, Wang Z, Schratt G, Richardson JA, Nordheim A, Olson EN (2002) Potentiation of serum response factor activity by a family of myocardin-related transcription factors*. Proc Natl Acad Sci U S A.* 99(23):14855-60.

Wang HY, Bakshi K, Frankfurt M, Stucky A, Goberdhan M, Shah SM, Burns LH (2012) Reducing amyloid-related Alzheimer's disease pathogenesis by a small molecule targeting filamin A. *J Neurosci.* 32(29):9773-84.

Wang Y, Falasca M, Schlessinger J, Malstrom S, Tsichlis P, Settleman J, Hu W, Lim B, Prywes R (1998) Activation of the c-fos serum response element by phosphatidyl inositol 3-kinase and rho pathways in HeLa cells. *Cell Growth Differ*. 9(7):513-22.

Wang Z, Wang DZ, Hockemeyer D, McAnally J, Nordheim A, Olson EN (2004) Myocardin and ternary complex factors compete for SRF to control smooth muscle gene expression. *Nature.* 428(6979):185-9.

Yagi H, Oka Y, Komada M, Xie MJ, Noguchi K, Sato M (2016) Filamin A interacting protein plays a role in proper positioning of callosal projection neurons in the cortex. *Neurosci Lett*. 612:18-24.

Yin D, Chen W, O'Kelly J, Lu D, Ham M, Doan NB, Xie D, Wang C, Vadgama J, Said JW, Black KL, Koeffler HP (2010) Connective tissue growth factor associated with oncogenic activities and drug resistance in glioblastoma multiforme. *Int J Cancer.* 127(10):2257-67.

Yuan Y, Shen Z (2001) Interaction with BRCA2 suggests a role for filamin-1 (hsFLNa) in DNA damage response. *J Biol Chem*. 276(51):48318-24.

Yue J, Huhn S, Shen Z (2013) Complex roles of filamin-A mediated cytoskeleton network in cancer progression. *Cell Biosci.* 3(1):7.

Yue J, Lu H, Liu J, Berwick M, Shen Z (2011) Filamin-A as a marker and target for DNA damage based cancer therapy. *DNA Repair*. 11(2):192-200.

Zhang K, Zhu T, Gao D, Zhang Y, Zhao Q, Liu S, Su T, Bernier M, Zhao R (2014) Filamin A expression correlates with proliferation and invasive properties of human metastatic melanoma tumors: implications for survival in patients. *J Cancer Res Clin Oncol*. 140(11):1913-26.

Zhang X, Azhar G, Chai J, Sheridan P, Nagano K, Brown T, Yang J, Khrapko K, Borras AM, Lawitts J, Misra RP, Wei JY (2001) Cardiomyopathy in transgenic mice with cardiac-specific overexpression of serum response factor. *Am J Physiol Heart Circ Physiol.* 280(4):H1782-92.

Zhang X, Chai J, Azhar G, Sheridan P, Borras AM, Furr MC, Khrapko K, Lawitts J, Misra RP, Wei JY (2001) Early postnatal cardiac changes and premature death in transgenic mice overexpressing a mutant form of serum response factor. *J Biol Chem.* 276(43):40033-40.

Zhao XH, Laschinger C, Arora P, Szászi K, Kapus A, McCulloch CA (2007) Force activates smooth muscle alpha-actin promoter activity through the Rho signaling pathway. *J Cell Sci*. 120(Pt 10):1801-9.

Zhou AX, Hartwig JH, Akyürek LM. (2010) Filamins in cell signaling, transcription and organ development. *Trends Cell Biol.* 20(2):113-23.

12 Publications

Parts of the results of this thesis have been published in a peer-reviewed journal.

- **Kircher P**, Hermanns C, Nossek M, Drexler MK, Grosse R, Fischer M, Sarikas A, Penkava J, Lewis T, Prywes R, Gudermann T, Muehlich S.

  Filamin A interacts with the coactivator MKL1 to promote the activity of transcription factor SRF and cell migration
  Science Signaling, 2015 Nov

- Muehlich S, Hermanns C, Meier M, **Kircher P**, Gudermann T.

  Unravelling a new mechanism linking actin polymerization and gene transcription
  Nucleus, 2016 Apr

Poster

- **Kircher P**, Nossek M, Drexler MK, Chinchilla P, Grosse R, Hermanns C, Lewis T, Prywes R, Gudermann T, Muehlich S.

  80. Annual Meeting of the German Society of Pharmacology and Toxicology, Hannover, 2014

13 Acknowledgements

Zuerst möchte ich mich bei meinen Eltern bedanken, die mich während meiner gesamten Ausbildung liebevoll begleitet und gefördert haben und ohne deren Unterstützung ich diese Arbeit nicht hätte durchführen können.

Mein besonderer Dank gilt Frau Dr. Susanne Mühlich für ihre exzellente Betreuung, stets aufmunternde Art und tatkräftige Unterstützung. Des weiteren für ihre motivierenden thematischen Diskussionen, methodischen Ratschläge und Problemlösungen.

Meinem Doktorvater Herrn Prof. Dr. Thomas Gudermann danke ich sehr, dass er mir die Möglichkeit gab, meine Forschung am Walther-Straub-Institut für Pharmakologie und Toxikologie durchzuführen.

Herrn Prof. Dr. Martin Biel danke ich ausserordentlich für die Übernahme der externen Fachvertretung im Bereich der Pharmazie.

Ferner möchte ich meinen Kolleginnen und Kollegen der Arbeitsgruppe Dr. Mühlich, Constanze Hermmans, Maria Draxler, Veronika Hampl, Natalie Frank, Claudia Martin, Clara-Mae Beer und Josef Penkawa für ihre Unterstützung danken. Vielen Dank für die schöne Zeit am WSI!